THE ASTROPHYSICAL JOURNAL

AN INTERNATIONAL REVIEW OF SPECTROSCOPY AND ASTRONOMICAL PHYSICS

VOLUME 91 JUNE 1940 NUMBER 5

ATMOSPHERIC ABSORPTION OF INFRARED SOLAR RADIATION AT THE LOWELL OBSERVATORY

III AND IV. THE SPECTRAL INTERVALS: 8.0–11.0 μ AND 11.0–14.0 μ

ARTHUR ADEL AND C. O. LAMPLAND

ABSTRACT

The detailed transmission of the earth's atmosphere throughout the spectral intervals from 8.0 to 11.0 μ and from 11.0 to 14.0 μ is investigated empirically in its dependence upon water vapor, ozone, and carbon dioxide. The transmission is given in both tabular and curve form for the following liquid water equivalents of atmospheric water vapor: (8.0–11.0 μ) 2.1, 3.2, 6.1, 10.8, 21.4, and 41.5 mm; (11.0–14.0 μ) 1.3, 4.1, 6.5, 17.9, 20.3, and 23.3 mm. The integrated transmissions for these spectral regions are moderately high, being, in the region 8–11 μ, 83.6 per cent for 2.1 mm of water and 47.4 per cent for 41.5 mm of water; and, in the region 11–14 μ, 76.2 per cent for 1.3 mm of water and 49.3 per cent for 23.2 mm of water. This is in sharp contrast to the atmospheric transmission of the spectral region between 5.5 and 8 μ, which, as shown in Part II of this series of analyses, is merely 13 per cent for 1 mm of water and as little as 5 per cent for 10 mm of water. The absorption by atmospheric ozone, now correctly placed between 9 and 10 μ, is much more intense than was formerly thought to be the case. The cessation of atmospheric transmission occurring normally at 13.9 μ recedes to 13.5 μ when the carbon dioxide in the path of the radiation has been increased to the amount resident in two or more air masses. Numerous small absorption lines due to water vapor have been recorded. Their existence has been established by repeated duplication.

This is the third in a series of papers describing the degree of absorption suffered by incoming infrared radiations as a consequence of the absorption spectrum of the earth's atmosphere—an analysis of considerable importance in the Observatory's program of astronomical radiometry and in meteorological investigations. In all these studies the sun serves as the source of radiation and the earth's atmosphere as the absorbing medium.

The first paper[1] in the series dealt with the continuous absorption spectrum of the atmosphere, the second[2] with the combined continuous and discrete absorptions throughout the spectral region 5.5–8.0 μ, while the present communication is concerned with a treatment similar to the latter for the regions 8.0–11.0 μ and 11.0–14.0 μ. The two regions currently being considered will in the future be designated as regions III and IV, respectively.

The distribution of solar intensity in regions III and IV at the earth's surface is shown by original records in Figures 1 and 2.[3] The wave-length scale is graduated in tenths μ on the dispersion of rock salt, and the intensities are proportional to the corresponding ordinates. The continuous absorption by water vapor creates a modified solar energy envelope differing from the original incident at the outer limits of the atmosphere, and upon this the discrete absorptions of water vapor, ozone, and carbon dioxide are impressed. Whereas the absorption discussed in Part I is governed mainly by water vapor and the absorption of Part II is due to water vapor and the oxides of nitrogen, the transmission in region III is determined by water vapor and ozone and that in region IV by water vapor and carbon dioxide. Many of the water lines which occupy regions III and IV are quite unsaturated and are, consequently, amenable to the law which states that the absorption is proportional to the square root of the optical thickness. The ozone band and the absorption by carbon dioxide at the long wave-length limit of transmission, on the other hand, being quite saturated, follow a more complicated pattern. This behavior is in contrast to the region between 5.5 and 8.0 μ, where it is water vapor which produces saturated absorption while the oxides of nitrogen exercise only moderate absorption.

The particular observations to be discussed here and reduced to curves of transmission are typical of a large number of observations made over a period of two years and with a wide variety of atmospheric water-vapor contents. The reduction of such curves as those

[1] A. Adel, *Ap. J.*, **89**, 1, 1939.

[2] A. Adel and C. O. Lampland, *Ap. J.*, **91**, 1, 1940.

[3] The difficulties usually encountered in the long wave-length region (occasioned by drift and by contaminating radiations of shorter wave length) were eliminated through the use of the periodic radiometer and suitable shutter plates.

PLATE V

FIG. 1

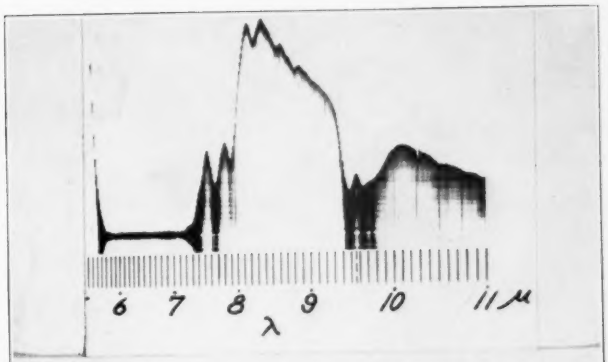

FIG. 2

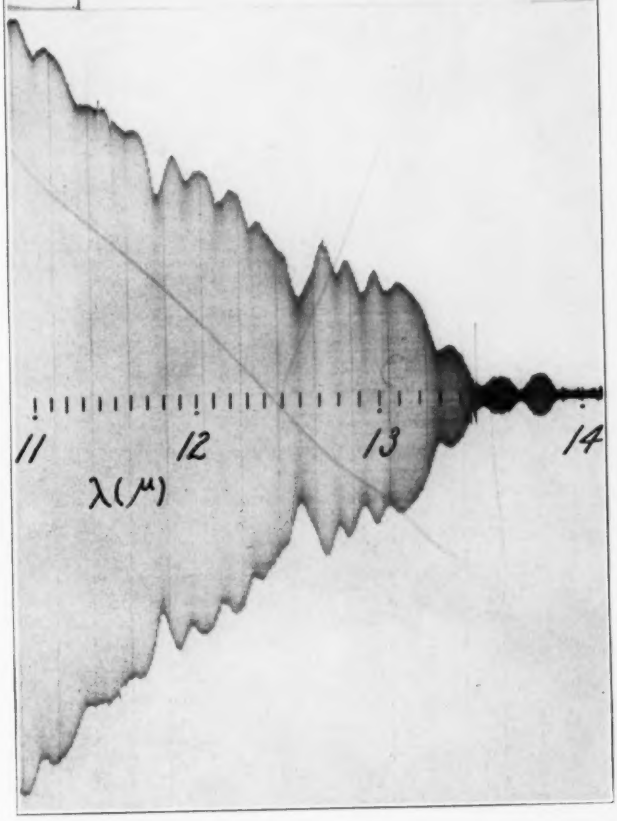

FIGS. 1 AND 2.—ROCK-SALT PRISMATIC SOLAR SPECTRUM

UNIV. OF MICH.

shown in Figures 1 and 2 to curves of transmission is accomplished by the combined application of the curve of distribution of solar intensity at the outskirts of the atmosphere, found by extrapolation through the use of Beer's law,[1] and the coefficient of continuous absorption at 11.0 μ. The atmospheric water-vapor content was in each case spectroscopically determined. Six observations reduced in this manner for region III are summarized in Table 1 and in Figure 3, while six observations similarly reduced for region IV are summarized in Table 2 and in Figure 4. It will be noted in Figure 4 that the curve of continuous-absorption coefficient in this spectral region does not rise as rapidly in the direction of longer wave lengths as was indi-

TABLE 1

ATMOSPHERIC TRANSMISSION: 8–11 μ

Wave Length in μ	*A*	*B*	*C*	*D*	*E*	*F*
8.0	20.3	25.6	44.6	47.8	52.4	60.7
8.1	37.6	44.2	65.8	73.3	70.8	79.5
8.2	34.4	47.2	68.7	76.5	80.5	85.9
8.3	47.1	52.7	78.1	82.7	89.5	91.4
8.4	49.5	64.8	83.7	89.7	93.7	97.3
8.5	47.5	63.2	82.5	88.3	93.3	96.6
8.6	54.8	70.0	84.8	90.5	93.6	97.1
8.7	53.1	71.5	83.3	89.8	93.4	95.6
8.8	51.8	69.5	81.6	88.0	91.7	94.3
8.9	56.5	75.1	86.2	92.7	95.7	97.9
9.0	54.0	72.3	82.8	91.0	95.2	97.6
9.1	57.6	74.2	85.2	91.4	94.7	97.1
9.2	58.2	73.7	84.2	90.8	91.8	95.0
9.3	51.2	62.4	77.6	84.7	85.7	88.5
9.4	26.2	30.7	42.7	43.2	40.4	41.9
9.5	21.5	23.2	32.0	34.7	27.3	28.5
9.6	24.6	27.8	35.1	39.8	31.6	32.6
9.7	24.6	27.3	35.3	41.8	33.1	34.3
9.8	30.0	34.2	43.3	50.8	43.0	45.4
9.9	40.8	45.8	57.6	65.8	60.9	64.2
10.0	49.6	59.2	74.2	82.3	80.2	82.7
10.1	57.5	69.2	83.8	92.5	91.7	94.8
10.2	56.7	70.0	83.8	93.9	94.2	98.5
10.3	53.3	68.5	82.2	92.5	94.5	98.7
10.4	56.4	71.5	80.6	91.0	95.1	99.0
10.5	52.3	68.5	78.4	89.0	91.6	97.0
10.6	55.1	70.7	80.8	92.3	93.8	97.7
10.7	56.3	72.7	82.0	93.5	94.2	97.8
10.8	50.0	66.3	75.4	90.5	92.3	96.6
10.9	53.0	70.5	78.8	93.6	94.7	96.2
11.0	51.0	64.4	78.9	92.0	93.6	96.6

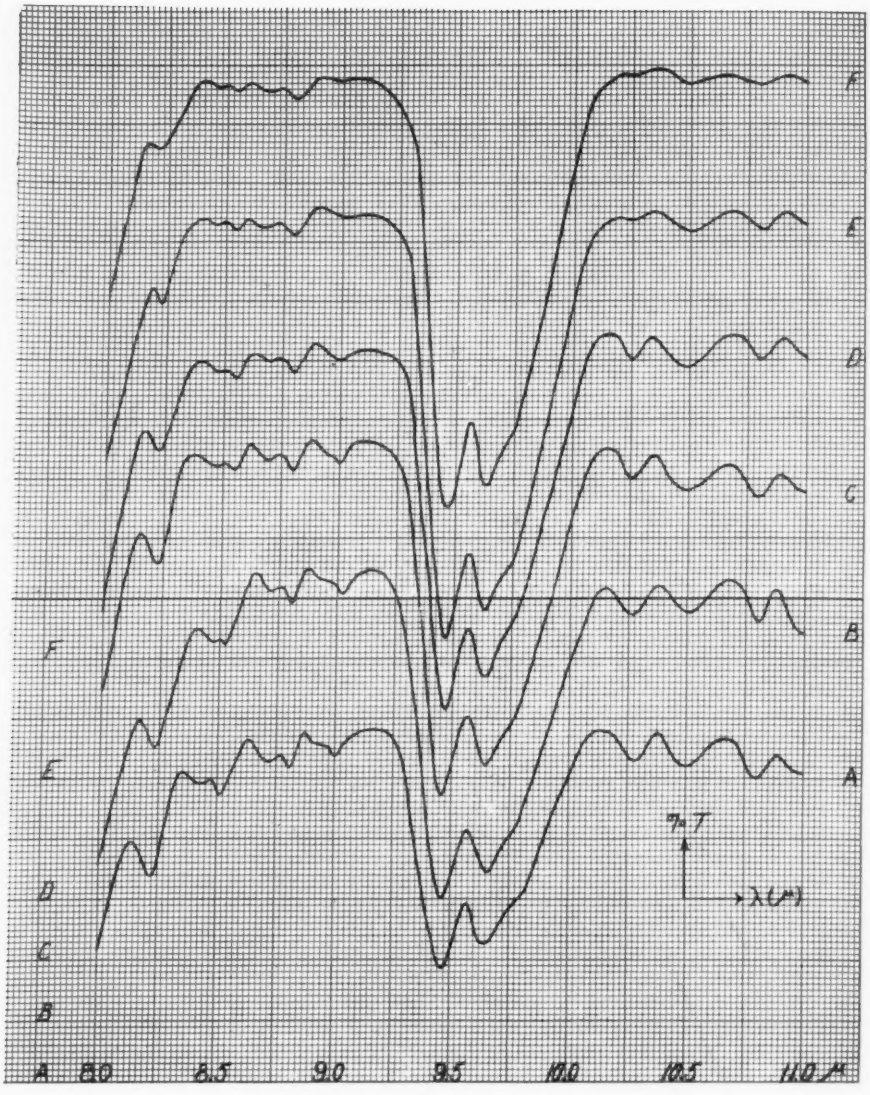

FIG. 3.—Atmospheric transmission: 8–11 μ

cated by the earlier preliminary measurements.[1] The liquid water equivalents corresponding to the observations of Figure 3 are: *A*, 44.0–39.0 mm; *B*, 22.2–20.5 mm; *C*, 11.2–10.4 mm; *D*, 6.2–6.0 mm; *E*, 3.3–3.1 mm; and *F*, 2.1–2.1 mm. The first, or larger, number corresponds to 11.0 μ, while the second number corresponds to 8.0 μ, the latter having in each instance been observed at a slightly smaller zenith distance of the sun than the former. Similarly, for Figure 4 we have *A*, 24.2–22.5 mm; *B*, 21.5–19.1 mm; *C*, 19.6–16.2 mm; *D*, 6.7–6.3 mm; *E*, 4.1–4.1 mm; and *F*, 1.3–1.3 mm. As before, the larger number corresponds to 14.0 μ and the smaller to 11.0 μ.

TABLE 2

ATMOSPHERIC TRANSMISSION: 11–14 μ

Wave Length in μ	*A*	*B*	*C*	*D*	*E*	*F*
11.0	67.7	71.3	75.5	89.5	92.2	97.4
11.1	71.3	75.0	78.5	91.3	94.2	97.5
11.2	70.3	73.1	77.1	90.3	92.2	96.6
11.3	63.7	68.0	71.7	86.7	90.7	95.2
11.4	67.3	70.8	73.5	88.1	92.5	95.8
11.5	68.7	71.4	73.7	88.1	92.2	95.7
11.6	67.0	70.8	73.0	87.2	91.3	94.8
11.7	65.7	71.7	72.5	87.6	88.5	93.3
11.8	55.4	59.5	63.3	76.8	87.0	93.4
11.9	70.2	72.5	75.0	86.7	90.8	95.5
12.0	65.5	72.1	72.6	85.7	91.2	95.7
12.1	67.5	72.5	74.5	89.1	89.9	96.2
12.2	68.8	72.1	74.5	85.2	91.7	95.5
12.3	64.1	67.5	70.3	86.8	88.5	95.7
12.4	62.2	64.8	68.1	84.5	87.3	94.5
12.5	55.0	57.0	59.3	79.2	80.4	91.6
12.6	36.2	40.4	43.5	63.1	70.3	85.7
12.7	63.1	65.2	65.4	78.1	83.2	93.0
12.8	54.8	59.0	60.1	77.5	85.1	96.6
12.9	51.3	56.3	57.7	79.3	82.7	95.6
13.0	63.3	64.8	64.8	84.9	86.1	96.7
13.1	62.0	60.3	60.1	79.1	80.6	90.4
13.2	52.2	52.0	50.3	72.8	67.1	76.7
13.3	23.2	24.9	22.8	42.3	45.4	56.0
13.4	22.6	24.9	18.5	39.0	35.0	39.0
13.5	6.5	8.7	2.8	17.3	14.7	18.3
13.6	9.9	9.0	0.0	13.5	14.9	16.3
13.7	3.8	5.0	0.0	7.1	10.0	13.7
13.8	12.5	12.9	0.0	16.4	15.9	17.1
13.9	0.0	0.0	0.0	0.0	0.0	0.0
14.0	0.0	0.0	0.0	0.0	0.0	0.0

The transmissions listed in Tables 1 and 2 are given at intervals

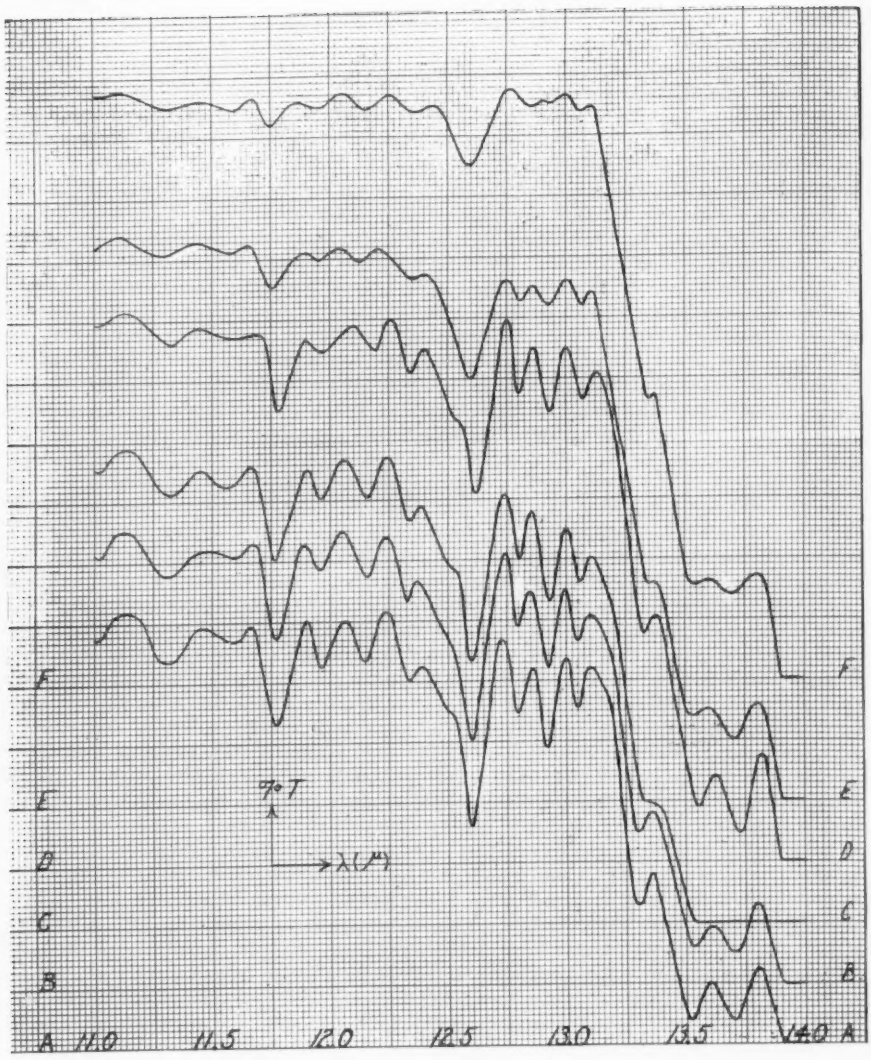

FIG. 4.—Atmospheric transmission: 11–14 μ

of 0.1 μ. Figures 3 and 4 give continuous curves of transmission based on Tables 1 and 2, supplemented by additional points such as the maxima and minima of salient features. In Figures 3 and 4 the plots are on the scale of normal dispersion. The dispersion axis for a given curve lies opposite the left-hand letter corresponding to the

TABLE 3

ATMOSPHERIC TRANSMISSION

Curve	Region of 8–9 μ	Region of 9–10 μ	Region of 10–11 μ	Region of 8–11 μ	Mean Water Content (Mm)	Mean Air Mass
A	47.9	39.3	54.9	47.4	41.5	1.6
B	61.3	47.2	69.5	59.3	21.4	1.6
C	78.4	57.7	80.6	72.2	10.8	1.4
D	84.8	64.0	91.8	80.2	6.1	1.3
E	88.2	60.1	93.3	80.5	3.2	1.6
F	91.8	61.9	97.2	83.6	2.1	1.5

TABLE 4

ATMOSPHERIC TRANSMISSION

Curve	Region of 11–12 μ	Region of 12–13 μ	Region of 13–14 μ	Region of 11–14 μ	Mean Water Content (Mm)	Mean Air Mass
A	66.3	59.7	22.1	49.3	23.3	1.2
B	70.3	62.9	23.1	52.1	20.3	1.3
C	72.9	65.1	18.7	52.2	17.9	2.1
D	87.3	81.2	32.5	67.0	6.5	1.3
E	91.3	84.8	32.9	69.7	4.1	1.4
F	95.8	94.2	38.7	76.2	1.3	1.4

curve. The termini of the curves are given by the letters on the right. Each vertical division is equal to 1 per cent on the scale of 100 per cent.

Tables 3 and 4 list the integrated transmissions obtained from Figures 3 and 4 for the intervals: 8.0–9.0 μ, 9.0–10.0 μ, 10.0–11.0 μ, 8.0–11.0 μ; and 11.0–12.0 μ, 12.0–13.0 μ, 13.0–14.0 μ, 11.0–14.0 μ. The mean air mass of each observation is also given. It is now apparent that the recession of the limit of transmission in *C* of Figure 4 is due to the relatively large carbon dioxide content of air mass 2.

LOWELL OBSERVATORY
FLAGSTAFF, ARIZONA

ABSOLUTE *f*-VALUES BY THE METHOD OF TOTAL ABSORPTION*

ROBERT B. KING AND DONALD C. STOCKBARGER[1]

ABSTRACT

A special furnace has been constructed for the purpose of measuring the absolute *f*-values of lines in spectra of astrophysical interest. The method, that of total absorption, is described, and results obtained in the course of the preliminary work are given. For the line λ 3261 of cadmium an *f*-value of 0.0023 was obtained, in good agreement with the values obtained by other investigators. For the copper resonance lines λλ 3247 and 3274 the results are 0.62 and 0.32, respectively.

The work described here was undertaken with the purpose of determining experimentally the absolute *f*-values of lines in the spectra of elements of astrophysical importance. The field for investigation is limited by a number of factors, but several elements, among them iron and nickel, offer the possibility of such determinations. The present paper describes the experimental technique and the preliminary results obtained in the course of checking its accuracy.

Numerous experimental methods have been employed to measure absolute *f*-values or, in the case of resonance lines, the lifetime of the excited states.[2] These have been concerned mainly with resonance lines in the spectra of elements of relatively easy excitation. Most of these methods encounter serious practical difficulties when applied to the lines of the higher melting-point elements. A survey of the possibilities showed that the method of "total absorption" offered the most promising means of attack on these elements.

The primary requisite of the method of total absorption is knowledge of the absolute number of atoms in the column of absorbing vapor. Hence, reliable vapor-pressure data at the temperatures to be used must be available, and the temperature and the length of the column of absorbing vapor must be accurately known. It has

* *Contributions from the Mount Wilson Observatory, Carnegie Institution of Washington*, No. 629.

[1] Of the Massachusetts Institute of Technology.

[2] A discussion of these methods and a bibliography is given in Mitchell and Zemansky, *Resonance Radiation and Excited Atoms*, Macmillan, 1934.

been our experience that sufficient vapor density may be obtained at temperatures well below the melting-points to observe in absorption the ultimate lines of the metals of the iron group. A furnace was therefore constructed in which temperatures up to 1300°–1400° C could be closely regulated and accurately measured and in which a pure metal could be heated without the formation of an alloy affecting the vapor pressure.

APPARATUS

The essential features of the furnace are shown in Figure 1. Unless otherwise specified, the parts of the furnace are of Alundum, of mixture RA 98, rated to withstand temperatures of over 2000° C.[3] A core *A* of $1\frac{1}{2}$ inches inner diameter, 10 inches long, wound with 0.020-inch molybdenum wire, twelve turns per inch, is the main heating element. It is surrounded by another core *B*, of 2 inches inner diameter. Two inches at each end of core *B* are also wound with 0.020-inch molybdenum wire, nine turns per inch. The windings of both cores are coated with a layer of Alundum cement, RA 518. The cores are inserted in holes drilled in the centers of the disks *C*, 4 and 5 inches in diameter, fastened together. These disks serve as insulators and support two cylindrical nickel baffles *D* which surround the heating elements. The disks are drilled with numerous holes to permit evacuation of the space between the cores and the baffles.

A system of baffles *F*, formed by attaching disks to the ends of thin-walled cylinders *E* by means of molybdenum wires, helps to maintain a uniform temperature within the center cylinder. A $\frac{3}{8}$-inch hole in the center of each disk permits passage of light from the source of the continuous spectrum. The absorption cell *G*, an evacuated pyrex or quartz tube about 25 mm diameter and 38 mm long, containing the element to be studied is placed in the central cylinder.

A thermocouple for temperature measurements is mounted in a small double-holed porcelain tube *J*. The hot junction is located directly over the absorption cell.

The apparatus illustrated in Figure 1 is inclosed in a vacuum chamber (not shown) consisting of a 6-inch steel pipe 18 inches long,

[3] Obtained from the Norton Co., Worcester, Mass.

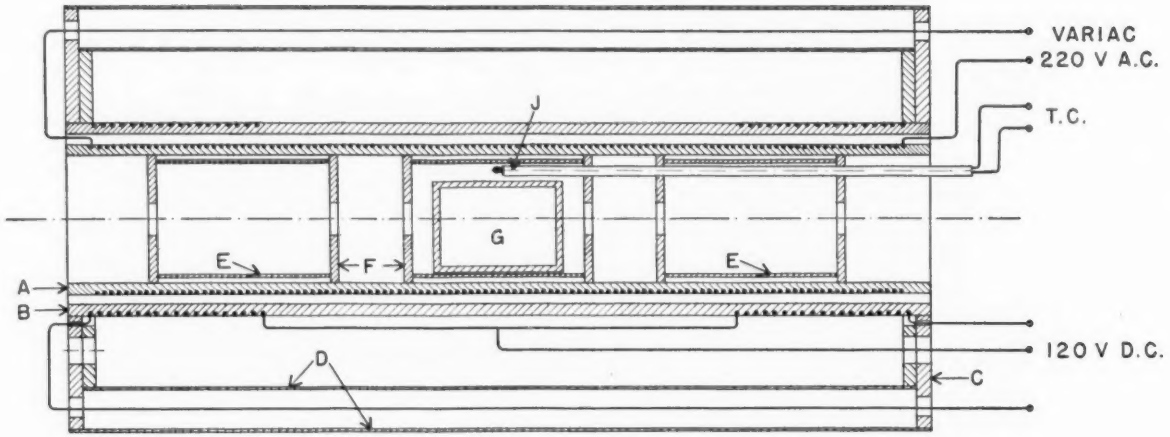

FIG. 1.—Cross section of interior of electric furnace designed for measurement of absolute *f*-values

closed permanently at one end by a cast-iron pipe cap. The furnace parts and the wiring are attached to a cast-iron faceplate, which is clamped to a flange at the other end of the pipe. The joint between flange and faceplate is sealed effectively by universal wax, pressed into a groove at the outer periphery. All the cast-iron parts are painted with several coats of Glyptal lacquer.

The 6-inch steel pipe is surrounded by a water jacket. The cap, faceplate, and brass window holders in cap and faceplate are cooled by coils of copper tubing. In addition, three nickel disks, not shown in the figure, mounted at each end of the furnace core, reduce heat transfer to the ends. These cooling devices, together with the cylindrical nickel baffles inclosing the furnace cores, allow a furnace temperature of 1300°–1400° C to be maintained without overheating the wax joints.

Pressures of 0.01–0.05 mm of *Hg* are readily maintained in the furnace by means of a Megavac pump. Pressures within this range were used in all the experiments described here.

The wirings of the two heating elements *A* and *B* are independent of each other. The current in the winding of the inner core *A* is closely controlled by a Variac attached to the 220-volt A.C. line. The windings at the ends of the outer core *B* are in parallel with each other and are connected in series with a lamp rheostat to a 12-kw D.C. generator. By slide-wire rheostats the proportion of current in each may be varied, and the total current controlled by the lamps. All the heating wires and the thermocouple wires pass through the faceplate. The former are attached to spark plugs, and the latter are led through vacuum-tight insulated fittings screwed into the faceplate.

The heating elements were designed to maintain a uniform temperature over 6 or 7 cm of the central portion of the furnace. The currents required in each coil to remove temperature gradients within this region were found by shifting back and forth a movable thermocouple, controlled from without the furnace by a simple magnetic arrangement. This was done at various temperatures. It was found that the temperature variations could be kept within 1° C at all temperatures.

Temperature measurements were made with a platinum, platinum-

rhodium (10 per cent) thermocouple calibrated by the Bureau of Standards. Fine wires, 0.007 of an inch in diameter, insured quick response to temperature changes in the furnace. The thermocouple e.m.f. was measured by a Wolff potentiometer, calibrated by a Weston standard cell. The cold junction of the couple was kept at room temperature. Changes in e.m.f. corresponding to temperature changes of less than $\frac{1}{2}^\circ$ C were easily observed with the aid of a galvanometer. During 30-minute exposures the furnace temperature could be held constant to 1° C without difficulty.

The source of continuous radiation in the ultraviolet was a 50-ampere Philips cinema lamp with quartz bulb. A $2\frac{1}{2}$-inch-focus quartz lens, sealed to the window holder at the closed end of the furnace chamber, sent a parallel beam of light through the furnace tube. Emerging through a plane quartz window in the faceplate, the beam was brought to a focus on the slit of the spectrograph by two additional quartz lenses.

METHOD OF MEASUREMENT

The total absorption, or the equivalent width, of an absorption line as a function of the number of atoms active in absorbing the line is given by the well-known curve of growth. The linear, faint-line portion observed for a very small concentration of the absorbing atoms has been used to derive the relative *f*-values of lines of *Fe* I and *Ti* I from measures of equivalent width of absorption lines produced in the graphite-tube electric furnace.[4,5] In the course of these investigations it was shown[4] that the shape of this portion of the curve of growth, derived from lines photographed in the second order of the 15-foot concave-grating spectrograph, followed the course of the theoretical curve within the limits of observational error. The fact that the shape of the curve was defined well into the Doppler portion where the relation between the equivalent width and the number of absorbing atoms is not linear but approaches the horizontal was good evidence that the spectrograph introduced no large errors into the absolute values of total absorption as a function of

[4] R. B. and A. S. King, *Mt. W. Contr.*, No. 528; *Ap. J.*, **82**, 377, 1935.

[5] R. B. and A. S. King, *Mt. W. Contr.*, No. 581; *Ap. J.*, **87**, 24, 1938.

the number of absorbing atoms. The present work, however, requires a more precise check.

Under the circumstances, the most satisfactory way of accomplishing this is to measure the equivalent width of a line for which the number of absorbing atoms may be calculated. Thus a check is provided not only on the action of the spectrograph and the photometric method but on the furnace and the temperature measurement as well, since the number of active atoms is calculated from conditions assumed to exist in the furnace.

The linear and lower Doppler portions of the theoretical curve of growth of an absorption line may be represented by the equation:[6]

$$\frac{A_\lambda}{2\Delta\lambda_D} = \frac{\sqrt{\pi}}{2} C \left[1 - \frac{C}{2!\sqrt{2}} + \frac{C^2}{3!\sqrt{3}} - \frac{C^3}{4!\sqrt{4}} + \dots . \right], \qquad (1)$$

from which $A_\lambda/2\Delta\lambda_D$, the equivalent width divided by twice the Doppler breadth, both in angstrom units, may be calculated as a function of C for values of $C < 3$. Here

$$C = k_0 \cdot nlf, \qquad (2)$$

where k_0, the absorption coefficient per oscillator, is given by

$$k_0 = \frac{\sqrt{\pi}\, e^2}{mc^2} \cdot \frac{\lambda}{\Delta\lambda_D} \cdot 10^{-8} \qquad (3)$$

and where n is the number of atoms per cubic centimeter in the low-energy state involved in the transition, l the length of the column of absorbing vapor, and f the f-value or "oscillator strength" of the line. For any state, n is given by the Boltzmann formula

$$n = n_0 \frac{g_i e^{-\frac{E_i}{kT}}}{\sum g_s e^{-\frac{E_s}{kT}}}, \qquad (4)$$

where n_0 is the number of neutral atoms per cubic centimeter obtained from the vapor-pressure data for the temperature T, g_i is the

[6] A. Unsöld, *Physik der Sternatmosphären*, Springer, 1938.

statistical weight $(2j + 1)$, and E_i the excitation energy of the state in question measured from the ground state. The summation is taken over all states of the atom. For a single ground state without neighbors close enough to have appreciable populations at low temperatures (which is the case for *Cd* and *Cu*), the summation is equal to the statistical weight of the ground state and the expression reduces to $n = n_0$. The Doppler breadth is given by

$$\Delta\lambda_D = \frac{\lambda}{c}\sqrt{\frac{2RT}{M}}, \tag{5}$$

where T is the absolute temperature, M the atomic weight, and R the gas constant. By means of equations (1)-(5) the equivalent width A_λ can be calculated as a function of nlf which gives the course of the linear and lower Doppler portions of the curve of growth for specified values of λ, T, and M.

Therefore, if the factors n, g, E_i, l, λ, T, and M are known, the absolute f-value of a line may be derived from observations of the equivalent width, when the equivalent widths lie on the linear and lower Doppler parts of the curve of growth. Since the equivalent widths must be small in order to satisfy this requirement, a combination of low vapor density and small f-value is desired.

Most of the lines for which experimental absolute f-values are available are resonance lines (usually having large f-values) of elements for which a high vapor density may be produced at low temperatures. In most cases a rough calculation shows that the desired equivalent width can be obtained only at very low temperatures. Usually either the vapor-pressure data are not available at these temperatures or the Doppler breadth is so small as to prevent observation of the linear portion of the curve of growth. In some cases the lines lie in parts of the spectrum not conveniently observed with our apparatus. By a process of elimination it was found that perhaps the most favorable line for investigation was λ 3261 of cadmium. In addition, the copper resonance lines $\lambda\lambda$ 3247 and 3274 have been investigated.

MEASUREMENTS OF THE CADMIUM LINE λ 3261

The cadmium line λ 3261 arises from the intersystem transition between the normal state $^1S_0$ and the state $^3P_1^o$. Its measured *f*-value is small in comparison with that of the ultimate line λ 2288 ($^1S_0 - {}^1P_1$). Its absolute *f*-value has been determined by three independent methods. Kuhn,[7] from measurements of magneto-rotation, found $f = 0.0019$, H. D. Koenig and A. Ellett[8] found 0.0019, and Ellett[9] found 0.0021, from measurements of the lifetime of the $^3P_1^o$ state. Hence this line has one of the best-determined *f*-values. An approximate calculation showed that at a temperature of about 200° C, λ 3261 should have an equivalent width observable by the spectrograph and should lie near the upper limit of the linear portion of the curve of growth.

Vapor-pressure curves for solid cadmium are given by A. C. Egerton[10] and K. K. Kelley.[11] The equation of Egerton is derived from measurements of the vapor pressure of solid cadmium. Kelley has derived free-energy equations for solid and liquid cadmium from a critical consideration of all available vapor-pressure and other data included in the derivation of the equations. Since Kelley's is the later and more comprehensive work, his curve has been adopted for the reduction of our observations. Kelley's value for the vapor pressure at 200° C is about 17 per cent larger than Egerton's. Hence the *f*-values derived with the aid of Kelley's curve will be smaller than those obtained with Egerton's by this amount.

A Pyrex tube 25 mm in diameter and 38 mm long with plane Pyrex windows sealed to the ends was evacuated and baked out. A deposit of pure cadmium metal was introduced by distillation into the tube, which was then sealed off and placed in the central portion of the furnace.

The absorption line was photographed in the second order of the 15-foot, concave-grating spectrograph, dispersion 1.86 A/mm. Equivalent widths as small as 0.001 A are measurable on Eastman

[7] W. Kuhn, "Die Stärke der anomalen Dispersion in nicht leuchtendem Dampfe von Thallium und Cadmium," *Habilitationsschrift*, Zürich, 1926.

[8] *Phys. Rev.*, **39**, 576, 1932.

[9] *Phys. Rev.*, **33**, 124 (A), 1929.

[10] *Phil. Mag.*, **33**, 33, 1917.

[11] *U.S. Bureau of Mines Bulletin*, No. 383, 1935.

IV O plates with this instrument. Plate calibration and photometry and reduction to equivalent width were carried out in a manner described in a previous paper.[4] Twenty-five observations of equivalent width, ranging from 0.002 to 0.006 A, were made at temperatures between 182° and 208° C. From a curve of growth computed for a temperature of 205° C and with the aid of the vapor-pressure curve of Kelley, a mean f-value of 0.0023 for λ 3261 was derived. Egerton's vapor-pressure curve yields $f = 0.0027$. The average deviation of a single measure from the mean was about 8 per cent, with no indication of systematic differences.

Considering the nature of the measurements, the agreement between our value $f = 0.0023$ and the values $f = 0.0019$ and 0.0021 obtained by the earlier investigators is good. The difference may be due to uncertainty in the vapor-pressure curve for solid cadmium, which is less well determined than that of the liquid. Kuhn's work[7] was done at temperatures well above the melting point. It is noteworthy that the points cited in his paper (522° and 560° C) fall on Kelley's vapor-pressure curve.

The agreement between our result and those of other investigators indicates that the present method, for low temperatures at least, and the spectrograph are free from all but very small sources of systematic error.

THE COPPER LINES λλ 3247 AND 3274

No previous measurements of the f-values of the copper resonance lines λ 3247 and λ 3274 are available. However, the domination of the spectrum by the resonance lines indicates that they should be observed at temperatures well below the melting point. Vapor-pressure curves for copper in the neighborhood of the melting point are given by H. A. Jones, I. Langmuir, and G. M. J. Mackay,[12] by P. Harteck,[13] by K. K. Kelley,[11] and by A. L. Marshall, R. W. Dornte, and F. J. Norton.[14] The curve given by the free-energy equation of Kelley, based in part on Harteck's measurements (1419°–1463° K), has been adopted for the present work. This curve is in excellent agreement with the later data of Marshall, Dornte,

[12] *Phys. Rev.*, **30**, 201, 1927.

[13] *Zs. phys. Chem.*, **134**, 1, 1928.

[14] *J. Amer. Chem. Soc.*, **59**, 1161, 1937.

and Norton (1268°–1466° K) from measurements of rates of evaporation of copper. The agreement is shown by the fact that both give 81,240 cal/gm atom as the "best" value of the heat of vaporization of copper at 0° K as derived from the vapor-pressure data.

A sheet of high-purity, triple-plated electrolytic copper, obtained through the kindness of Dr. R. N. Rhines and Dr. Gerhard Derge of the Metals Research Laboratory of the Carnegie Institute of Technology, was placed in a quartz tube 25×38 mm, similar in size to the pyrex tube used for *Cd*. The tube was evacuated, baked out with hydrogen, and finally evacuated, baked out, and sealed off. No change in the bright surface of the metal was observed after repeated heatings in the furnace. Measurements of equivalent widths of λλ 3247 and 3274 were made at temperatures ranging from 897° to 952° C. A curve of growth computed for a temperature of 900° C and the vapor-pressure data of Kelley were used in reducing the equivalent widths to *f*-values. The hyperfine structure of the lines must, however, in this case be considered in its effect on the shape of the curve of growth, which, for the equivalent widths observed at these temperatures, deviates slightly from linearity.

If the hyperfine-structure separation of a line is larger than the Doppler width, then each hyperfine-structure component should be treated as a separate line, each following its own curve of growth. If, as is the case for the copper lines, the hyperfine structure is not completely resolved by the spectrograph, the measured equivalent width is the sum of the equivalent widths of the components of the line. If the equivalent width of the blend lies on the truly linear portion of the curve of growth, the *f*-value of the line may be derived from the total area; but since our observed equivalent widths for the copper lines fall on the nonlinear part of the curve, the components must be treated separately.

The hyperfine structure of the lines λλ 3247 and 3274 has been observed by S. Frisch[15] and by R. Ritschl.[16] Both lines were found to be doublets with separations of about 0.04 A. In each case the intensity ratio of the components was observed as approximately 2:1, the component of longer wave length being the stronger. Since the nuclear moment of the copper atom is $\frac{3}{2}$, the theoretical hyperfine-

[15] *Zs. f. Phys.*, **71**, 89, 1931. [16] *Zs. f. Phys.*, **79**, 1, 1932.

structure pattern of the terms gives the $^2S_{\frac{1}{2}}$ term as split into two components, $^2P^o_{\frac{1}{2}}$ into two, and $^2P^o_{\frac{3}{2}}$ into four. The separations of the components of $^2P^o_{\frac{1}{2}}$ and $^2P^o_{\frac{3}{2}}$ are small compared to those of $^2S_{\frac{1}{2}}$. The selection rules allow four hyperfine-structure lines to arise from the transition $^2S_{\frac{1}{2}} - {}^2P^o_{\frac{1}{2}}$ (λ 3274) and six from $^2S_{\frac{1}{2}} - {}^2P^o_{1\frac{1}{2}}$ (λ 3247). Because of the small separation of the $^2P^o_{\frac{1}{2}}$ and $^2P^o_{1\frac{1}{2}}$ components, however, we should expect the observed hyperfine structure of each line to consist of two components of approximately equal separation arising from the splitting of the $^2S_{\frac{1}{2}}$ term. Each of these components should be an unresolvable blend due to the $^2P^o_{\frac{1}{2}}$ and $^2P^o_{1\frac{1}{2}}$ splitting. This is found to be the case in the analogous D lines of sodium.[17] In accordance with the statistical weights of the terms of the $^2S_{\frac{1}{2}}$ hyperfine structure, the theoretical intensity ratios of the observed doublet components will be 5:3, and the stronger component will in each case lie on the long wave-length side. Since the observations of Frisch and Ritschl indicate that this picture is correct, it seems best for our purpose to treat the lines as composed each of two simple components of intensity ratio 5:3.

In case of hyperfine structure the over-all f-value ($\bar{f}$) for a line is given by the relation

$$\bar{f} \cdot N = \sum_{jk} f_{jk} \cdot N_j ,$$

where

$$N = \sum_{j} N_j ,$$

and j and k refer to the lower and upper hyperfine-structure terms involved in the transition. The summation is taken over all components. In our case we may write for each line

$$\bar{f} = \frac{N_1 f_1 + N_2 f_2}{N} ,$$

where N_1 and N_2 are the numbers of atoms in the two $^2S_{\frac{1}{2}}$ hyperfine-structure terms, and f_1 and f_2 are the f-values associated with the

[17] C. M. van Atta and L. P. Granath, *Phys. Rev.*, **44**, 60, 1933.

transitions from these terms. Then if the measured total equivalent widths of the lines are divided into two parts of ratio 5:3, N_1f_1 and N_2f_2 may be read off the curve of growth. Dividing the sum by N, the number of atoms in the lower state, yields $\bar{f}$, the over-all f-value of the line. Here $N = nl$, where n is the number of normal atoms per cubic centimeter and l the length of the path.

Our observations of the copper lines suggested this hyperfine structure. The lines were broadened, and since the microphotometer tracings showed indications of a secondary maximum on the violet side of each line, the reduction of equivalent widths to f-values was carried out by the procedure just outlined.

The mean of 43 observations gave f-values of 0.62 for λ 3247 and 0.32 for λ 3274. The average deviation of a single measure from the mean was about 10 per cent, with no indication of systematic differences for different temperatures.

When the lines were treated as single simple lines, the f-values found were 0.76 and 0.36. But owing to the fact that the total equivalent widths from which these values were derived lie on the part of the curve of growth which deviates from linearity, rather large systematic differences with respect to equivalent width, or temperature, appeared, especially for λ 3247. The adopted method, which allows for the hyperfine structure, should give closer approximations to the true f-values. It may be noted that any reasonable division of the observed equivalent widths, say 2:1, brings the components down onto the more truly linear portion of the curve of growth, and the resulting f-values differ negligibly from those corresponding to an assumed ratio of 5:3. Hence, even if the lines were treated as complexes of four or six components, the resulting f-values would differ only slightly from 0.62 and 0.32 derived on the assumption of only two components.

For cadmium λ 3261 the theoretical hyperfine structure consists of three components, one strong, due to the isotopes of even atomic number whose nuclear spin is zero, and two weaker components, due to the isotopes of odd atomic number with nuclear spin $\frac{1}{2}$. The line has been observed only as double.[18,19] According to Ellett and Lar-

[18] W. A. McNair, *Phil. Mag.*, **2**, 613, 1926.

[19] A. Ellett and L. Larrick, *Phys. Rev.*, **39**, 294, 1932.

rick[19] the component due to the even isotopes coincides with the stronger of the two components due to the odd isotopes. These authors find an intensity ratio between the two observable components of 7:1, while the work of H. Schüler and J. E. Keystone[20] indicates a ratio of 12:1. In any case, the bulk of the intensity is due to one component. On our spectrograms the line appears single and very sharp. It has been treated here as a single simple line. The deviation of the curve of growth from linearity has in this case very little effect on the derived f-value.

THE f-SUM FOR COPPER

The Thomas-Kuhn f-sum rule[21] states that the sum of the f-values of all lines arising from a single atomic energy level shall equal the number of optical electrons, that is, the number of electrons which may take part in transitions giving rise to the optical spectrum including the continua beyond the series limits. For the alkali spectra the f-sum is about one,[22] since the inner closed electron shells are tightly bound and only the valence electron is active in producing the spectrum. In the case of copper the normal configuration is $3d^{10}4s$ with a closed d shell and single s electron, and an alkali-like doublet spectrum arises from transitions of the type 4s-np, 4p-nd, etc., involving only the outer electron. The resonance lines $3d^{10}4s\ {}^2S_{\frac{1}{2}} - 3d^{10}4p\ {}^2P^{\circ}_{\frac{1}{2}, 1\frac{1}{2}}$ belong to this spectrum. The d shell is not tightly bound, however, and configurations of the types $3d^9xx$, $3d^8xxx$, $3d^7xxxx$, etc., are theoretically possible, and an enormous number of transitions may occur between the normal state $3d^{10}4s$ and terms arising from these configurations. Transitions are observed between the normal configuration $3d^{10}4s$ and terms of the configuration $3d^94s4p$, giving rise to several moderately strong intersystem lines in the near ultraviolet. Therefore, since it is possible that any one or more of eleven electrons may be involved in transitions from the normal state (assuming the electrons in the inner shells are tightly bound), the f-sum should be eleven, to a close approximation. The

[20] *Zs. f. Phys.*, **67**, 433, 1931.

[21] *Naturwiss.*, **13**, 627, 1925; *Zs. f. Phys.*, **33**, 408, 1925.

[22] Experimental results are summarized in an article by S. A. Korff and G. Breit, *Rev. Mod. Phys.*, **4**, 471, 1932.

present investigation gives an *f*-sum of 0.94 for the resonance lines alone. It appears that although the resonance lines dominate the observed spectrum, the contributions of the enormous number of theoretically possible transitions, whose *f*-values are individually very small, together with the continuum beyond the series limit, amount to over 90 per cent of the total *f*-sum from the normal state.

SOURCES OF ERROR

The source and the amount of systematic error are difficult to determine in work of this sort. Errors may arise from a number of sources, including vapor-pressure data, temperature measurement, scattered light in the spectrograph, photographic photometry, and possible chemical reactions between the metal and its surroundings in the furnace which would alter the vapor pressure. While not definitive, the fact that successive exposures at the same temperature and exposures taken during repeated reheatings of the furnace gave accordant results for both *Cd* and *Cu* indicates that stable conditions of the vapors existed. It is noteworthy that the differences between our *f*-value for *Cd* λ 3261 and that of other investigators (2.3×10^{-3} against 1.9 and 2.1×10^{-3}) are in the sense opposite to what would be expected if the observed equivalent widths were affected by scattered light in the spectrograph. Filters used to cut down extraneous light had no influence on the measured equivalent widths. Measurements of thermocouple e.m.f. were made by a null method with apparatus of high precision whose error should be small. A systematic error in temperature measurement of 1° C would introduce an error of about 5 per cent in the *f*-value for *Cd* and 3 per cent in those for *Cu*. For the measurements with *Cu* two different thermocouples were used which gave results identical within the errors of measurement. From a consideration of the factors of uncertainty involved, it is evident that no claim of high accuracy can be made for measurements of this kind. Nevertheless, the good agreement between our *f*-value for *Cd* λ 3261 and those of other investigators indicates that the systematic errors of the method are small. Hence we may conclude that if the vapor-pressure data are good and the vapor of the pure metal can be obtained in the furnace, the

method of excitation, the temperature measurement, the spectrograph, and the photometry will yield reasonably accurate results for other elements.

This investigation was begun in the George Eastman Research Laboratory of Physics at the Massachusetts Institute of Technology and continued in the laboratory of the Mount Wilson Observatory. We wish to acknowledge the courtesy and co-operation of the physics department of the Institute in permitting the transfer of the apparatus. We also wish to thank Dr. Arthur S. King for his continued interest and many helpful suggestions and Dr. Rudolph Minkowski, Dr. Ralph W. Dornte, Dr. George H. Shortley, and Dr. Leo Goldberg for valuable advice on various points of the problem.

Carnegie Institution of Washington
Mount Wilson Observatory,
Physics Department
Massachusetts Institute of Technology
August 1939

THE PHOTOGRAPHIC DETERMINATION OF STELLAR PARALLAXES WITH THE 60- AND 100-INCH REFLECTORS*

SEVENTEENTH SERIES

ADRIAAN VAN MAANEN

ABSTRACT

Trigonometric parallaxes determined with the 60- and 100-inch reflectors are given for 25 fields, including 26 stars, 20 of which have photographic absolute magnitudes of +10 or fainter; 5 are even +15 or fainter. A list is given of the 21 stars known at present for which the absolute photographic magnitude is fainter than +15.

The present paper gives results for 26 stars in 25 fields, which have recently been measured for parallax. The work has been carried out in the same way as for the previously published series.[1] The results are given in Table 1. The magnitudes are those published by Willis or by the Radcliffe observers or derived from star-counts based on *Publications of the Astronomical Laboratory at Groningen*, **27,** Table IV, 1917. The parallaxes of Wolf 424 and of Luyten 789-6 are preliminary, based on 12 exposures each.

BD+20°5071 is a star of type R3 with dwarf characteristics; since the mean absolute parallax from McCormick and Mount Wilson is +0".004, the absolute magnitude is +1.8 visual.

For U Pegasi the motion in declination was also measured, giving $\delta = -0''.040 \pm 0''.001$.

Most of the stars were put on the program as faint stars of considerable proper motion with the hope of finding some more stars of very faint absolute magnitudes. Not less than 20 of the stars have a photographic absolute magnitude fainter than +10, while 5 are even fainter than +15, viz., the two components of Wolf 424, Wolf 457, Luyten 789-6, and Mayall's star. The total number of these

* *Contributions from the Mount Wilson Observatory, Carnegie Institution of Washington*, No. 630.

[1] *Mt. W. Contr.*, Nos. 111, 1916; 136, 1917; 158, 1918; 182, 1920; 204, 1921; 237, 1922; 270, 1923; 290, 1925; 321, 1926; 356, 1928; 391, 1929; 435, 1931; 468, 1933; 506, 1935; 553, 1936; 590, 1938.

very faint stars has now reached 21, and it seems worth while to give a complete list (see Table 2). Besides these 21 stars, 3 others are given by Luyten in *Harvard Bulletin*, No. 910; but for the parallaxes of these stars, as he has stated, "the accuracy is not as good as might

TABLE 1

Object	α 1900	δ 1900	Pg m	Mt. Wilson Spectrum	Relative Parallax	μ_α Rel.	P.E.	No. of Exp.	Instrument
vM-W 34*	$0^h10^m24^s$	+15° 21′	15.7	.....	+0″.014	+0″.131	7 4	16	100
Radcl. 8, BL= Wolf 44	0 55 8	+60 50	12.1	M2	+ .078	+0.350	6 4	20	60
Ross 11	1 33 36	+54 59	15.9	.....	+ .014	+0.578	5 6	16	60
Ross 21	2 24 6	+56 56	15.0	.....	+ .065	+1.099	4 3	18	60
Ross 367	2 53 48	+57 43	13.6	.....	+ .018	+0.107	5 4	20	60
Radcl. 10, 342	5 9 44	+60 24	15.4	.....	+ .021	+0.203	5 6	16	60
Lal. 15743 AB	7 58 50	+12 35	8.7	K2	+ .005	+0.109	10 4	18	60
Lal. 15743 C	7 58 50	+12 35	10.5†	.....	+ .023	+0.102	24 9	12	60
Radcl. 28, BL	8 36 33	+44 51	15.4	.....	+ .045	−0.393	6 4	18	60
Wolf 1438 = Ross 127	12 8 16	+17 16	13.3	.....	+ .030	−0.496	12 6	16	60
Wolf 424 AB	12 28 25	+ 9 34	13.7	M6e	+ .213	−1.737	17 4	12	100
Wolf 457	12 55 6	+ 4 2	15.6	.....	+ .078	−0.442	5 1	16	100
Wolf 534	14 14 0	− 6 50	14.5	.....	+ .077	−1.119	6 1	20	100
BD+16°2658= Ross 130	14 24 54	+15 57	12.4	M3	+ .092	−1.034	11 3	20	60
vM-W 10*	15 2 58	+29 36	14.1	.....	+ .033	−0.291	6 3	18	60
Ross 510	15 23 42	+17 4	14.7	.....	+ .034	−0.903	7 5	18	60
ϵ Herculis	16 56 28	+31 4	3.9†	Ao‡	+ .019	−0.045	16 2	18	60
Radcl. 61, 184	16 56 39	+29 51	13.0	.....	+ .013	−0.416	4 2	18	60
Wolf 834	18 11 17	+20 29	14.6	.....	+ .026	−0.463	6 8	18	60
Wolf 1373	20 52 49	+21 59	13.5	.....	+ .087	+0.771	8 1	20	100
Wolf 918	21 3 43	−13 40	12.2	M3	+ .079	+0.689	7 1	20	100
Wolf 1336	21 54 9	− 4 33	16.0	.....	+ .040	+0.022	9 2	18	100
BD+20°5071	21 59 40	+20 34	8.8†	R3	− .010	+0.050	5 1	16	60
Luyten 789-6	22 33 0	−15 52	14.3	.....	+ .328	+2.228	9 9	12	100
Mayall's star	23 45 48	+19 24	17.0	.....	+ .047	+0.866	6 6	20	100
U Pegasi	23 52 52	+15 24	Var.	G3	−0.030	−0.040	9 1	20	60

* *Mt. W. Contr.*, No. 412, 1930.

† Visual magnitude.

‡ Spectrum from *Henry Draper Catalogue*.

have been hoped, as seeing conditions during the early morning hours are generally of low quality." Accordingly, they are not included in the present list.

Six of the 21 stars are components of double stars.

Wolf 457, according to Kuiper, is of spectral type O; it is thus the faintest of the white dwarfs known at present.

PLATE VI

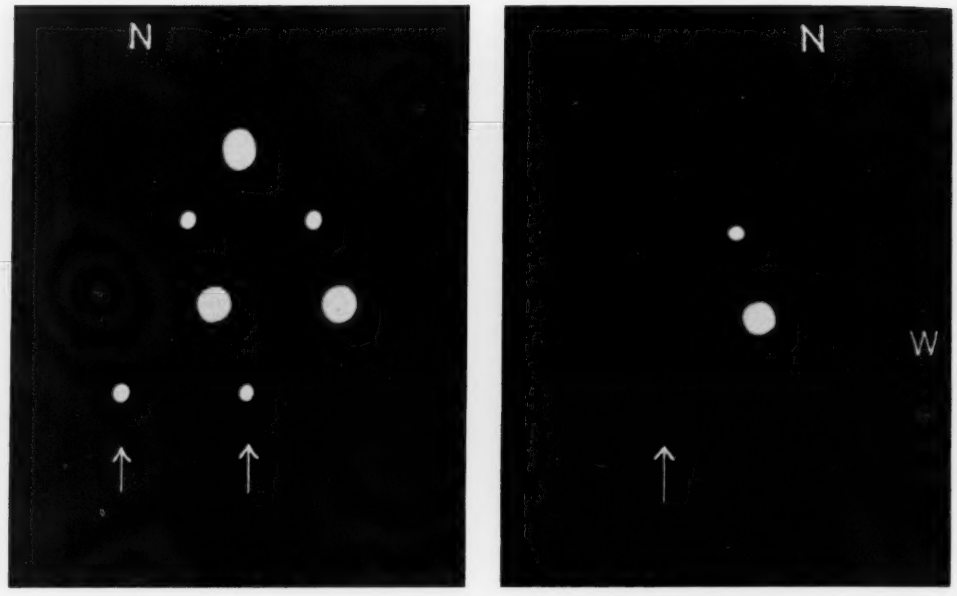

VARIABLE COMPANION OF LALANDE 21258

Left, May 11, 1939, two exposures at an interval of 36^m; Pg $m = 14.2$ and 14.5. The single image above is from a comparison field. *Right*, a single exposure showing the variable at normal brightness, Pg $m = 16.0$.

UNIV. OF MICH.

Wolf 489, too, has a spectrum of much earlier type than would be expected from the absolute magnitude, but it is doubtful if a star of type K should be called a white dwarf.

The companion of Lalande 21258 is at present the only star known of such low luminosity which has a variable magnitude. On more

TABLE 2

Object	α 1900	δ 1900	Pg m	Mt. Wilson Spectrum	μ	Parallax	Pg. M
Ross 614 B	6^h24^m	$-2°44'$	14.5*	.....	1".09	+0".262	+16.6*
Ross 619	8 7	+9 11	14.2	M6	5.40	+ .163	+15.3
Ross 92	9 35	+22 29	15.7	.....	0.72	+ .089	+15.4
Wolf 359	10 52	+ 7 36	15.4	M5e	4.84	+ .413	+18.5
Lal. 21258 B	11 0	+44 2	16.0	M6e	4.47	+ .173	+17.2
Wolf 424 A	12 28	+ 9 34	14.4	M6	1.87	+ .208	+16.0
Wolf 424 B	12 28	+ 9 34	14.4		1.87	+ .208	+16.0
Wolf 457	12 55	+ 4 2	15.6	O‡	1.05	+ .079	+15.1
Wolf 489	13 32	+ 4 13	15.2	K*	3.94	+ .134	+15.8
α Centauri C	14 23	−62 15	13.0	M	3.85	+ .752	+17.4
Ross 508	15 19	+17 51	15.4	.....	1.23	+ .088	+15.1
Barnard's star	17 53	+ 4 25	11.5	M5	10.30	+ .541	+15.2
Ross 154	18 44	−23 57	12.4	M6	0.74	+ .355	+15.1
Ci. 20, 1123	18 58	−13 42	16.3	.....	0.80	+ .069	+15.5
Ross 165 B	19 42	+26 55	15.0	.....	1.34	+ .119	+15.4
Lal. 38380 B	19 59	+29 36	16.5	.....	0.92	+ .061	+15.4
vM-W 112†	21 37	− 0 4	17.4	.....	0.45	+ .034	+15.1
Luyten 789-6	22 33	−15 52	14.3	.....	3.27	+ .330	+16.9
Ross 248	23 37	+43 39	13.8	M5	1.82	+ .319	+16.3
vM-W 119†	23 38	+ 0 22	16.5	.....	0.33	+ .056	+15.2
Mayall's star	23 46	+19 24	17.0	.....	0.89	+0.048	+15.4

* The asterisk indicates an uncertain value.

† *Mt. W. Contr.*, No. 412, 1930.

‡ Spectrum by Dr. Kuiper.

than two dozen exposures taken at Harvard and at Mount Wilson it is of about magnitude 16; but on two exposures taken by me on May 11, 1939, with an interval of 36 minutes, it is of magnitudes 14.2 and 14.5, respectively. The left part of Plate VI shows these two exposures, the arrows indicating the variable; the single image is a close double star in Selected Area 30 used as a companion field for the determination of the magnitude. To the right is one exposure on the star at its normal magnitude.

CARNEGIE INSTITUTION OF WASHINGTON
MOUNT WILSON OBSERVATORY
February 1940

SPECTROSCOPIC LUMINOSITIES OF STARS OF TYPES G AND K IN TWO SELECTED FIELDS

PHILIP C. KEENAN

ABSTRACT

Spectroscopic luminosities and revised spectral types were determined for stars brighter than the eighth visual magnitude having Henry Draper types G5–K5, in two fields—one in Cassiopeia (146 stars) and the other centered at the north galactic pole (120 stars). For this purpose the luminosity classes defined by Morgan were calibrated in terms of absolute magnitude by means of spectrograms of 235 bright stars of known trigonometric parallax.

From the data for the Milky Way field the main course of the luminosity function for K0 stars in the vicinity of the sun was derived. The numbers of stars per unit volume increase steadily with luminosity class, in going from supergiants to dwarfs. The zero point of the function was furnished by the giants, for which a space density of 8×10^{-5} stars per cubic parsec was found.

A plot of the distribution in distance of the individual stars indicates the marked falling-off in numbers of stars in the higher luminosity groups in the direction of the galactic pole at distances greater than about 200 parsecs from the sun.

It has been shown by W. W. Morgan[1] that by a careful selection of criteria involving estimated relative intensities of absorption lines it is possible to determine luminosities and spectral types from spectrograms of moderate scale (≈ 100 A/mm) with a precision comparable to that obtainable from high-dispersion plates. Thus the spectroscopic sampling of stellar populations can be extended to stars fainter than those within reach of spectrograph cameras designed for programs of accurate radial velocities.

In the present investigation these criteria have been applied to the two-dimensional classification of stars with visual magnitudes brighter than 8.0 in two fields: one near the galactic plane in Cassiopeia and the other centered at the north galactic pole. These samples represent the relatively near-by stars extending, respectively, in directions within, and perpendicular to, the plane of the Milky Way.

CRITERIA OF CLASSIFICATION

Spectra of the majority of the northern stars brighter than the fifth visual magnitude have been taken by Morgan and his assist-

[1] *Ap. J.*, **85**, 380, 1937; **87**, 460, 1938.

ants, and the systems of classification used in the present study were established from this material. The system of spectral types is that defined in Morgan's second paper,[1] and the criteria employed are given in his Table 1. For the late G- and K-type stars the decisive factor in the classification is the strength of *Ca* I 4226.

The luminosity criteria are listed in Table 1. Several fainter lines have been added to those used by Morgan. Although the intensity ratios of these additional lines are not as sensitive to luminosity changes as 4045/4077 and 4260/4215, they were included in order to minimize the accidental errors from defects in the film, since the length of the exposure times limited the material to one or two good spectrograms for most of the field stars.

TABLE 1

LINE INTENSITY DIFFERENCES FOR LUMINOSITY CLASSIFICATION

Spectral Range	4045 to 4077	4071 to *Hδ*	4260 to 4215	4352 to 4360, 4370 4376	4415, 4427 to 4435, 4444	4325 to 4290
G4–G9.....	√	√	√	×	×	√
K0–K1.....	√	√	√	√	×	√
K2–M0.....	√	√	√	√	√	×

The lines which tend to strengthen in stars of high luminosity are given in the bottom row. Where several lines are listed together, the estimated average intensity for the group was used in forming the corresponding intensity difference. The lines employed within a given spectral range are checked, while those omitted are marked with a cross (×). The last pair of lines is not useful for types later than K1 because, from this point on, λ 4290 becomes rapidly stronger toward later spectral types.

The procedure was to estimate intensities on a scale extending from 1 for the faintest perceptible line to 6 for a line of great strength, such as λ 4026 at K3. The scale was kept consistent by frequent intercomparison of spectrograms of the standard stars. For a given spectrogram the intensity sum was obtained by adding the individual differences, of which there were four for types G9 and earlier and five for the later spectral divisions.

The intensity sum obtained in this way is a purely observational parameter characterizing the luminosity of the star—it can be considered as a second dimension in the classification. However, the sums are estimated on an arbitrary scale, depending upon the observer and the dispersion of the spectrograph. By use of the standard stars they can be reduced either to absolute magnitudes or to the luminosity classes which were introduced by Morgan and are connected with the usual descriptions of luminosity in the following way:

Description	Luminosity Class (L_Y)
Supergiants	I
Bright giants	II
Giants	III
Subgiants	IV
Main-sequence dwarfs	V

Absolute magnitudes represent the most precise formulation of luminosities, but in practice it is desirable to tabulate also the luminosity classes. There are two reasons for this. First, as Morgan has pointed out,[2] they are observational data obtained directly from the spectra, while the scale of spectroscopic absolute magnitudes is subject to revision as our direct determinations of distances of the standard stars are improved and extended. In the second place, the luminosity classes offer a convenient grouping for taking means in relating intensity sums to absolute magnitudes. It may be further noted that with the use of intermediate classes (e.g., II–III) they provide a scale with nine divisions, which is ample for much spectrographic work done with low dispersion.

Spectrograms of 235 bright or near-by stars provide the data for the present calibration. For the great majority of these there were available two or more good spectrograms of each star. After a table had been prepared giving the mean intensity sum for each luminosity class and spectral type from G3 to M0, the next step was the determination of the corresponding mean absolute magnitudes. The reduction was necessarily carried out somewhat differently for the several luminosity classes.

[2] *Ibid.*, first paper, p. 389.

Class V.—This class represents precisely the main sequence. Morgan has found that his spectral types for dwarfs between G4 and K2 agree closely with those assigned at Mount Wilson. Consequently, to the rather small numbers of dwarfs within this range of types which were photographed here were added all stars listed in the Mount Wilson parallax catalogue[3] whose trigonometric parallaxes were large enough to assure membership in the class. The trigonometric absolute magnitudes were weighted inversely as the relative errors in the parallax, in order to eliminate distortion of the mean due to the larger effect of negative errors in the parallaxes, and the averages were taken for each spectral type separately. The means for types K2–Mo were based upon only a few stars bright enough to be photographed here, but the dispersion in luminosity of the main sequence is known to be small in this range.[4]

Class III.—In calibrating the giants, it was necessary to work directly with the trigonometric parallaxes rather than with absolute magnitudes, because of the presence of negative parallaxes. The procedure was similar to that followed by Russell,[5] in that the observed parallax, p, of each star was reduced to the parallax p' which the star would have if its apparent magnitude were an arbitrarily fixed constant—in this case, 4.0. The means were taken for the groupings of spectral types shown in Table 2. In the third column are given the averages which were obtained by weighting each reduced parallax inversely as the square of its probable error derived from the value given in the Yale catalogue. There are two objections to this procedure. In the first place, if the true dispersion is a considerable fraction of the parallaxes and is comparable to their accidental mean error, the absolutely brighter stars will be systematically favored. In the second place, if one or two stars have much larger weights than the remainder in the same group, the number of stars is effectively reduced, and the sampling errors may become large. To test for the presence of these effects, unweighted means were formed and are tabulated in the fourth column. The considerable differences between the two means are not systematic and are evidently due to the

[3] *Ap. J.*, **81**, 187, 1935.

[4] Cf. Morgan, *Ap. J.*, **87**, 589, 1938.

[5] *Ap. J.*, **87**, 389, 1938.

sampling effect in the weighted parallaxes. In almost every case the larger differences can be traced to the presence of one or two very high weights, as at K1, where Arcturus, with a reduced parallax of $0''.0151$, has nearly as much weight as the other 21 stars together.

Some weighting is desirable, and as a compromise the simple means of the values in the two columns were taken as the adopted mean parallax in the fifth column. The corresponding absolute magnitudes were plotted against spectral types, and the final values of $M_{\overline{\pi}}$ in the sixth column were read from a smooth curve passing

TABLE 2

CALIBRATION OF CLASS III

Spectral Types	No. of Stars	Weighted Mean Parallax	Unweighted Mean Parallax	Adopted Mean Parallax	$M_{\overline{\pi}}$
G3–G6.....	6	$0''.0160$	$0''.0207$	$0''.0184$	$+0^{m}.33$
G7–G8.....	18	.0171	.0207	.0189	+ .40
G9.....	21	.0230	.0220	.0225	+ .75
K0.....	26	.0199	.0185	.0193	+ .45
K1.....	22	.0184	.0196	.0190	+ .40
K2.....	14	.0157	.0161	.0159	+ .00
K3–K4.....	19	.0128	.0178	.0153	− .10
K5–M0.....	16	0.0122	0.0100	0.0111	−0.78

through the points. The desired mean absolute magnitude $\bar{M}$ is related to $M_{\overline{\pi}}$ by

$$\bar{M} = M_{\overline{\pi}} + 5(\overline{\log \pi} - \log \overline{\pi}) .$$

The reduction factor was determined from the estimated true dispersion σ_i of the parallaxes.[6] If σ_t is the accidental mean error of the parallax determinations and σ is the total dispersion of the unweighted means, the numerical values found were

$$\sigma_t = 0''.0119 , \qquad \sigma = 0''.0138 , \qquad \sigma_i = 0''.0070 ,$$

yielding $\bar{M} = M_{\overline{\pi}} - 0.15$.

The minimum in mean absolute magnitude near type G9 is in agreement with the general run of the luminosities of giants derived

[6] For the derivation of convenient formulae for the reduction see R. E. Wilson, *Ap. J.*, **90**, 360, 1939.

by Russell[7] from all available trigonometric parallaxes, although he did not find such a rapid rise in brightness for the late K's. The absolute values are about the same as those generally assigned to the giants, even though class III represents a narrower range of luminosities.

Classes II and IV.—These were treated in the same way as class III, with the exception that the small numbers of stars included made it necessary to take the means for all spectral types together. For the late K stars the values for classes II and II–III were raised slightly to keep pace with the increasing luminosity of the stars of class III.

Class I.—Since the supergiants are too remote to be reached by trigonometric parallaxes, it is necessary to fall back upon other methods of estimating their distances. The few direct determinations, mostly from the magnitudes of the companions to supergiants in binary systems, are listed below:[8]

α Per	F5	-4^m4	In the Perseus cluster
α UMin	F7	4.2	
ζ Aur	K0	3.4	
η Per	K2	4.8	
α Sco	K5+	−4.0	From diffuse nebulosity

Distance can also be estimated by a comparison of the star's radial velocity with the differential effect of galactic rotation, though the method is not as satisfactory for late types as for type B, since the data are sparse and the peculiar velocities are known to increase toward later spectral types. However, Greenstein[9] has recently been able to make a preliminary reduction of the velocities of 49 stars of types A8–M, finding $\bar{M} = -4.4$ with a mean error of about 1 mag.

The general agreement of the results suggests the adoption of -4^m5 for supergiants of all types later than F0. This value is consistent with the trigonometric absolute magnitudes for the stars of class II but is naturally subject to considerable uncertainty.

[7] *Op. cit.*, Table 4 on p. 411.

[8] This list is due to Morgan; see *Ap. J.*, **87**, 466, 1938.

[9] *Proc. Nat. Acad. Sci.*, **26**, 263, 1940.

The complete calibration table for converting luminosity classes to absolute magnitudes is given in Table 3. The absolute magnitudes are means for stars brighter than a given apparent magnitude and, since the field stars are selected in the same way, the table can be applied as it stands.

TABLE 3

REDUCTION OF LUMINOSITY CLASSES TO ABSOLUTE MAGNITUDES

Class	G3	G4	G5	G6	G7	G8	G9	K0	K1	K2	K3	K4	K5	K6	M0	No. of Stars
I	−4.5	−4.5	−4.5	−4.5	−4.5	−4.5	−4.5	−4.5	−4.5	−4.5	−4.5	−4.5	−4.5	−4.5	−4.5	49
II	−2.0	−2.0	−2.0	−2.0	−2.0	−2.0	−2.0	−2.0	−2.0	−2.1	−2.2	−2.3	−2.4	.....	−2.8	7
II–III	−0.8	−0.8	−0.8	−0.8	−0.8	−0.8	−0.8	−0.8	−0.8	−0.9	−1.0	−1.1	−1.2	.....	−1.8	11
III	+0.1	+0.2	+0.2	+0.2	+0.3	+0.4	+0.4	+0.4	+0.2	+0.0	−0.1	−0.4	−0.6	.....	−1.2	142
III–IV	+1.4	+1.5	+1.5	+1.5	+1.5	+1.5	+1.5	+1.5	+1.5	+1.5	+1.4	.....	.....	.....	.....	10
IV	+3.0	+3.1	+3.2	+3.3	+3.3	+3.3	+3.3	+3.3	+3.3	+3.3	.....	.....	.....	.....	.....	11
V	+5.0	+5.1	+5.2	+5.3	+5.5	+5.6	+5.8	+5.9	+6.1	+6.4	+6.8	+7.2	+7.7	+8.5	+9.3:	116

ACCURACY OF THE DATA

The mean error of an estimate from a single spectrogram is about ±1.3 tenths of a spectral class between G1 and G9 and ±0.4 between K0 and K5. The uncertainty of the absolute magnitudes varies somewhat with position in the reduction table, but, except for supergiants, the mean error of an estimate from one satisfactory spectrogram probably does not exceed $\pm 0^{m}.8$.

OBSERVATIONAL DATA

The observing program was planned to include about 140 stars near the plane of the Milky Way and a similar number in the direction of the galactic pole. The limit of apparent visual magnitude was set at 8.0 by the exposure times for the Bruce one-prism spectrograph on the Yerkes 40-inch telescope. With the Moffitt camera, giving a scale of 110 A/mm at $H\gamma$, exposures of roughly $1\frac{1}{2}$ hours were necessary on Agfa Super Plenachrome Press films for late K-type stars of the limiting magnitude, but the average exposure time for the program stars was of the order of half a hour.

The areas covered are specified in Table 4, the equatorial coordinates referring to 1900. In Cassiopeia the fields extend from 0° to −12° in galactic latitude and from 75° to 100° in galactic longitude. They were so chosen in order to avoid the conspicuous dark

absorbing clouds lying along the northern edge of the Milky Way in this constellation. At the galactic pole the fields were arranged to avoid the cluster in Coma Berenices.

The stars placed on the program were all those brighter than the eighth magnitude lying within these areas and having spectral types between G5 and K5, inclusive, in the *Henry Draper Catalogue*. Since the *Draper Catalogue* lists practically all stars brighter than $m_v = 8.25$, completeness of the sample at type Ko was assured.

TABLE 4

THE FIELDS OF OBSERVATION

Galactic Plane (Area, 237.5 Sq. Deg.)			Galactic Pole (Area, 501 Sq. Deg.)		
Field	Limits in α	Limits in δ	Field	Limits in α	Limits in δ
1....	0^h05^m to 0^h59^m	$+51°50'$ to $+59°30'$	1...	11^h02^m to 12^h02^m	$+29°45'$ to $+39°45'$
2....	0 59 to 1 58	51 00 to 61 00	2...	12 02 to 13 02	29 45 to 39 45
3....	23 02 to 0 05	48 15 to 58 15	3...	12 32 to 13 32	19 46 to 29 36
			4...	13 02 to 14 02	29 45 to 39 45

Altogether, 432 satisfactory spectrograms were taken and used in the classification of 278 stars. The slit width was kept constant for stars of all brightnesses; and, as far as possible, the spectrograms were treated uniformly in order to avoid systematic effects in the classification.

CLASSIFICATION OF THE SPECTRA

The procedure of classification was to assign first the spectral type of the star by direct comparison with an extensive set of spectrograms of standard stars. The luminosity differences were then estimated, and the sum was taken. Since all the spectrograms of the stars in both fields had previously been mixed together, the order of selection was entirely at random, and usually the identity of the star being classified was not noted until after the intensity estimates had been made. Later the results from duplicate spectrograms were combined, and means were taken after a careful comparison of the films.

After the intensity sums had been reduced to luminosity classes

and absolute magnitudes, distances were computed from the apparent magnitudes of the stars, allowing for interstellar absorption.

The correction for absorption was derived primarily from the photoelectric colors of B stars given in the most recent list of Stebbins, Huffer, and Whitford.[10] Fifty of the stars in their catalogue lie within our Cassiopeia field. The material was divided into two groups according to whether the galactic latitude was greater or less than 5°, and for each group the total visual absorption (taken as $6E_1$, where E_1 is the color excess on the photoelectric scale) was plotted against distance. In view of the large scatter of the points the variation of absorption with distance was estimated by forming normal points and by drawing the best smooth curve through them.

An independent check on the absorption was furnished by 11 of the field stars for which color indices on the International System had been measured here on Tikhoff plates with a mean error of about $\pm 0^m05$. The excesses over the normal colors for corresponding spectral classes and luminosities were multiplied by 4 to give total visual absorptions and were plotted against distances, which were all between 300 and 500 parsecs. For $b > 5°$ the straight line through the mean of the points indicated a visual absorption of 0^m54 in the first thousand parsecs, in satisfactory agreement with the value of 0.48 mag/kpsc derived from the photoelectric colors, considering the low weight of each determination.

On the assumption that the absorbing material is concentrated near the galactic plane, the correction curve for the galactic-pole field was drawn to start with the same slope for the first 100 parsecs as in the galactic plane and then to approach a limit of 0^m2 at 500 parsecs.[11]

The adopted corrections are shown in Table 5. That the size of the corrections in the Cassiopeia region is reasonable is suggested by Bok's discussion[12] of the absorption in the neighborhood of Selected Area 18, which lies within our field. His density analyses in this vicinity were carried out on the assumption that the rate of photographic absorption was either 0.5 or 1.0 mag/kpsc. It should

[10] *Ap. J.*, **91**, 20, 1940.

[11] See, e.g., Stebbins, Huffer, and Whitford, *Ap. J.*, **90**, 209, 1939.

[12] *Ap. J.*, **90**, 249, 1939.

be further noted that there appear to be patches of greater absorption along the northern part of this field, but it did not appear feasible to correct for them. Their effect will be to make the computed star densities slightly too low.

The catalogues of spectral types and luminosities for the two regions follow in Tables 6 and 7. In each table the columns are arranged in the following order: the number of the star in the *Henry Draper Catalogue*, the equatorial co-ordinates for 1900, the galactic latitude from the Lund tables, the apparent visual magnitude, the Henry Draper spectral type, the revised spectral type, the luminosity class, the visual absolute magnitude, and the distance in parsecs. The last column contains additional identifications, Mount Wilson spectroscopic absolute magnitudes and spectral types of those stars for which such data are available, and trigonometric absolute magnitudes for a few of the nearer stars. For a small number of stars which were found, on classification, to lie outside the range of types to be studied, only the spectral type is given. Several others from the original observing-list have been omitted because they were found to be definitely fainter than the eighth magnitude.

TABLE 5

TOTAL VISUAL ABSORPTION IN MAGNITUDES

DISTANCE (PARSECS)	CASSIOPEIA		GALACTIC POLE
	($b>5°$)	($b<5°$)	
100	0^m05	0^m07	0^m05
200	.11	0.16	.10
300	.16	0.24	.14
400	.22	0.32	.17
500	.27	0.40	.19
1000	.54	0.80	.20
1500	.73	1.11	.20
2000	0.82	1.29	0.20

Not quite all the stars on the program were observed. In Cassiopeia, 146 stars were classified out of a total of 165, and at the galactic pole 120 out of 139 were taken. Since care was taken to see that the stars left out were not systematically concentrated with

TABLE 6

CATALOGUE OF STARS IN THE NORTH-GALACTIC-POLE FIELD

HD Star	α 1900	δ 1900	b	m_V	HD Sp.	Y Sp.	Lum. Class	M_V	d (Parsecs)	Remarks
96496	11^h02^m1	+37° 19′	+67°	8^m0	K2	Ko	IV	$+3^m3$	77	
96677	03.1	36 31	68	7.30	Ko	G8:	III	+0.4	230	
96778	03.7	30 35	69	7.18	G5	G5	III	+1.0	170	
96921	04.5	33 04	69	7.26	Ko	K1	III–IV	+2.5	90	
97287	06.8	37 26	68	7.56	G5	Ko	III	+0.4	280	
97322	07.0	35 19	69	7.17	Ko	K1	IV	+3.3	60	
97371	07.3	36 22	69	7.9	Ko	K1	III	−0.5	460	
97438	08.0	33 59	69	6.75	Ko	K1	III:	+0.4	180	
98262	13.1	33 38	70	3.71	Ko	K3	III	−0.5	69	ν UMa, MW −0.1, K3
98317	13.4	36 02	70	6.94	Ko	K1	III	0.0	225	
98397	14.1	33 21	71	8.0	Ko	Ko	III	+0.4	310	
98500	14.8	30 40	71	7.42	K5	Mo	III	−1.0	440	
98746	16.7	35 53	71	8.0	Ko	K2	III	0.0	370	
98812	17.2	35 34	71	7.60	Ko	K2	III	−0.5	390	
99504	21.8	33 41	72	7.9	Ko	G8	III	+0.4	290	
99720	23.2	39 52	70	7.82	Ko	G8	III	+1.0	220	
100149	26.4	31 31	74	7.94	Ko	Ko:	III	−0.5	440	
100204	26.7	30 48	74	7.9	Ko	Ko	III	+0.4	290	
100235	26.9	36 47	72	6.56	Ko	Ko	III	+0.4	165	
100338	27.7	34 35	73	7.42	K2	K2+	III–IV	+2.5	150	
100470	28.6	37 23	72	6.33	Ko	Ko	III	0.0	180	S 3509
101151	33.3	34 12	74	6.36	K2	K2	III	−0.5	220	
101178	33.5	39 45	72	7.42	K5	M1:	III:	−1:	440:	
101501	35.7	34 46	75	5.46	G5	G6	V	+5.3	11	61 UMa, M_{trig} +5.6, MW +5.2, G6
101855	38.3	32 19	76	6.84	Ko	Ko−	III	−0.5	280	
102160	40.4	31 02	77	8.0	Ko	Ko	III	0.0	370	
102493	42.7	33 02	77	8.0	K5	K2	III	−0.5	460	
102686	44.3	30 03	78	7.56	Ko	G9	IV	+3.0	80	
102909	45.8	34 10	76	7.20	Ko	K1	I	−4.5	1990	
102941	46.0	37 23	75	7.8	Ko	K1	III	0.0	330	
103095	47.2	38 26	75	6.46	G5	G7p	V	+5.6	10	Groombridge 1830, M_{trig} +6.6, MW +6.3, G5
103520	50.1	39 19	75	7.07	Ko	K1:	III	−0.5	290	
103684	51.3	35 28	77	7.54	Ko	Ko	III	−0.5	350	
104017	53.6	38 26	76	8.0	K2	K3:	III	+0.5	290	
104075	54.1	33 43	79	6.02	Ko	K2−	III	−0.5	200	
104438	56.5	36 36	77	5.62	Ko	Ko	III	0.0	130	S 3613, M_{trig} +3.3 MW +0.5, K1
104862	59.5	36 07	78	7.52	Ko	K1	III	+0.2	270	
105341	12 02.7	30 58	81	8.0	K5	K5:	III:	0.0:	370:	
105424	03.2	30 49	81	7.78	K2	Mo	III	−0.8	480	
105586	04.3	30 01	82	7.81	Ko	K1	III	−0.5	420	
106365	09.1	33 20	81	6.78	Ko	Ko	III	+0.4	180	S 3671, MW +0.7, K3
106760	11.5	33 37	82	5.4	Ko	Ko	III:	+1.0	76	S 3687, MW +0.5, Ko
107341	15.4	38 28	78	6.67	Ko	Ko	III	0.0	200	S 3715, MW +0.7, G7
107485	16.2	38 35	78	7.40	Ko	K1	II	−3.0	1100	
107486	16.2	35 15	81	7.17	Ko	K1	III–IV	+1.5	135	
107634	17.1	33 39	81	7.9	Ko	G9	III	+0.4	290	
108078	19.9	31 35	85	7.66	Ko	Ko	IV	+2.5	105	
108174	20.5	38 54	78	7.64	Ko	K1	III	+0.4	260	
108225	20.9	39 34	78	5.22	Ko	G9	III	0.0	110	6 Can Ven, M_{trig} +2.5, MW +0.9, G4
108299	21.5	37 39	80	8.0	Ko	K3	III	−0.1	390	
109305	28.6	38 38	79	6.72	Ko	K1	III	−0.2	225	Hydrogen lines rather strong
109317	28.7	33 48	83	5.43	Ko	Ko	III–IV	+1.5	60	S 3799, MW +0.6, G7
109345	28.9	+33 57	+83	6.37	Ko	K1+	III	0.0	175	

TABLE 6—*Continued*

HD Star	α 1900	δ 1900	b	m_V	HD Sp.	Y Sp.	Lum. Class	M_V	d (Parsecs)	Remarks
109649	12h31m1	+32° 33′	+85°	7m46	K2	K3	III	−0m5	350	
110194	35.3	34 42	83	7.52	K2	K4	III	+1.0	190	
110501	37.5	34 14	84	6 62	Ko	Ko	IV	+3.3	46	
110788	39.4	28 32	89	8.0	Ko	G9	III–IV	+1.5	190	
110883	40.2	27 57	90	7.53	Ko	K2	III	0.0	290	
110987	40.9	38 55	79	8.0	Ko	F	.....	.....	.....	
110988	40.9	34 06	84	7.52	G5	Ko	III–IV	+1.5	155	
111254	42 9	23 16	85	7.8	K2	K2	III	0.0	330	
111255	42 9	22 11	84	7.8	Ko	K2	III	0.0	330	
111285	43.1	24 39	86	7.31	G5	G6	III	+1.0	180	
111318	43.4	30 56	87	7.74	Ko	G8	IV	+3.5	70	
111366	43.7	36 53	81	8 0	K2	K3:	III	−0.5:	460:	
111395	43 9	25 24	87	6 39	G5	K1	IV	+3.3	42	S 3864, M_{trig} +4.1, MW +4.9, G6
111483	44 5	35 52	82	7 9	Ko	K3	III	−0.1	370	
111541	44 9	26 58	88	6 89	Ko	Ko	III	+1.0	150	
111591	45.3	23 24	85	6.46	Ko	K1	III–IV	+1.5	96	
111628	45 6	36 15	82	8 0	K5	Mo	III	−0.5	460	
112127	49 1	27 19	88	7 10	K2	K1	III–IV	+1.0	160	
112234	50 1	20 10	82	6 69	Ko	K1	III	+0.2	180	
112353	51 0	32 32	85	6.93	G5	K1	III	−0.5	280	
112973	55 4	35 27	82	7 72	G5	K1	III	−0.5	410	
112989	55 5	31 20	85	5 08	Ko	G9p:	II–III:	−1.0:	160:	37 Comae, hydrogen lines strong, M_{trig} +1 1:, MW +0 1, G9
113021	55 7	32 18	85	6 72	G5	G6	III	+0.2	190	
113094	56 2	24 51	85	7 86	Ko	K1	III	+0.2	310	
113170	56 7	21 48	83	7 20	K5	K4:	III:	−0.6:	330:	
113320	57 8	23 30	84	7 99	Ko	Ko	III–IV	+1 0	230	
113380	58 2	23 44	84	7 54	Ko	K1	III	0.0	300	
113516	59 2	22 25	.....	7 76	G5	F	.....	.....	.....	
113771	13 00 9	27 07	85	7 8	Ko	K1	III	−0 5	420	
113996	02 4	28 10	85	4 90	K5	K4	III	−0.6	125	41 Comae, MW +0 2, K5
114037	02 7	27 03	85	7 60	Ko	K2:	III	−0.4	370	
114092	03 2	28 04	85	6 40	K5	K4	III	−0.4	220	
114093	03 2	25 21	84	6 90	Ko	G9	III	0.0	220	
114037	06 7	22 28	82	6 83	G5	G4	II–III	−1.0	340	
114724	07 3	24 48	83	6 46	Ko	K1	III	+0.2	170	
114744	07 4	37 27	.....	8 0	Ko	F8:	.....	.....	.....	
114819	08 0	20 28	80	7 42	Ko	K2	III	−0 5	350	
114976	09 0	30 20	83	7 9	Ko	Ko	III	−0 5	440	
115256	10 9	29 17	83	7 36	Ko	K1:	III	−0 4	330	
115927	15 2	36 54	78	7 68	G5	Ko	II–III	−1.0	480	
115968	15 5	38 42	77	7 91	Ko	G6	IV	+3.3	82	S 4007, M_{trig} +4 9
116204	17 0	39 25	76	7 22	K2	K1−	III	0.0	260	
116232	17 2	26 31	82	7 72	Ko	G7	III–IV	+2.0	135	
116287	17 6	30 49	81	6 92	Ko	K2+	III	0 0	220	
116288	17 6	21 14	79	7 56	Ko	K3	II–III	−1.5	570	
116515	19 0	26 04	81	7 38	Ko	G8	IV	+4 0	47	
117203	23 7	31 39	80	7 12	K2	K4	III	−0.6	320	
117555	26 0	24 44	79	7 96	G5	G5	III	+0 5	290	Weak lines
117730	27 1	27 08	.....	7 83	K5	M1:	.....	.....	.....	
117876	28 1	24 52	79	6 18	G5	Ko:	III	+0.4:	140:	S 4068
117893	28 2	31 16	79	7 54	Ko	K1	III	+0.2	280	
117981	28 9	34 10	78	6 80	Ko	K1	III	−0.4	250	
118234	30 4	21 19	77	8 0	Ko	G9	III–IV	+1.0	230	
118296	30 9	35 30	77	7 8	Ko	G7:	III:	0.0:	340:	
118670	33 3	23 02	77	7 05	G5	K1	IV	+2.5	80	
119035	35 8	31 31	77	6 08	G5	G5	II:	−2.0:	390:	
119914	41 1	35 10	75	7 52	G5	G9	III	0 0	300	
120048	42 0	39 00	73	6 00	Ko	K1	II–III	−1 0	230	
120164	42 7	39 03	73	5 57	Ko	Ko	III–IV	+1 5	65	S 4129, MW +0 6, G9
120245	43 2	38 23	73	7 10	K2	Ko	III	+0 4	210	
120364	43 9	+30 21	+76	8 0	Ko	Ko	III	0 0	370	

TABLE 6—*Continued*

HD Star	α 1900	δ 1900	b	m_V	HD Sp.	Y Sp.	Lum. Class	M_V	d (Parsecs)	Remarks
120420...	13^h44^m2	+31°41′	+76°	5^m81	Ko	Ko	III	-0^m5	175	S 4139, MW +1.0, G7
120531...	44.9	31 12	75	7.8	Ko	Ko	IV	+4.0	58	
120819...	46.7	35 10	74	6.00	Ma	Mo	III	−1.2	260	
120933...	47.4	34 57	74	4.96	Ma	K5	III	−0.8	140	
121212...	49.0	34 17	74	7.20	Ko	K4	III	−0.4	310	
121934...	53.5	33 05	74	7.9	Ko	Ko	III	−0.5	440	
122326...	56.2	39 31	70	6.70	K2	K3−	III–IV	+1.5	110	
122456...	56.9	32 02	73	7.06	Ko	K4	III	−0.8	350	
122517...	57.3	36 43	72	7.50	Ko	G7	IV	+2.0	120	
122968...	59.9	37 51	71	8.0	Ko	G7:	IV:	+3.3:	86:	
123351...	14 02.0	+31 20	+72	7.58	Ko	K1:	III	−0.5	390	

respect to either spectral type or apparent magnitude, the densities computed in the next section could be corrected by multiplying by the appropriate factor for completeness.

LUMINOSITY FUNCTION AND DISTRIBUTION OF THE STARS IN SPACE

The luminosity-spectrum diagrams for the two regions are shown in Figure 1. All the stars classified between types G3 and Mo are included; however, the material is essentially complete only for the range G7–K2. Among the stars later than K2, none was classified as a subgiant; this was true also of the calibration stars.

The distribution in distance of the individual stars is represented in Figure 2, in which distance from the sun is given by the vertical co-ordinate. In the horizontal direction the points are plotted at random between parabolas of the form $x = ay^2$, so that equal increments of volume in space are represented by equal areas in the figure. There was no room in the drawing to show the continuation of the bounds beyond 500 or 600 parsecs distance, but they should extend to infinity. For the first 100 parsecs they were replaced by straight lines in order to leave enough space to show the nearest observed stars.

In such a diagram uniform space density of stars would appear as uniform areal density of the plotted points; and since the two figures are drawn to the same scale, they may be compared directly. The limits of completeness for the different luminosity classes are defined as the distance of a star of the eighth apparent magnitude having

TABLE 7

CATALOGUE OF STARS IN THE CASSIOPEIA FIELD

HD Star	α 1900	δ 1900	b	m_V	HD Sp.	Y Sp.	Lum. Class	M_V	d (Parsecs)	Remarks
37	00 00^{m}3	+49°58′	−12°	8^{m}07	Ko	Ko	II–III	−0^{m}6	490	
58	00.4	52 37	9	7.30	Ko	K1	III	+0.2	250	
71	00.5	55 09	7	7.11	Ko	Ko	II–III	−1.0	360	
185	01.6	53 57	8	8.0	Ko	Ko	III	+0.4	300	
509	04.5	51 28	10	8.0	Ko	Ko	III	0.0	370	
516	04.6	50 52	11	8.0	Ko	K1:	III	−0.2	400	
638	05.6	56 25	5	7.7	Ko	K1	III	+0.2	280	
663	05.8	57 04	5	6.71	Ko	K1	III	−0.2	220	
697	06.3	59 13	2	8.0	G5	Ko	II	−2.0	750	
871	08.0	51 17	10	8.0	K5	K3	III	−0.1	380	
936	08.7	59 27	2	7.05	Ko	Ko	II	−1.5	410	
973	09.0	54 43	7	7.72	K2	K2:	III	−0.5	400	
1044	09.7	53 31	8	7.85	G5	G8:	II	−2.0	750	Hydrogen lines strong
1071	09.9	53 01	9	7.91	Ko	K1+	III	+0.1	340	
1427	13.3	52 23	9	7.9	Ko	K3+	III	+0.8	240	
1536	14.5	55 10	7	7.91	K2	K3	II	−1.0	490	
1598	15.2	56 00	6	6.79	G5	G1	III	.....	.....	
1811	17.4	54 05	8	7.30	G5	G8	I–II	−3.5	1110	Weak lines
1951	18.7	56 33	5	7.7	K2	K2	III–IV	+2.0	135	
2112	20.3	54 27	7	6.92	K2	K3	II	−3.0	810	
2152	20.6	54 56	7	7.32	Ko	K1	II	−2.0	590	
2506	23.7	58 55	3	7.8	G5	G8	III	+1.0	210	
2701	25.5	55 09	7	6.78	G5	K2	II–III	−0.8	290	
2774	26.2	52 17	9	5.69	Ko	K1	III	+1.0	86	S 128, MW +0.3, K2
2824	26.6	55 27	6	7.41	Ko	K1	III	+0.5	230	
2825	26.6	53 16	9	7.05	K2	K4	II–III	−1.0	380	
2826	26.6	52 28	9	7.8	K2	Ko	III	+0.4	280	
2900	27.2	54 43	7	8.0	Ko	G9	III	0.0	370	
2901	27.2	53 34	8	7.10	K2	K2p	III	0.0	250	4215 weak
2952	27.7	54 21	8	6.14	Ko	Ko	III	+0.4	135	
3027	28.5	54 23	8	8.0	Ko	Ko	III	0.0	370	
3250	30.6	56 45	5	7.60	K2	Ko	III	+0.4	250	
3345	31.3	54 25	8	7.26	K2	K4	III	−0.8	370	
3368	31.5	54 41	7	7.8	K2	G6:	III	0.0	340	
3409	31.9	58 37	3	8.0	Ko	Ko	III	+0.4	290	
3681	34.5	58 54	3	7.17	Ko	K1	III	+0.2	220	
3699	34.7	58 57	.....	7.57	K2	M1:	.....	.....	.....	
3712	34.8	55 59	6	2.47	Ko	K1	II–III	−0.8	45	α Cass, M_{trig} −2.3, MW −0.4, G7
3933	36.8	58 01	4	7.9	Ko	G5	III	+0.4	280	
4029	37.7	55 59	6	7.8	Ko	G9	III	+0.4	270	
4285	40.2	54 07	8	8.0	K2	K2−	III	−0.5	450	
4362	40.9	59 02	.....	6.49	G5	F9	I:	.....	.....	MW −1.7, cF9
5234	49.0	58 26	4	4.95	Ko	K2−	II–III	−1.0	140	υ^1 Cass, MW +0.1, K2
5258	49.2	56 44	5	7.90	K5	K5	III:	−0.8:	440:	
5395	50.7	58 38	3	4.83	Ko	G7	III–IV	+2.0	37	υ^2 Cass, M_{trig} +2.8, MW +2.6, G4
5430	51 0	56 57	5	7.9	Ko	K1	III	+0.5	270	
5477	51.5	52 46	9	7.95	Ko	K2	III′	+0.5	290	
5747	54.0	59 59	2	7.16	G5	G9:	III:	+1.0:	150:	S 284, MW +0.3, G8
5981	56.1	55 48	6	6.93	Ko	Ko	III	0.0	210	
6027	56.5	58 45	3	7.7	K2	K3	III–IV	+1.5	160	
6098	57.2	58 34	3	8.0	Ko	K2−	III	−0.5	430	
6147	57.5	58 23	4	7.03	K5	K4	III	−0.6	290	
6211	58.1	51 58	10	6.27	K2	K3	III	+0.5	140	
6238	58.3	56 35	5	7.10	Ko	G9	III	0.0	240	
6497	01 00.9	56 24	5	6.58	Ko	K1:	III–IV	+0.8	140	
6540	01.2	52 58	9	6.49	Ko	K2	III	−0.5	230	
6582	01.6	54 26	7	5.26	G5	G5	V	+5.3	10	μ Cass, M_{trig} +5.8, MW +5.4, G4
6634	02 □	+59 37	−2	8.0	G5	G9	IV	+2.5	120	

TABLE 7—*Continued*

HD Star	α 1900	δ 1900	b	m_V	HD Sp.	Y Sp.	Lum. Class	M_V	d (Parsecs)	Remarks
6810	01^h03^m7	+52° 20′	−10°	7^m8	K0	G8	III	0^m0	340	
6833	03.9	54 13	8	7.10	K0	K1	III	−0.4	290	
7010	05.4	59 58	2	7.9	K0	K0	III	0.0	340	S 357, MW +1.4, K0
7177	07.0	57 03	5	8.0	K5	K5	III	−1.0	510	
7416	09.2	59 59	2	8.0	K0	K1:	III	+1.0	220	
7444	09.5	51 12	11	7.55	K0	K2	III	0.0	300	
7587	10.8	55 58	6	8.0	K0	G7	III	−0.1	360	
7666	11.5	56 06	6	6.78	K0	K0	III	+0.4	160	
8365	17.8	53 50	.....	8.0	G5	G0	.....	.....	.....	
8372	17.9	58 25	3	8.0	K0	K0	III	+0.8	240	
8397	18.1	56 40	5	7.7	K5	K3	III	−0.5	380	
8654	20.3	52 36	9	7.69	G5	K0	III	+0.4	260	
8784	21.5	51 17	10	7.8	K0	K1:	III	+0.5	200	
8929	22.9	51 10	10	7.22	G5	K0	III–IV	+2.0	110	
8992	23.5	58 15	.....	7.6	G5	Late F	.....	.....	.....	
9022	23.8	59 16	2	7.25	K5	K2	III	−0.4	300	
9154	25.1	60 51	1	7.7	K0	K2	II	−2.5	710	
9352	27.0	57 49	4	6.0	K0, A0	K2	I	−4.5	900	S 453, MW −2.0, cK1
9354	27.0	55 18	6	7.31	K0	G8:	II:	−2.5:	630:	
9366	27.1	54 26	7	7.17	K5	K3p	I:	−4.5	1550	Strong hydrogen lines
9408	27.4	58 44	3	4.88	K0	K0	III	0.0	93	χ Cass, M_{trig} +1.3, MW +0.9, G6
9635	29.4	51 39	10	7.7	K2	K2	III	+0.5	400	
9839	31.0	54 33	7	7.62	K0	G5	II	−2.0	690	
9900	31.6	57 28	4	5.74	K0	K1	I	−4.0	650	S 476, MW −0.9, G9
10110	33.8	53 22	8	6.64	K2	K5	III	−0.6	250	
10181	34.5	53 04	8	7.58	K2	K3	II–III	−1.0	430	
10332	35.9	60 03	1	7.36	K2	K1+	II–III	−1.0	410	S 500, MW, −0.2, K1
10437	36.7	59 08	2	6.75	G5	K1	III	−0.5	250	
10498	37.3	51 01	10	6.80	K5	K4+	III	−0.8	300	
10680	39.2	59 14	2	7.78	K0	K1	II	−1.5	570	
10806	40.7	57 32	4	6.95	K0	K0	II	−2.5	600	
11103	44.1	56 17	5	7.9	K2	K2	III–IV	+2.0	140	
11544	48.3	56 05	.....	6.99	G5	F9	I	.....	.....	
11555	48.4	53 41	7	7.50	G5	K0	III	−0.5	370	
11658	49.3	51 11	9	7.25	K0	G9	III–IV	+2.5	88	
11716	49.9	60 45	0	8.0	K0	K3:	III	−0.6	440	
11773	50.4	51 59	9	7.7	K5	K1	III	+0.2	300	
11922	52.0	52 35	8	7.8	G5	G6:	III	−0.4:	400	
11996	52.7	59 31	1	7.7	K5	K4	III:	−0.8	420	
218416	23 02.8	52 17	7	6.26	K0	G9	III	0.0	180	
218766	05.5	49 27	10	7.41	K0	K0	III	+0.4	230	
218803	05.8	56 55	3	7.10	G5	G8	IV	+3.3	58	
219015	07.5	48 42	11	8.0	K0	K1+	III	+0.1	350	
219134	08.5	56 37	3	5.65	K2	K3	V	+6.8	6	S 7259, M_{trig} +6.5, MW +6.6, K5
219135	08.5	56 00	.....	7.6	G5	F8:	I	.....	.....	
219599	11.9	50 07	9	7.77	K5	K5	III	−0.6	430	
219901	14.4	54 00	6	7.7	K2	K5	III	−1.0	490	
220241	17.1	50 44	9	8.0	K5	K2	III	−0.5	450	
220274	17.4	48 15	11	7.45	K0	K0	III	+1.0	190	
220370	18.1	53 41	6	7.9	K2	K3	III	0.0	330	
220383	18.2	50 30	9	7.72	K2	K2	III	−0.5	400	
220444	18.7	51 33	8	8.0	K0	G4	II	−2.5	980	
220639	20.3	54 33	6	7.55	G5	K0	III	−0.5	370	
220653	20.4	55 35	5	7.61	K0	K2	III	−0.5	350	
220747	21.2	52 50	7	7.9	K5	K2	III	0.0	350	
220806	21.7	52 37	8	7.8	K5	K5	III	−0.6	430	
221023	23.5	50 49	10	7.7	K0	K2	III	0.0	310	
221124	24.2	53 07	7	7.10	K0	K0	III	0.0	240	
221168	24.6	54 36	6	7.8	K0	K1:	III:	+0.2:	300:	
221203	24.9	48 34	12	8.0	K0	K0:	III	+0.4	310	
221246	25.3	+48 36	−12	6.38	K2	K5	III	−0.6	230	

TABLE 7—*Continued*

HD Star	α 1900	δ 1900	b	m_V	HD Sp.	Y Sp.	Lum. Class	M_V	d (Parsecs)	Remarks
221378	23h26m6	+48° 58′	−10°	7m47	Ko	K1	III	+0m2	260	
221538	27.9	53 08	7	7.02	Ko	G6	III	+0.2	220	
221587	28.2	49 48	11	8.0	Ko	K1−	III	0.0	370	
221625	28.6	56 52	4	7.40	G5	G6	III	+0.6	210	
221863	30.6	51 44	9	7.02	Ko	Ko	III	0.0	230	
221913	31.0	50 43	10	7.22	Ma	Mo	III	+1.0	170	
222077	32.4	55 20	5	7.51	K5	K5–Mo	III	−1.0	430	
222154	33.1	52 16	8	7.9	K5	Mo	III	−1.2	580	
222218	33.6	58 06	3	7.22	Ko	G9	III	−0.5	290:	
222265	34.0	53 53	7	7.49	Ko	G9	III	+0.4	240	
222490	36.0	52 00	9	7.56	G5	G9	III	+0.4	250	
222618	37.1	56 43	4	6.33	G5	K1−:	III	−0.5	210	
222748	38.2	51 23	9	6.60	Ko	Ko	III	0.0	200	
222887	39.5	54 39	6	7.31	K2	K3	III	−0.5	330	
223046	41.1	50 07	11	7.62	Ko	G9	III	+0.4	260	
223165	42.1	58 06	3	5.09	Ko	K1	III	+0.2	90	τ Cass, MW +0.7, G9
223173	42.2	56 54	4	5.78	Ko	K3	II–III	−0.8	185	S 7430, MW −1.1, K3
223298	43.3	49 19	11	7.9	Ko	G9	II–III	−0.8	500	
223321	43.5	54 09	7	7.8	Ko	K4:	III:	−0.4:	400:	
223457	44.6	55 05	6	7.91	Ko	G9	III	−0.5	410	
223615	46.0	50 51	10	7.9	Ko:	G9	III	0.0	350	
223626	46.1	50 47	10	8.0	K2	K1	III–IV	+1.5	190	
223734	47.1	49 33	12	7.64	Ko	K2	III	−0.5	380	
223916	48.5	50 58	10	6.97	Ko	Ko	III	+0.4	200	
223969	49.0	55 56	5	7.48	K2	K4	III	−0.8	400	
224140	50.4	48 23	13	8.0	K2	K2	III	0.0	370	
224152	50.5	52 11	9	6.77	Ko	K2	III	−0.5	260	S 7474, MW +0.4, K3
224320	51.8	55 17	6	7.01	Ko	G8	II	−2.0	530	
224405	53.1	49 53	11	6.83	G5	G5	IV	+3.5	46	S 7488, MW +4.6, G2
224541	53.7	52 50	9	7.74	Ko	K1	III	+0.2	300	
224612	54.2	49 58	11	7.37	G5	G5	III:	−0.5	350	
224870	56.3	49 25	12	6.36	Ko	G7	II–III	−0.8	250	
224968	57.1	49 13	12	7.94	G5	Ko	III	−0.5	450	
225172	59.0	+49 19	−12	7.44	Ko	Ko	III	+0.4	240	

the faintest absolute magnitude included in the given class. Most of the stars in the class will have higher luminosities, and consequently a considerable proportion of those observed lie beyond the limit of completeness. The effect of absorption is apparent in the differences in these limits for the two regions.

Although the range of penetration into space is not sufficient to permit density gradients to be derived, comparison of the two figures brings out strikingly the galactic concentration of at least the more luminous stars. Out to about 200 parsecs the giants appear equally numerous in the two directions, but beyond this point they begin to thin out toward the galactic pole. More conspicuous are the differences for stars of classes I and II, but the presence of one star of each of these classes in the north-galactic-pole field shows that highly

luminous stars are to be found occasionally at distances of several thousand parsecs from the galactic plane.[13]

The supergiant in the north-galactic-pole field is HD 102909, of apparent magnitude 7.20, spectral type K1, and luminosity -4^m5. In each field two dwarf stars occur at such small distances that they scarcely show in Figure 2. In the north-galactic-pole field they are 61 UMa (G6) and Groombridge 1830 (G7p), and in the Cassiopeia

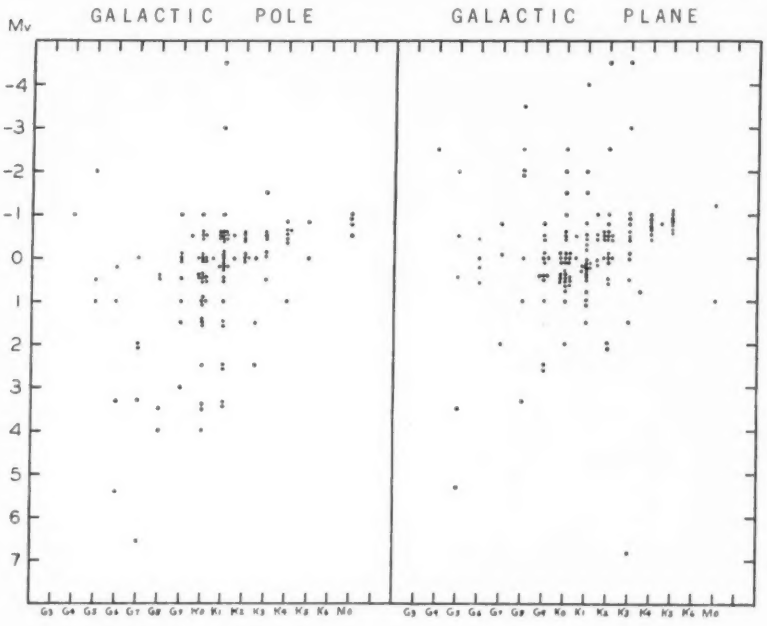

FIG. 1.—Luminosity—spectrum diagrams

field, S 7259 (K2) and μ Cas (G5). These are all well-known dwarfs with large trigonometric parallaxes.

The data of the catalogue of the Cassiopeia field are well suited to a determination of the luminosity function for types G7–K2 in the neighborhood of the sun. For this purpose the total number of stars in each luminosity class was divided by the volume of space corresponding to the distance of an eighth-magnitude star having the mean absolute magnitude of that class. The resulting relative num-

[13] Cf. Shapley, *Proc. Nat. Acad. Sci.*, **25**, 428, 1939.

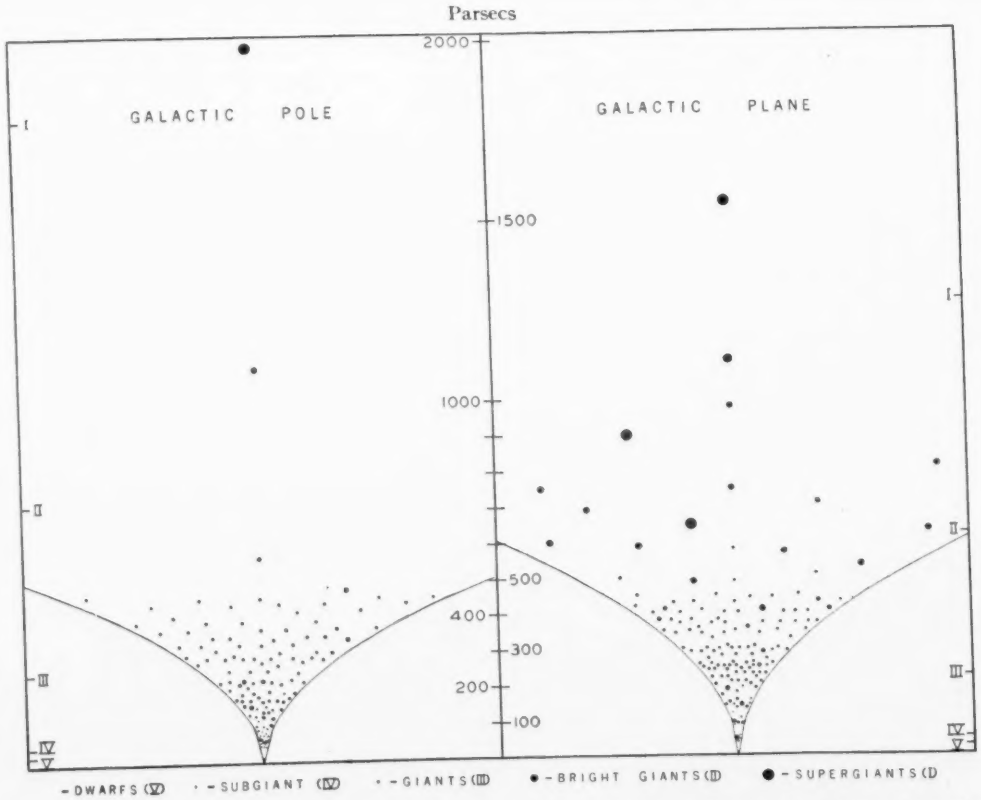

FIG. 2.—Distribution in distance of G4–Mo stars brighter than visual mag. 8.0. Distance from the sun is given by the vertical scale in the center. Limits of completeness are indicated at the edges.

bers of stars per unit volume were reduced to actual space densities by means of the giants, since class III was the only one containing enough stars within the limit of completeness to provide a significant value of the density. To a distance of 220 parsecs, 18 class III stars were counted in the Cassiopeia field. The volume of space was 2.57×10^5 cubic parsecs, and the completeness factor was 1.14, giving a density of 8.0×10^{-5} stars per cubic parsec. Since the fluctuations in so small a number may be considerable, a check was provided by the 56 giants within 320 parsecs, which gave the slightly lower density of 6.5×10^{-5}, as was to be expected.

The computed space densities for the different luminosity classes appear in the fifth column of Table 8. The mean absolute magni-

TABLE 8

SPACE DENSITIES IN CASSIOPEIA FOR STARS OF TYPES G_7–K_2

Luminosity Class	Range in Absolute Magnitude	Mean Absolute Magnitude	Number of Stars Observed	Stars per Cubic Parsec
I	−3.0 to −4.5	−3.8	3	2.2×10^{-8}
II	−1.5 to −3.0	−1.5	9	4.4×10^{-7}
III	+1.5 to −1.0	+0.8	85	8.0×10^{-5}
IV	+4.5 to +1.5	+3.5	7 15	1.1×10^{-4}
V	+6.5 to +5.5	+6.0	1 1	.....

tudes for each luminosity class, tabulated in the third column, were computed with weights based upon the luminosity function itself and are averages referred to a given volume of space. Their uncertainty may be several tenths of a magnitude. In classes IV and V the observed stars were so close to the sun that the data of the north-galactic-pole field could safely be included also. In the last two rows of the fourth column the upper numbers refer to the north-galactic-pole field and the lower numbers to the Cassiopeia field. The density for class IV is a mean from the two fields, each of which gave almost the same value. For class V the density is omitted because of the scantiness of the data.

For comparison with determinations from other sources the densities were next divided by the range in luminosity included within

each class. The logarithms of the resulting numbers of stars per cubic parsec per interval of one absolute magnitude are plotted as ordinates in the graphical representation of the luminosity function in Figure 3. Here the density for class V was included merely to show that the observed number of dwarfs was consistent with the number to be expected from our relatively complete knowledge of the stars within a few parsecs of the sun. The cross in the diagram,

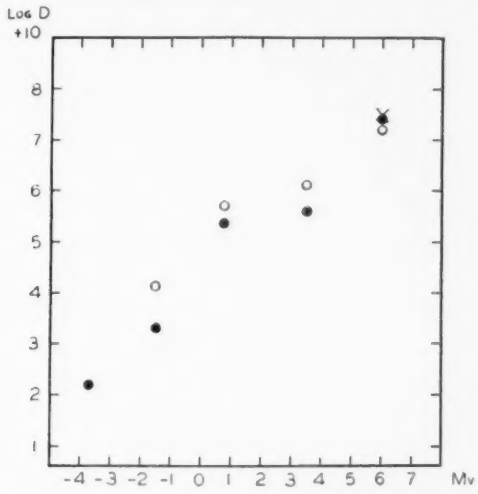

FIG. 3.—Luminosity function for G7–K2 stars with apparent magnitude brighter than 8.0 (filled circles). Logs of space density are plotted as ordinates. Open circles represent Gratton's data. The cross shows the frequency of dwarfs indicated by Luyten's table.

which is almost coincident with the filled circle at $M_v = 6.0$, represents the density derived from Luyten's luminosity function for stars of all types within a radius of 5 parsecs,[14] on the assumption that all stars in his table with absolute magnitudes between +5.5 and +6.5 were main-sequence stars of types G7–K2.

The open circles in the diagram represent corresponding points on the luminosity function for stars of Henry Draper classes K0 and K2 derived by L. Gratton[15] from proper motions and radial velocities. Thus his range in spectral type is similar, though not identical, to that of the present study. For comparisons with other luminosity

[14] *Pub. U. Minnesota Obs.*, **2**, No. 7, 123, 1939. [15] *B.A.N.*, **6**, 85, 1933.

functions based upon proper motions reference should be made to the discussion in Gratton's paper, but the essential point is that Gratton found a density increasing continuously toward lower luminosities, without any indication of the minimum between the giants and dwarfs which had been suggested by the earlier results of Strömberg and others. The confirmation of the general course of Gratton's curve by the present data, which provide a completely independent and more direct determination, is evidence of the freedom from systematic errors of the method of proper motions.

That the subgiants at K0 are actually more numerous than the giants appears now to be established, but the accuracy of the spectroscopic parallaxes is not sufficient to define the finer structure of the luminosity function—at least not until much richer material is at hand. The apparent absence of subgiants of types later than K2 and the very small dispersion in the luminosities of the late K dwarfs suggest that the luminosity function is changing rapidly in this spectral range and probably possesses a minimum between the giants and the main sequence. This point can probably be best investigated by measuring trigonometric parallaxes of all subgiants and dwarfs within 40 or 50 parsecs, the stars having been selected by means of low-dispersion spectrograms.

The spectroscopic luminosity curve is of greatest value at the high-luminosity end in spite of the few stars included, for these stars are at distances such that parallaxes determined by other methods are extremely uncertain. The density observed for the supergiants is probably slightly too low, for the volume of space surveyed extends to a height of about 300 parsecs above the galactic plane at a distance of 1500 parsecs, and the mean space density is presumably less than that characteristic of galactic latitude zero.

The apparent vertical displacement of the two curves in Figure 3, amounting to a ratio of about 3 in the densities, may be due in part to the different spectral ranges involved and to the presence of the absorption patches mentioned previously, but it is possible that the space density in Cassiopeia is less than the average for the Milky Way. This is suggested by the survey of four galactic fields by Schalén,[16] who separated giants and dwarfs by the cyanogen criterion

[16] *Upsala Medd.*, No. 55, 1932.

applied to slitless spectrograms. Schalén's space densities for giants of Henry Draper types G5 to K2 should be roughly comparable to the values in the fifth column of Table 8, although his inclusion of stars of classes I and II among the giants should raise his densities by about 10 per cent as compared to our value for class III. For the mean of four fields in Cygnus, Cepheus, Cassiopeia, and Auriga he found 2.1×10^{-4} giants per cubic parsec to a distance of about 200 parsecs, after a factor of 1.1 had been applied to correct for interstellar absorption. For his Cassiopeia field alone, which partially overlaps the one observed here, the density was 1.2×10^{-4}, about half the mean of the other three.

I am indebted particularly to Dr. Morgan for his many suggestions in regard to this program and for the opportunity of making use of his extensive collection of spectrograms of bright stars. Mr. F. R. Sullivan took part in all the observations at the telescope.

YERKES OBSERVATORY
January 1940

THE DISTRIBUTION OF COLOR IN SPIRALS*

CARL K. SEYFERT

ABSTRACT

This investigation is based on a photometric study of red- and blue-sensitive plates of the seven spirals, NGC 598, 891, 2403, 3031, 4631, 5194, and 5457. The plates, calibrated by means of exposures with a tube sensitometer, have been measured in two photometers and by means of recording-microphotometer tracings across the principal axes of the spirals. These plates, taken with the Yerkes 24-inch reflecting telescope, have been supplemented by red-, yellow-, and blue-sensitive plates taken with the 82-inch reflector of the McDonald Observatory and with a 6-inch refractor.

The results show that the nebulous condensations in the arms of the spirals have red indices close to 0^m0 and are considerably bluer than the spiral nuclei. The spirals appear to have a general background intensity which decreases smoothly outward from the nucleus and on which the arms seem to be superimposed. This background is of approximately the same color as that of the nucleus. The color of the arms alone is blue, of red index close to 0^m0, and hence they are approximately of the same color as that of the individual condensations. The colors of emission nebulae in the spirals is discussed, and the anomalies in the blue-yellow color indices of emission nebulae suggest a rapid method of detecting such objects in extragalactic nebulae. Measures of the distribution of color in one dark-lane spiral (NGC 891) give no indication of reddening within the dark lane.

From an examination of photographic and photovisual plates F. H. Seares[1] in 1916 showed qualitatively that the nebular condensations in the arms of the spirals M 51, M 94, and M 99 were much bluer than the nuclear regions. This problem was investigated photometrically by E. F. Carpenter,[2] who confirmed the results of Seares for M 51. Carpenter showed that the knots or nebular condensations in this spiral were as blue as -0^m3, whereas the color index near the nucleus was $+0^m6$. The color of the nucleus was estimated as $+1^m6$, a value which Carpenter considered uncertain.

The present paper contains a reinvestigation of this problem for a number of spirals, using principally blue-red color indices instead of blue-yellow (referred to hereafter as "red indices" and "color indices," respectively). Not only have the surface brightnesses of the nebulous *condensations* relative to the nuclear regions in the two colors been determined, but the distribution of color of the *general background* in several spirals has also been investigated. The scale

* *Contributions from the McDonald Observatory, University of Texas*, No. 20.

[1] *Proc. Nat. Acad. Sci.*, **2**, 553, 1916. [2] *Pub. A.S.P.*, **43**, 294, 1931.

of both magnitude systems has been established by means of sensitometric exposures impressed on the plates. For most of the spirals an attempt was made to establish the zero point of the color system as well. However, the chief aim of the investigation has been to determine the *differences* between the colors of various parts of the same spiral.

I. THE PLATE MATERIAL

Two red-sensitive and two blue-sensitive plates were obtained on each of the following objects: NGC 598, 891, 2403, 3031, 4631, 5194, and 5457. The plates were taken with the Yerkes 24-inch aluminized reflector (focal length, 93.5 inches). The red-sensitive plates, Eastman 1-C Special emulsion, were exposed behind a Wratten No. 28 red filter for approximately 60 minutes each. The blue-sensitive plates, Eastman 1-O emulsion, were exposed without filter for approximately 30 minutes each. The effective wave length of the red plate and filter combination is approximately λ 6300; that of the blue-sensitive plates about λ 4250 for dwarf G5 stars. The latter value was determined by the author from objective grating plates of the Pleiades taken with the 24-inch reflector. Additional red-sensitive films (Agfa Super Pan Press and Wratten No. 29 filter), yellow-sensitive plates (Eastman 1-G emulsion and Wratten No. 8 filter), and blue-sensitive plates (Eastman 1-O emulsion) were taken of NGC 5194 and 5457 with the 82-inch reflector of the McDonald Observatory for the purpose of checking the accuracy of the results obtained from the smaller-scale Yerkes 24-inch reflector plates.

Each plate was standardized by means of an exposure of approximately 30 seconds made with a tube sensitometer. The same filters employed at the telescope were used for the standardizing exposures, which were impressed on the sky-fog background of the plates. Since the average exposures on the nebulae were much longer than the sensitometric exposures, it was necessary to investigate possible changes of the slope of the characteristic curve of the plates as a function of time of exposure. Accordingly, plates of all emulsions used were exposed in the tube sensitometer for intervals varying from 20 seconds to 1 hour. The resulting densities were kept approximately constant for the long and short exposures by using neutral screens and by varying the distance of the light source from the

plate. It was found that the characteristic curves were so nearly identical for the long and short exposures that no correction was necessary.

II. THE RELATIVE COLORS OF KNOTS AND NUCLEUS FOR FIVE SPIRALS

Eight to ten of the brightest and largest nebular condensations were measured on the plates of each of the spirals NGC 598, 2403, 4631, 5194, and 5457. For all but NGC 4631, the nucleus of each spiral was measured also. In the case of NGC 4631, a spiral seen edge on and in which no well-marked nucleus is visible, the nucleus of the small companion nebula, NGC 4627, was measured instead. These plates were measured in the Ross photometer[3] of the Yerkes Observatory, using a diaphragm which produces a beam at the plate of 0.22 mm diameter, or 19″ on the scale of the 24-inch reflector plates. The plates were remeasured in the McDonald photometer[4] with a diaphragm producing a beam of only 11″, considerably smaller than any of the features measured. The plates taken with the 82-inch reflector were also measured in the McDonald photometer. The relative surface brightnesses of the nucleus and knots of each object were determined by means of the sensitometric exposures on each plate. The determination of the zero point of the colors of the knots in each object will be discussed in Section IV.

Since the standardizing exposures were impressed on the sky fog of the plates, only small corrections for the variation in the general fog background had to be made. It was necessary, however, to make substantial corrections for the fact that the measured intensity of each knot represents a combination of the brightness of the knot plus the brightness of the arm, or the general background intensity of the spiral in which it is situated. Hence measures were made of the intensity of the arm in the vicinity of each knot and subtracted from the intensity of knot plus arm to give a measure of the brightness of the knot alone. No similar corrections were made for the measures of the nucleus. The accuracy of the results in some cases is reduced considerably by these background corrections. Magni-

[3] For a description of this instrument see *Ap. J.*, **84**, 241, 1936.

[4] A description of this instrument may be found in *Ap. J.*, **91**, 117, 1940.

tudes of knots for which the correction for background is unusually large have been indicated in the tables by a colon.

The final mean values of the blue and red magnitudes and colors are listed in Tables 1–5. Successive columns give (1) the designation of the knot; (2 and 3) the X and Y co-ordinates of the knots

TABLE 1

POSITIONS AND COLORS OF THE KNOTS IN NGC 598 (M 33)

(1) Knot	(2) ΔX	(3) ΔY	(4) Δm_{pg}	(5) Δm_{red}	(6) ΔR.I.	(7) R.I.	(8) Spectrum
1 (NGC 588)	−843″	− 43″	+1^{m}32	+1^{m}85	−0^{m}53	+0^{m}37	Emission
2	−644	−530	+1.20	+1.90	−0.70	+ .20	Emission
3	−502	−978	+1.43	+1.91	−0.48	+ .42	Emission
4 (NGC 595)	−223	+118	+0.96	+1.40	−0.44	+ .46	Emission
5	−211	−339	+1.20	+2.36:	−1.16:	− .26:	
6	+ 62	+356	+1.15	+1.45	−0.30	+ .60	
7	+ 93	−389	+0.97	+2.12:	−1.15:	− .25:	
8	+316	−140	+1.28	+2.13	−0.85	+ .05	Emission
9 (NGC 604)	+537	+452	+0.04	+0.35	−0.31	+0.59	Emission
Mean R.I.	+0^{m}24 ± 0.07 (p.e.)						

TABLE 2

POSITIONS AND COLORS OF THE KNOTS IN NGC 2403

(1) Knot	(2) ΔX	(3) ΔY	(4) Δm_{pg}	(5) Δm_{red}	(6) ΔR.I.	(7) R.I.
1	−195″	+ 51″	+0^{m}85	+1^{m}44	−0^{m}59	+0^{m}21
2	−136	−145	+1.55	+2.18	−0.63	+ .17
3	− 80	+ 17	+1.23	+2.34	−1.11	− .31
4	− 37	+ 47	+0.91	+1.59	−0.68	+ .12
5	+ 6	+ 34	+1.27	+2.04	−0.77	+ .03
6	+ 39	+ 72	+1.92:	+2.75:	−0.83:	− .03:
7	+ 65	− 15	+2.33:	+2.57:	−0.24:	+ .56:
8 (NGC 2404)	+ 97	+ 28	+0.60	+1.37	−0.77	+ .03
9	+157	−249	+1.16	+1.93	−0.77	+ .03
10	+175	− 27	+1.55	+1.91	−0.36	+0.44
Mean R.I.	+0^{m}12 ± 0.05 (p.e.)					

relative to the nucleus; (4 and 5) the magnitude of the knot *minus* the magnitude of the nucleus for blue and red light, respectively;

(6) the red index of the knot relative to the nucleus (i.e., col. 4 *minus* col. 5); and (7) the red index of the knot (determined from col. 6 after the zero point of the color scale was established; cf. Sec. IV).

TABLE 3

POSITIONS AND COLORS OF THE KNOTS IN NGC 4631
(Both Relative to the Companion Nebula NGC 4627)

(1) Knot	(2) ΔX	(3) ΔY	(4) Δm_{pg}	(5) Δm_{red}	(6) ΔR.I.	(7) R.I.
1	−248″	−148″	+0^{m}81	+1^{m}58	−0^{m}77	+0^{m}03
2	−179	−141	+ .96	+1.60	− .64	+ .16
3	−140	−141	+ .93	+1.38	− .45	+ .35
4	− 54	−133	+ .23	+1.06	− .83	− .03
5	+ 78	−145	+ .81	+1.27	− .46	+ .34
6	+148	−116	− .34	+0.34	− .68	+ .12
7	+218	−103	+ .83:	+1.42:	− .59:	+ .21
8	+282	−111	+0.96:	+1.65:	−0.69:	+0.11
Mean R.I.	+0^{m}16 ± 0.03 (p.e.)					

TABLE 4

POSITIONS AND COLORS OF THE KNOTS IN NGC 5194 (M 51)

(1) Knot	(2) ΔX	(3) ΔY	(4) Δm_{pg}	(5) Δm_{red}	(6) ΔR.I.	(7) R.I.	(8) ΔC.I.
1	−102″	− 5″	+1^{m}69	+2^{m}37	−0^{m}68	+0^{m}32	−0^{m}65
2	− 90	− 82	+1.30	+2.13	− .83	+0.17	− .99
3	− 83	−108	+1.19	+1.95	− .76	+0.24	− .80
4	− 61	−127	+1.97	+2.71	− .74	+0.26	− .61
5	+ 20	+ 26	+1.11	+1.84	− .73	+0.27	− .69
6	+ 64	−155	+2.07	+2.93	− .86	+0.14	− .41
7	+ 97	+ 80	+1.65	+2.17	− .52	+0.48	− .55
8	+103	−118	+1.75	+2.51	− .76	+0.24	− .74
NGC 5195	+ 72	+266	+0.19	+0.08	+0.11	+1.11	+0.12
Mean R.I. for knots	+0^{m}26 ± 0.02 (p.e.)						

The mean of the red indices of the knots is given at the bottom of the table, together with the probable error of this average value. The values given for NGC 5194 and 5457 include the measures obtained from the red and blue plates taken with the 82-inch reflector.

In the tables of the measures of these two spirals, an eighth column is also included, which gives the *color indices* of the knots relative to the nucleus as determined from the photographic and photovisual plates taken with the McDonald reflector. An additional column is added for NGC 598 and 5457, to denote whether the knot is a known emission nebula. These last data are taken from the papers of E. Hubble,[5] N. U. Mayall and L. H. Aller,[6] and C. K. Seyfert.[7] The positions of the knots measured in each object are also indicated by arrows in Plates VII–IX.

TABLE 5

POSITIONS AND COLORS OF THE KNOTS IN NGC 5457 (M 101)

(1) Knot	(2) ΔX	(3) ΔY	(4) Δm_{pg}	(5) Δm_{red}	(6) ΔR.I.	(7) R.I.	(8) ΔC.I.	(9) Spectrum
1 (NGC 5447)	−391″	−262″	+0^m.77	+1^m.49	−0^m.72	+0^m.07	−0.57	Emission
2 (NGC 5447)	−378	−277	+0.97	+1.86	− .89	− .10	−0.77	Emission
3 (NGC 5453)	−143	−145	+1.16	+2.10	− .94	− .15	−0.83	
4 (NGC 5455)	−103	−387	+0.65	+1.42	− .77	+ .02	−0.50	Emission
5	− 92	− 51	+1.46	+2.26	− .80	− .01	−1.10	
6 (NGC 5458)	− 4	−181	+1.23	+2.22	− .99	− .20	−0.97	
7 (NGC 5461)	+250	−113	+0.60	+0.96	− .36	+. 43	−0.20	Emission
8 (NGC 5462)	+346	+ 50	+1.20	+1.92	− .72	+ .07	−0.45	Emission
9 (NGC 5462)	+359	+ 68	+1.00	+1.81	− .81	− .02	−0.64	Emission
10 (NGC 5471)	+670	+170	+0.39	+0.97	−0.58	+0.21	−0.20	Emission
Mean R.I.	+0^m.03 ± 0.04 (p.e.)							

The red indices of the knots in NGC 5194 and 5457, as measured from the plates taken with the 82-inch reflector, average 0^m.12 bluer than those obtained from the 24-inch reflector plates. This systematic difference between the two sets of plates is small enough to give confidence in the measures from the smaller-scale plates from which most of the material was obtained.

The accidental errors of measurement are as follows: the probable error of a magnitude obtained from one photographic plate is ±0^m.10; the probable error of a magnitude determined from a single red- or yellow-sensitive plate is ±0^m.12. Since the published measures are the mean of at least two plates, the probable error of a final color is ±0^m.11.

[5] *Ap. J.*, **63**, 236, 1926. [6] *Pub. A.S.P.*, **51**, 112, 1939. [7] *Ap. J.*, **91**, 261, 1940.

III. THE DISTRIBUTION OF COLOR ACROSS THE MAJOR AXES OF FIVE SPIRALS

Tracings across the major and minor axes of the five spirals NGC 598, 891, 3031, 5194, and 5457 were obtained by means of the recording microphotometer of the Yerkes Observatory. The measures were made at intervals of 1 or 2 mm on the tracings, corresponding to intervals of 0.1 and 0.2 mm on the plates. Various slit sizes were used for the different spirals, ranging from 2″ to 6″ in width and from 6″ to 45″ in length. The standardizing exposures on the plates made it possible to reduce the measures to a magnitude scale with an arbitrary zero point.

Since the nuclear regions of NGC 3031 and 5194 were too strongly exposed for measurement in the microphotometer, four additional plates of short exposure (two red-sensitive and two blue-sentitive plates) were obtained and measured as indicated above. The blue plates were exposed for 5 minutes and the red plates for 10 minutes. Measures on the tracings of these short-exposure plates gave the distribution of brightness around the nucleus. For a number of points in these spirals, measures could be made on both long- and short-exposure plates, thus making it possible to combine the two sets of measures. The region of overlap is approximately $1^m.0$ for each spiral. The accuracy with which the two sets of measures agree is illustrated in the diagrams of the measures (Fig. 2).

The probable error of a single photographic or red magnitude determination is $\pm 0^m.06$, and hence that of a single red index is $\pm 0^m.09$. Since the published values are the mean of two plates, the probable error of a final red index is $\pm 0^m.06$.

The measures are given in the form of diagrams, Figures 1–3, inclusive. The ordinates are magnitudes with an arbitrary zero point, and the abscissas are the distances in millimeters from the nucleus as measured on the plates. Each curve gives the mean intensity distribution determined from two plates, the upper curve from blue-sensitive plates and the lower curve from red-sensitive plates. At the bottom of each figure are the curves representing the distribution of red index (also with an arbitrary zero point) across the axes of the spiral. The red index of the nucleus is indicated by a horizontal line. On the page opposite each set of curves are given two photographs of

PLATE VII

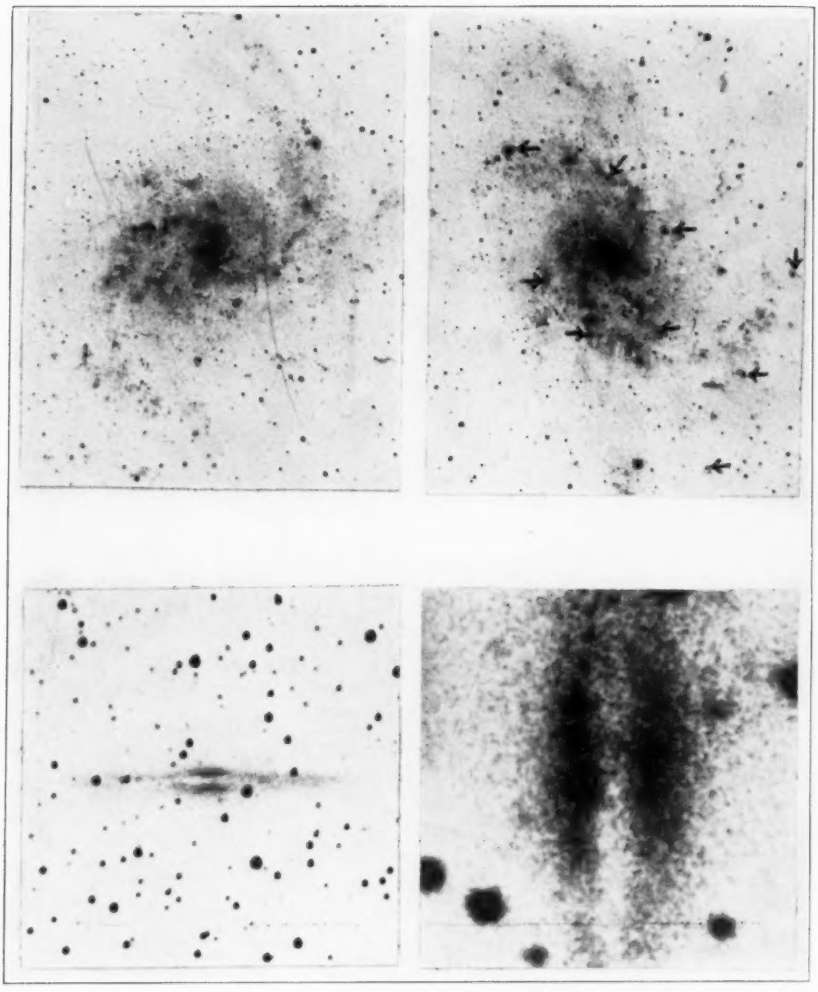

PHOTOGRAPHS OF NGC 598 (*a* AND *b*) AND OF NGC 891 (*c* AND *d*)

The intensity measures given in Figure 1 correspond to horizontal diameters of objects on the plates shown above; the horizontal scales are the same. Nebular condensations measured in NGC 598 have been indicated by arrows in *b*.

UNIV. OF MICH.

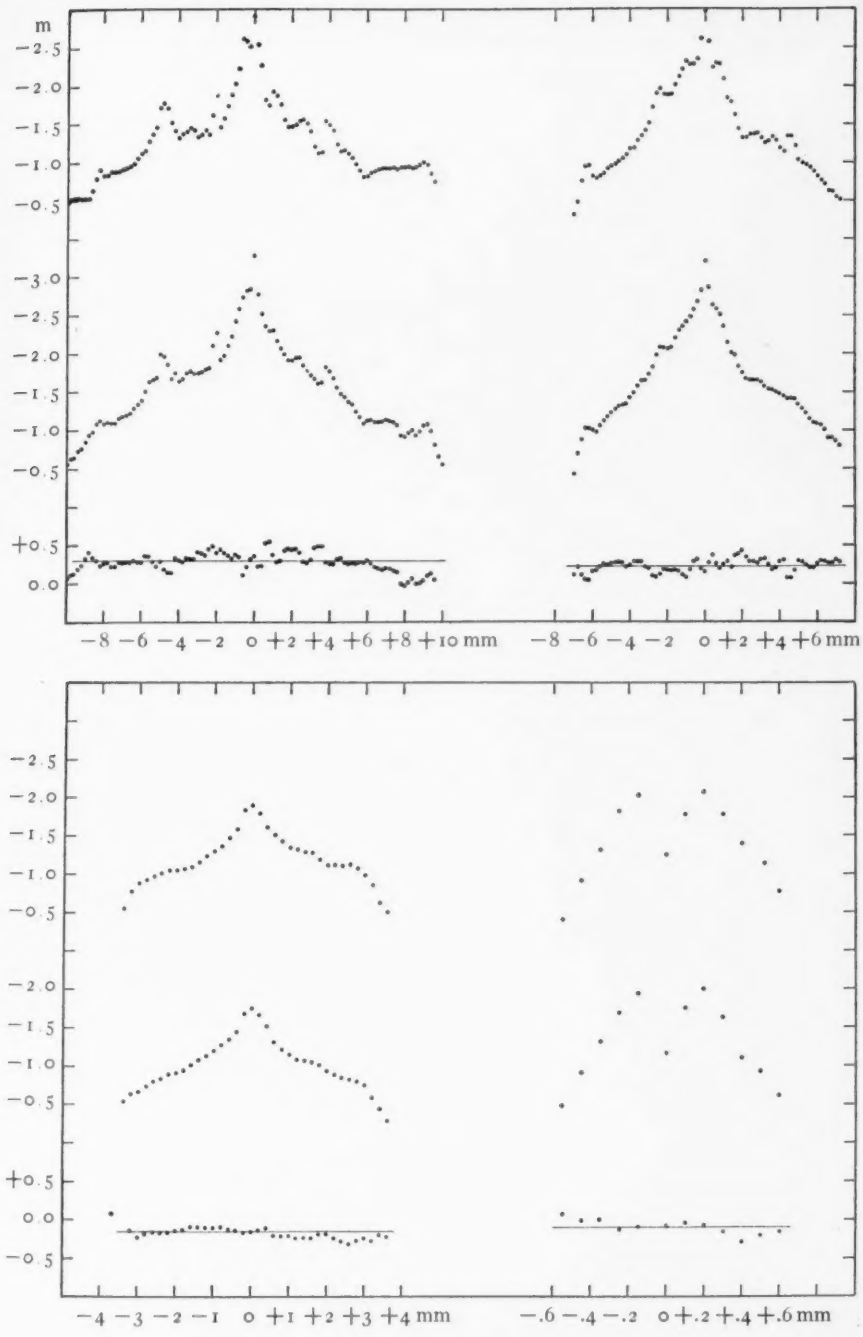

FIG. 1.—Measures of distribution of intensity and red index in NGC 598 (*upper*) and NGC 891 (*lower*). Measures along the major axis (north-south axis for NGC 598) are on the left, and along the minor axis (east-west axis for NGC 598) are on the right.

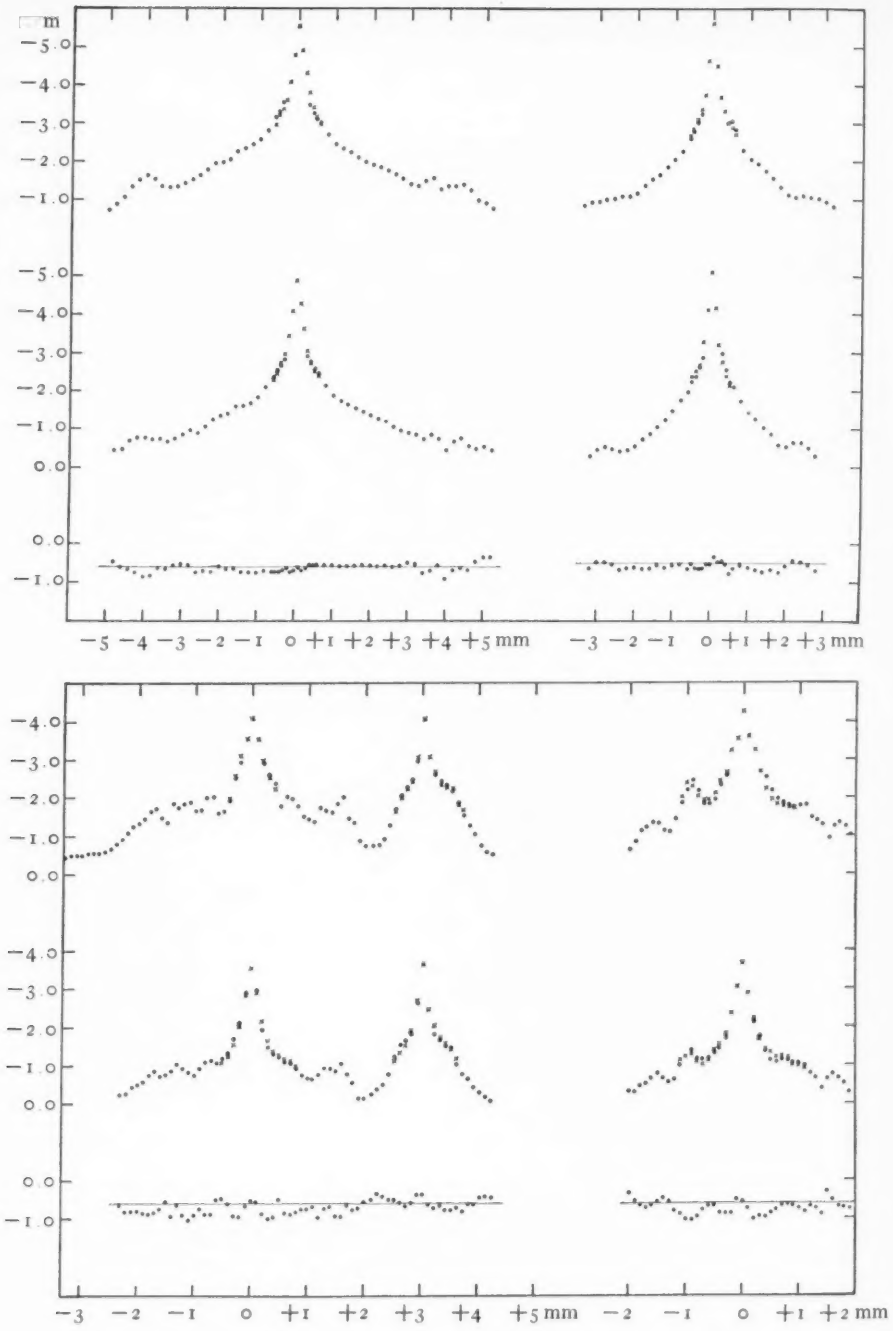

FIG. 2.—Measures of distribution of intensity and red index in NGC 3031 (*upper*) and NGC 5194 (*lower*). Measures along the major axis are on the left, and those along the minor axis are on the right. Filled circles represent measures from long-exposure plates, and crosses from short-exposure plates.

PLATE VIII

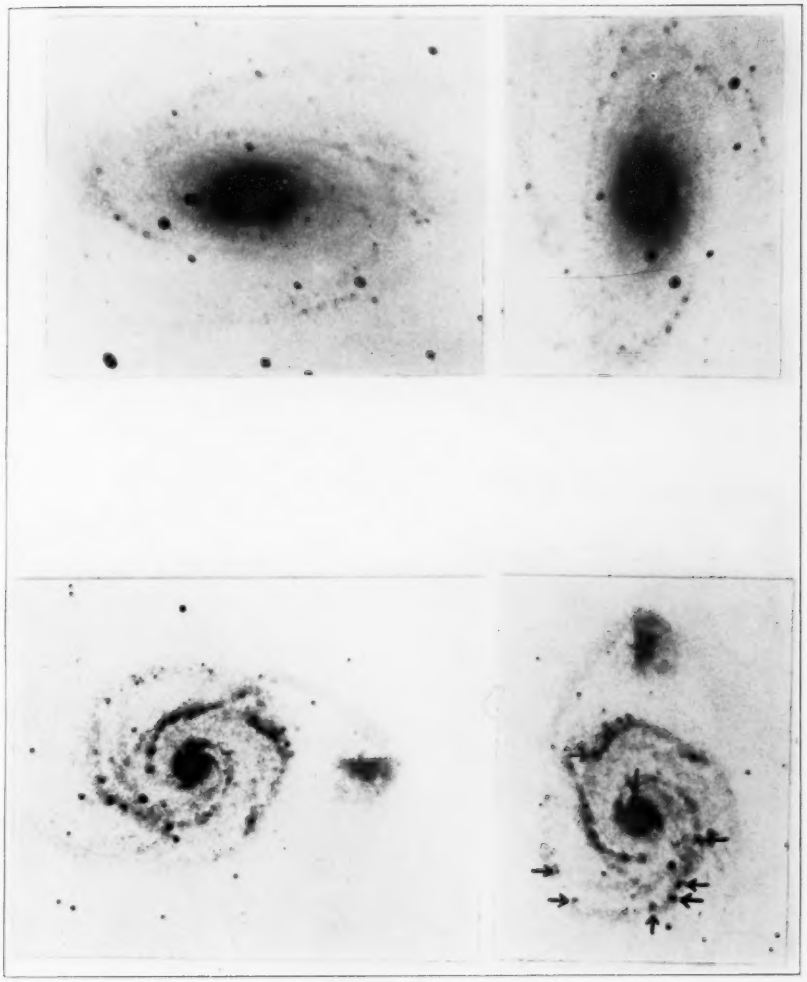

PHOTOGRAPHS OF NGC 3031 (*a* AND *b*) AND OF NGC 5194 (*c* AND *d*)

The intensity measures given in Figure 2 correspond to horizontal diameters of objects on the plates shown above; the horizontal scales are the same. Nebular condensations measured in NGC 5194 have been indicated by arrows in *d*.

UNIV. OF MICH.

PLATE IX

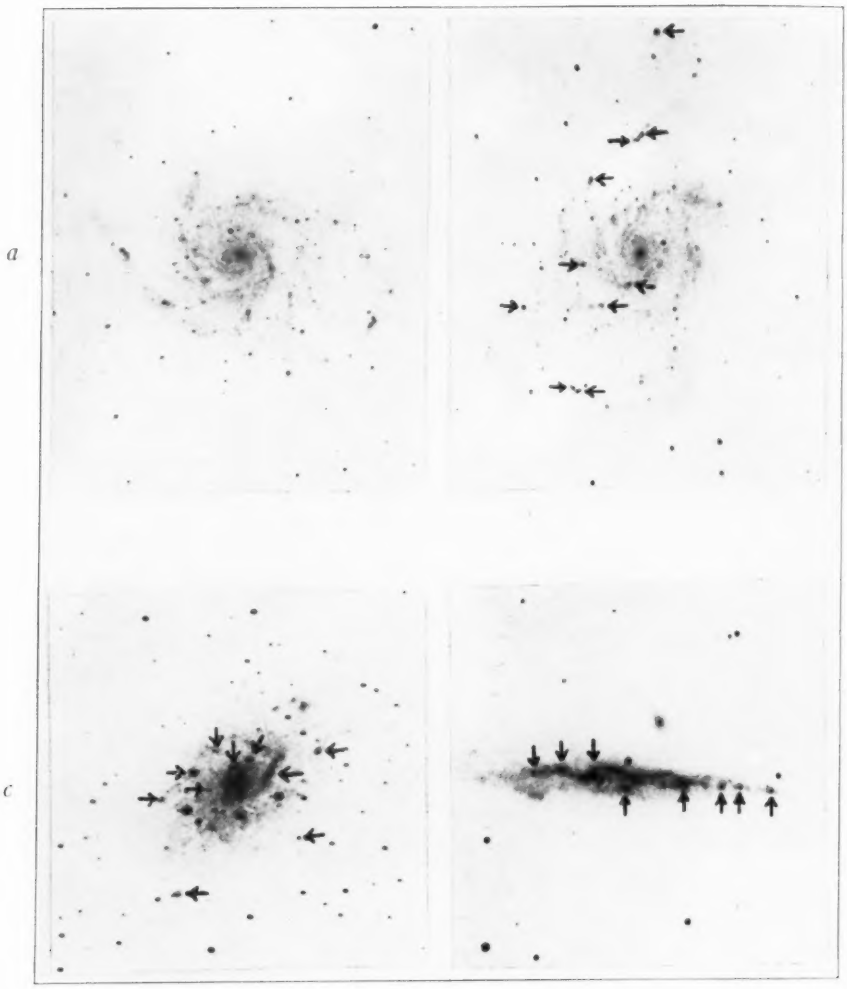

PHOTOGRAPHS OF NGC 5457 (*a* AND *b*), NGC 2403 (*c*), AND OF NGC 4631 (*d*)

The intensity measures given in Figure 3 correspond to horizontal diameters of NGC 5457 on the plates shown above; the horizontal scales are the same. Nebular condensations measured have been indicated in *b*, *c*, and *d*.

UNIV. OF MICH.

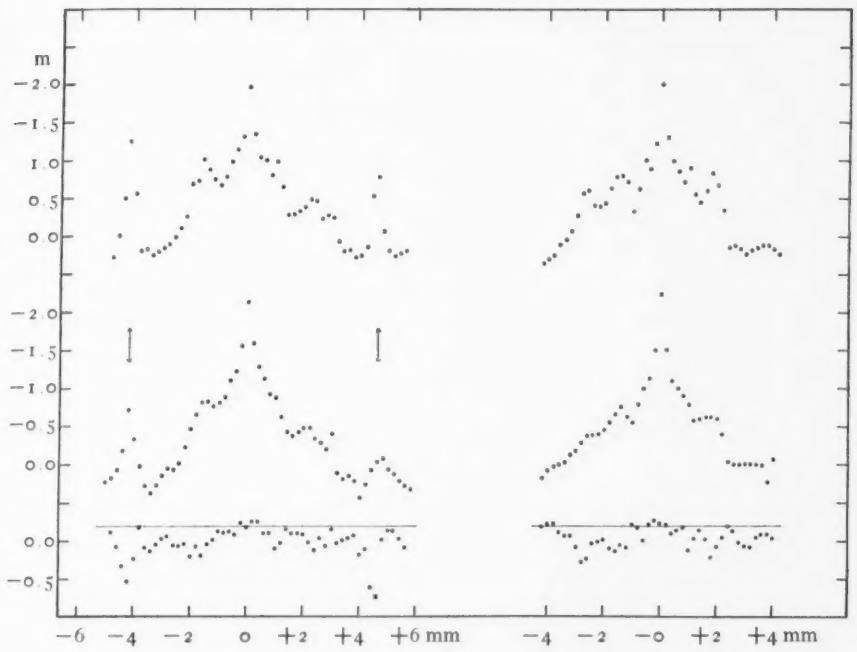

FIG. 3.—Measures of distribution of intensity and red index in NGC 5457. Measures along the major axis are on the left, and those along the minor axis are on the right.

the spiral on the same scale as that of the curves and oriented in such a manner that the direction of the corresponding microphotometer run is horizontal and through the nucleus.

IV. DISCUSSION OF THE RESULTS

NGC 598 (M 33).—This large late-type spiral has a semistellar nucleus seemingly imbedded in a heavy mass of diffuse material. The arms, which are not very distinct, contain many nebulous condensations of various sizes. This fact, together with its large angular dimensions (60′×40′), makes M 33 an excellent object for study.

On the average, the nine knots measured in M 33 are $0^m.66 \pm 0.07$ (p.e.) bluer than the nucleus on the red-index scale, with individual values ranging from $0^m.30$ to $1^m.16$ (Table 1).

In order to determine the zero point of the relative colors of M 33, red-sensitive (Afga Super Pan Press film and Wratten No. 29 filter), yellow-sensitive (Eastman 1-G emulsion and Wratten No. 15 filter), and blue-sensitive plates (Eastman 1-O emulsion) of this object and of the North Polar Sequence were taken with the Yerkes 6-inch UV telescope, now at the McDonald Observatory. Total integrated magnitudes of the brightest condensation, knot No. 9 (NGC 604), were estimated. The red index, as determined from these plates, is $+0^m.6$. Since knot No. 9 is $0^m.31$ bluer than the nucleus (Table 1), the red index of the nucleus is therefore $+0^m.9$.[8] This value for the red index of the nucleus of M 33 makes it possible to transform the color differences of Table 1 to red indices on the system established by Mrs. Payne-Gaposchkin.[9] These red indices for the individual knots, given in column 7 of Table 1, range from $+0^m.60$ to $-0^m.26$ and have an average value of $+0^m.24$.

It is of interest to note that the red indices of the known emission nebulae in M 33 are not conspicuously different from the nonemis-

[8] Stebbins and Whitford (*Ap. J.*, **86**, 247, 1937) have determined the photoelectric color of the nucleus of M 33. Their determination is equivalent to $+0^m.65$ when reduced to the red-index scale. The discrepancy between the photoelectric color of the nucleus of M 33 and that determined above is probably accounted for by the presence of emission lines in the spectrum of the nucleus of M 33, as has been pointed out by Mayall and Aller (*loc. cit.*).

[9] *Harvard Ann.*, **89**, 93, 1935.

sion nebulae. Probably the reason for this is that the strong *Hα* emission is roughly balanced by the emission of the other Balmer lines and the [*O* II] doublet λ 3727 in the blue and violet. For the blue-yellow indices, however, the situation is quite different; for, if the yellow filter cuts off the strong N_1 and N_2 lines, no strong emission lines remain in the yellow region of an emission nebula to offset those in the photographic region, and the photovisual magnitude results primarily from the weak yellow continuum of the exciting stars. This fact is clearly illustrated by colors of knot NGC 604 in M 33, determined from the above-mentioned plates taken with the Yerkes 6-inch UV telescope. The red index for this knot is $+0^m.6$, but the blue-yellow index is $-1^m.5$. Qualitative examples of this effect for galactic emission nebulae have been shown earlier by O. Struve,[10] who employed red-sensitive plates to discover emission nebulae in the Milky Way. The striking difference between the strength of an emission nebula in yellow and red light is clearly shown in Plate I of his paper.

The measures of the intensity dlstribution in red and blue light for M 33, made with the recording microphotometer, show very little color variation out to a distance of 10′ from the nucleus (Fig. 1). There seems to be a slight tendency toward increased blueness at the extreme ends of the north-south run, but this may be due to the difficulty of measuring accurately the low densities far from the nucleus. The arms of the spiral are extremely indistinct, but for those that can be detected the integrated color of arm plus nebulous background ranges from $0^m.0$ to $0^m.15$ bluer than the nucleus. It will be noted in Figure 1 that the arms of the spiral seem to be superimposed on a background intensity which decreases smoothly from the nucleus to the periphery. The same effect is found to be true for the other spirals studied. It is surprising that this general nebulous background should be smooth in such broken spirals as M 33 and M 101.

NGC 891.—A spiral seen edge on, with a major diameter of 12′.0 and a minor diameter of 1′.0, NGC 891 has a total integrated magnitude estimated as $12^m.2$ by Shapley and Ames.[11] This object was

[10] *Ap. J.*, **86**, 94, 1937.

[11] *Harvard Ann.*, **88**, 43, 1932.

chosen for measurement because of the well-defined dark lane running along the major axis.

The measures are shown diagramatically in Figure 1. Since a long, narrow slit was used ($2'' \times 45''$), the microphotometer measures along the major axis represent an integration of dark lane and bright edges. Since the characteristic curves in the two wave lengths used happen to have nearly the same slope, the comparison of the two sets of measures can be made in spite of the effect of integration. It appears from Figure 1 that the color along the major axis is roughly constant.

The measures along the minor axis show the dark lane very well and indicate that it has the same color as the bright edges of the spiral. In addition, the plates of NGC 891 were measured in the McDonald photometer to check this latter result. The brightest parts of the edges of the spiral were found to be $0^m.9$ brighter than the darkest parts of the lane, whereas the corresponding difference found from the microphotometer tracings was only $0^m.6$ (Fig. 1). The discrepancy between the results found from two different methods of measurement is accounted for by the considerable irregularities in the dark lane. The photometer measures confirmed the measures in the microphotometer in showing that the dark lane has the same color as that of the bright edges of the spiral, within the accuracy of the measures.

NGC 2403.—This object, a late-type spiral with a large diffuse nucleus, measures $16' \times 10'$, with a total integrated magnitude of $10^m.2$.[11] Several conspicuous condensations are present in the main body of the spiral, ten of which were measured, as shown in Table 2. One of these condensations, No. 3, is probably not a knot but may be either a piece of an arm or an extended star cloud. Despite the rather uncertain character of this particular object, the measures of it have been included with the others in forming means. On the average, the knots of NGC 2403 are $0^m.68 \pm 0.05$ (p.e.) bluer than the nucleus, with values ranging from $0^m.24$ to $1^m.11$.

The zero point of the relative red indices in Table 2 was established by means of red- and blue-sensitive plates of NGC 2403 and the North Polar Sequence taken with the UV telescope (cf. M 33). From these plates, red indices of several of the brightest knots in

NGC 2403 were determined; and by making use of the red indices of these knots relative to the nucleus (Table 2), the red index of the nucleus was found to be $+0^{m}.80$, approximately $0^{m}.15$ redder than the color to be expected from the observed spectral type, F8.[12] Using this value for the color of the nucleus of NGC 2403, the color differences of the knots were translated into red indices (Table 2, col. 7). The average value of the red indices of the knots in NGC 2403 is $+0^{m}.12 \pm 0.05$ (p.e.).

NGC 3031 (M 81).—This is a large intermediate-type spiral with an integrated magnitude of $8^{m}.9$.[11] The apparent diameter along the major axis is 16′; along the minor axis, 10′. There are no condensations in this object of sufficient brightness to be measured in the photometer. From the recording microphotometer measures there seems to be no definite indication of a variation of red index across either axis (Fig. 2). The measures from the tracings in the vicinity of the arms indicate that the integrated color of the arms plus the general background intensity is just slightly bluer than the nucleus ($0^{m}.1$ or $0^{m}.2$ on the red index scale). Since the arms are extremely indistinct and difficult to distinguish from the general background intensity of the spiral, this result must be termed provisional.

NGC 4631.—This is a large irregular spiral, seen edge on. The diameters along the axes are 12′.0, and 1′.2, and the total integrated brightness of this object is $9^{m}.6$.[11] The red indices of eight knots were measured in the photometer; but since no definite nucleus is visible, the magnitudes, colors, and positions of the knots are referred to the small companion nebula, NGC 4627. The knots or condensations in NGC 4631 are, on the average, $0^{m}.64 \pm 0.05$ (p.e.) bluer than the companion nebula (Table 3).

Stebbins and Whitford[13] have measured the color of NGC 4631 with the photoelectric cell. Their color, when reduced to the red index scale, is $+0^{m}.12$. Stebbins and Whitford's color measures in large spirals refer to the nucleus due to the limitations of the size of the diaphragms they used. In the case of NGC 4631 their measures undoubtedly refer to what would appear in the telescope to be the nucleus, knot No. 6 in Table 3, which is by far the brightest feature of the spiral. If we assume this to be the case, knot No. 6 has a red

[12] *Ap. J.*, **83**, 10, 1936. [13] *Loc. cit.*

index of $+0^{m}.12$, and hence the red-index differences of the condensations in NGC 4631 may be transformed into red indices. These latter values, tabulated in column 7 of Table 3, indicate that the individual condensations in NGC 4631 have red indices ranging from -0.03 to $+0.35$, with an average value of $+0^{m}.16$.

NGC 5194 (M 51).—This fine late-type spiral, $12' \times 16'$ in diameter, is seen almost perfectly in plan. The arms are very distinct, and the nucleus is well defined. One of the most remarkable features of this spiral is the presence of a secondary nucleus at the end of one of the arms. The latter object, listed as a separate nebula in Dreyer's *New General Catalogue* (5195), has an integrated magnitude of $11^{m}.1$,[11] as compared to $10^{m}.1$,[11] for the integrated magnitude of M 51. The measures of the brightness and color of the individual condensations in M 51 are given in Table 4. On the red-index scale, the knots average $0^{m}.74$ bluer than the nucleus, with a small range of the individual values ($0^{m}.52$–$0^{m}.86$). The secondary nucleus (NGC 5195) has very nearly the same color as the primary nucleus ($0^{m}.11$ redder than the primary). A spectrogram of this spiral taken with the slitless spectrograph of the 82-inch reflector revealed no conspicuous emission nebulae, though two condensations were suspected of having weak *Hα* emission. Additional observations with the Yerkes 6-inch UV telescope fitted with a 30° objective prism show that the spectra of the two nuclei are quite similar in energy distribution, with no evidence of emission lines. Small-scale red-, yellow-, and blue-sensitive plates using appropriate filters have been employed to determine the color of the primary and secondary nuclear regions of M 51, so that the color differences listed in Table 4 might be reduced to the red and yellow color-index systems. The results are as follows:

Primary Nucleus		Secondary Nucleus (NGC 5195)	
m_{pg}	$11^{m}.9$	m_{pg}	$12^{m}.5$
m_{pv}	11.2	m_{pv}	11.7
m_{red}	10.9	m_{red}	11.4
C.I.	+ 0.7	C.I.	+ 0.8
R.I.	+ 1.0	R.I.	+ 1.1

Carpenter[2] gives the color index ($m_{pg} - m_{pv}$) of the region near the primary nucleus of M 51 as $+0^{m}.6$, a result in close agreement with the value given above ($+0^{m}.7$) for the color index of the primary

nucleus and nuclear region of M 51. Measures of plates of M 51 taken with the 82-inch reflector indicate that the primary nucleus has the same color as the region near the nucleus, within the accuracy of the measures. Hence, the present material indicates that the nucleus itself has a color index of $+0^{m}.7$ and a red index of $+1^{m}.0$. Carpenter's value for the color index of the nucleus of M 51 is $+1^{m}.6$, a value considered quite uncertain by him, however. Adopting the present values of $+0^{m}.7$ and $+1^{m}.0$ respectively, for the color index and red index of the primary nucleus of M 51, the color differences of the condensations in M 51 may be translated into color indices and red indices. On the average, the knots measured in M 51 have a color index of $+0^{m}.02$ and a red index of $+0^{m}.26$. The individual values of the red indices are listed in column 7 of Table 4.

Dr. Carpenter has kindly supplied me with his individual measures of the color indices of the knots in M 51, and for the eight knots measured by both of us the agreement is excellent (using the present blue-yellow color differences listed in column 8 of Table 4 and the value $+0^{m}.7$ for the color index of the primary nucleus). The systematic difference between our two sets of measures is negligible ($0^{m}.01$), and the average difference without regard to sign is ± 0.18.

The measures of M 51 with the recording microphotometer indicate little or no change in the integrated color of the spiral passing outward from the nucleus (Fig. 2). The integrated color of the arms plus nebulous background averages $0^{m}.3$ bluer than the nucleus on the red-index scale, with individual values ranging from $0^{m}.10$ to $0^{m}.45$. For M 51 the arms are sufficiently distinct to make it possible to subtract them from the general background intensity of the spiral. If this is done, the arms themselves average $0^{m}.6$ bluer than the nucleus, in close agreement with the foregoing value for the average color of the individual condensations in the arms.

NGC 5457 (M 101).—This late-type spiral, one of the largest in the sky, is approximately round, with a diameter of $22'$. The arms, which are fairly distinct, are broken up into a great number of nebulous condensations. These knots average $0^{m}.76$ bluer than the nucleus on the red-index scale and $0^{m}.62$ bluer than the nucleus on the color-index scale (Table 5). The author[7] has shown that many of the condensations in M 101 have emission spectra. A comparison of

the differences between red index and color index for the knots in emission in M 101 reveals no conspicuous anomalies such as were found for the brightest condensation (NGC 604) in M 33. The reason for this is undoubtedly that for M 101 the yellow-sensitive plates were photographed, as mentioned before, through a No. 8 Wratten filter, a light yellow filter which transmits about 50 per cent of the light at the strong emission line N_1 [*O* III]. This caused the images on the yellow-sensitive plates to be quite strong when N_1 is strong, resulting in fairly normal color indices in contrast to the large negative color index found for the emission knot NGC 604 in M 33.[14]

Red and blue-sensitive plates of M 101 and the North Polar Sequence were taken with the 6-inch UV telescope in order to determine the red indices of the nucleus and three of the brightest knots in M 101. Knowing the red index of each of these knots relative to the nucleus (Table 5, col. 6), four determinations of the red index of the nucleus were thus available. The average of these determinations yielded a red index for the nucleus of M 101 of $+0^m.79 \pm 0^m.08$ (p.e.). Using this value, the red indices of all the knots in M 101 were determined and tabulated in column 7 of Table 5. A glance at the table shows that the red indices of the knots average very close to $0^m.0$.

The recording microphotometer tracings across the two axes of M 101 indicate no appreciable progression in color from the nucleus outward (Fig. 3). The red index in the vicinity of the arms is approximately $0^m.35$ smaller than that of the nucleus, with a rather small scatter about this mean value. If allowance is made for the general background intensity of the spiral, the red index of the arms becomes $0^m.7$ smaller than that of the nucleus, or close to $0^m.0$. The microphotometer tracings across one axis included two pairs of knots, as indicated by arrows in Figure 3. The red indices of these knots, as determined from the tracings, are $0^m.8$ smaller than the nucleus, a result consistent with the values found above.

[14] *Note added in proof.*—The validity of this explanation is indicated by subsequent photovisual plates of M 101 obtained with the McDonald reflector and exposed behind a heavy yellow filter (Wratten No. 15; zero transmission at λ 5000). These plates showed the emission condensations to be greatly reduced in brightness relative to the nucleus and to the nonemission knots when compared with the corresponding images on the photovisual plates described in the text.

The present investigation has shown that the red indices of the nebular condensations in the arms of several large spirals are considerably smaller than that of their nuclei. The condensations have red indices close to 0.0, and we can therefore conclude that these condensations are composed largely of early-type stars, some of which are the source of exciting emission nebulae. The blue-red indices of these known emission nebulae are not very different from the nonemission nebular condensations. However, if care is taken to remove the strong N_1 and N_2 lines from the photovisual determinations, the blue-yellow indices would probably be abnormally low, as has been shown to be the case for the brightest emission nebula in M 33. In view of the fact that the color of a nebula is influenced to such a marked extent by the presence of strong emission lines, it follows that it is unsafe to draw conclusions regarding the composition of objects found in extragalactic nebulae on the basis of colors determined on one single base line. However, appropriate blue-, yellow-, and red-sensitive plates would undoubtedly afford a rapid method of detecting objects having strong emission spectra in extragalactic nebulae.

It is of interest to note that these giant emission nebulae, such as NGC 604 in M 33, have no known counterpart in our own Milky Way. The total absolute magnitude of the great nebula in Orion (NGC 1976), including the exciting stars, is only -5^m8,[15] whereas the absolute magnitude of knot NGC 604 in M 33 is approximately -10^m0, or of brightness comparable to that of the great emission nebula 30 Doradus (absolute magnitude approximately -12)[16] in the Large Magellanic Cloud.

I wish to thank Dr. Jesse L. Greenstein for his helpful suggestions concerning this investigation and for his kind co-operation in securing supplementary data at the Yerkes Observatory.

McDonald Observatory
January 8, 1940

[15] The total apparent magnitude of nebula plus stars is obtained from a paper by J. Hopmann (*Verh. der U. zu Leipzig*, **4**, 1, 1934). The distance, 540 parsecs, is taken from a paper by R. J. Trumpler (*Pub. A.S.P.*, **43**, 255, 1931).

[16] The apparent magnitude is from a paper by Shapley and Paraskevopoulos (*Ap. J.*, **86**, 340, 1937). The distance was assumed to be 26,000 parsecs.

SPECTROGRAPHIC OBSERVATIONS OF PECULIAR STARS*

P. SWINGS† AND O. STRUVE

ABSTRACT

1. The spectra of several absorption O-type stars showing vestiges of Wolf-Rayet emission have been investigated from λ 3300 to λ 6700. The absorption spectrum consists mainly of *H*, *He* II, *He* I, *O* III, *O* IV, *N* III, *N* IV, and *Si* IV. The emission lines show a P Cygni character and are confined to *H*, *He* I, and a few transitions of *He* II, *N* III, *N* IV, *N* V, *C* III, and *Si* IV. The location of the expanding shell giving rise to the emission and absorption lines is estimated.

2. The visual spectrum of P Cygni reveals strong *Fe* III lines originating from metastable levels (dilution effect). Lines of other elements show a peculiar selectivity of the emission lines.

The spectra of three other P Cygni type stars (Z Canis Majoris, BD+47°3487, and BD+11°4673) are described, especially in connection with the phenomena arising in expanding shells.

RY Scuti shows a strong system of forbidden [*Fe* III] lines, and the variations in the spectrum of this star are discussed.

3. The ultraviolet region of the spectrum of ζ Tauri shows several sets of absorption lines (*H*, *He*, and ionized metals) arising from the reversing layer and from various layers in the surrounding shell. The $a^5D - 4p^5P^o$ multiplet of *Fe* III was the most conspicuous feature in the visual region of γ Cassiopeiae in March, 1940. New data are given for the spectra of several other stars with extended shells (MtW 143, HD 218393, HD 160529, and HD 190073). A group of stars showing forbidden [*Fe* II] lines is discussed (WY Geminorum, W Cephei, B 1985, B 5481, and HD 45677); and new [*Fe* II] multiplets are found in the ultraviolet region of these objects.

4. The spectra of four binary systems showing simultaneously an M-type spectrum and forbidden lines of high excitation are described in detail. The spectroscopic phenomena accompanying the recent outburst of Z Andromedae are discussed; the continuous absorption in the shell plays an important role in the relative intensities of the emission and absorption components of the P Cygni type lines. The two stars AX Persei and CI Cygni have very similar bright-line spectra, of which the nebular part shows a very high excitation; besides *H*, *He* I, and *He* II, the strongest lines are due to [*Fe* VII] and [*Ne* V], and there is good evidence in favor of [*Fe* X]. The temperature of the nucleus exciting these nebular lines must be of the order of 150,000°, or more. Another multiple object of lower excitation is R Aquarii, and new spectroscopic data show the occultation effect of the nebula by the *TiO* atmosphere of the late-type component. There is good reason to believe that the binary nature of a star stimulates the process of shell formation.

The new quartz spectrograph of the McDonald Observatory is well suited for observations in the region between λ 3200 and λ 3900, where heretofore few peculiar stars have been observed. The purpose of the present investigation is to gather new material in this region, toward the study of extended stellar atmospheres. The stars

* *Contributions from the McDonald Observatory, University of Texas*, No. 22.

† Visiting scientist of the Belgian-American Educational Foundation.

which we have observed and the data of the observations are given in Table 1. All the stars have been observed previously in the ordinary photographic region. In two cases, namely those of P Cygni and γ Cassiopeiae, we have observed the visual region with a special grating spectrograph. In all other cases the prism spectrograph was used, for which the dispersion in the visual region is relatively insufficient. The photographic region, although observed previously by Merrill, H. H. Plaskett, and others, has been measured in most cases, partly to record changes which have taken place since the former observations were made and partly to study the lines of especially interesting atoms, such as [*Fe* III], [*Fe* VII], etc.

Our observations cover a short interval of time and are, therefore, not in themselves suitable for a study of the changes which take place in these interesting spectra. But in conjunction with the work of others and with additional observations, which we hope to secure in the future, they should be helpful in elucidating such remarkable phenomena as the outburst of Z Andromedae or the periodic changes of BD+11°4673.

Although the new material contains a wealth of information on various types of departures from thermodynamic equilibrium, on fluorescence processes, on the origin of the forbidden lines, and on the relative intensities of the forbidden lines, we have in most cases presented only the results of the observations and have in only a few instances attempted to interpret the results. The complete theoretical evaluation of the observations must wait until more material is available.

The material is presented in five sections: Section I deals with several absorption O stars which show vestiges of Wolf-Rayet character; Section II deals with P Cygni type stars; Section III is devoted to a number of interesting Be stars; Section IV discusses the spectra of several stars which combine features of very high and of very low excitation; and Section V contains some of our conclusions.

In the wave-length tables the individual wave lengths of the emission lines were adjusted to correspond with the laboratory values. Except in those cases in which radial velocity results are specifically mentioned, these wave lengths should not be used to determine the radial velocities of emission lines. The wave lengths of the absorption

TABLE 1

LIST OF OBSERVATIONS

HD	BD	Name	α 1900	δ 1900	Sp.	Mag.	Plate	Date	Mid. Exp. U.T.	Exp.	Dispersion at λ 3933
					Section I						
188001	+18°4276	9 Sagittae	19^h47^m9	+18°25′	O7	6.3	CQ 223	1939, Sept. 10	6^h11^m	3^h30^m	40 A/mm
							251	16	5 00	0 28	40
							260	23	3 53	1 00	40
190429	+35 3930 N.	.....	19 59.8	+35 45	O5	7.2	213	9	6 43	1 00	40
							261	23	5 43	2 00	40
34656	+37 1146	.....	5 14.0	+37 20	O6	6.7	228	10	10 07	0 30	40
190864	+35 3949	.....	20 1.9	+35 19	O6	8.0	259	22	5 56	2 06	40
	+21 1609	Nucleus of NGC 2392	7 23.3	+21 07	O	10.0	F/2q492	Oct. 6	10 18	1 04	100
							F/2g629	Dec. 16	12 24	0 16	50
							F/2q750	1940, Feb. 2	9 56	0 30	100
					Section II						
193237	+37°3871	P Cygni	20^h14^m1	+37°43′	B1p	4.7	G 6	1939, Sept. 20	3^h23^m	2^h00^m	26 A/mm
							G 7	20	5 56	3 00	26
53179	−11 1760	Z Canis Majoris	6 59.0	−11 24	Beq	8.4–11.5	F/2q493	Oct. 6	11 29	0 50	100
							F/2g594	Dec. 5	10 35	2 00	50
							F/2g668	Dec. 21	8 53	2 45	50
							F/2q749	1940, Feb. 2	6 39	1 12	100
	+47 3487	MWC 374	21 32.2	+47 25	B3eq	9.1	F/2g356	1939, Sept. 13	9 8	2 15	50
							F/2q386	25	5 24	1 36	100
							F/2q387	25	6 34	0 30	100
							F/2g409	29	4 08	0 30	50

TABLE 1—*Continued*

HD	BD	Name	α 1900	δ 1900	Sp.	Mag.	Plate	Date	Mid. Exp. U.T.	Exp.	Dispersion at λ 3933
					Section II—*Continued*						
207757....	+11°4673	AG Pegasi	$21^h46^m.2$	+12°09′	Bep	6.3–7.9	F/2g410	1939, Sept. 29	4^h33^m	0^h05^m	50 A/mm
							F/2g411	29	4 44	0 10	50
							F/2q456	Oct. 4	6 29	0 10	100
							F/2q457	4	6 41	0 05	100
							CQ 279	Nov. 14	2 10	2 40	40
							281	31	3 05	2 40	40
169515....	−12 5045	RY Scuti	18 19.9	−12 45	Pec.	9.6–10.4	F/2q354	1939, Sept. 9	2 59	1 47	100
							F/2g358	14	3 52	3 00	50
							CQ 258	22	3 08	3 00	40
							F/2g377	23	2 19	1 10	50
							F/2g383	24	1 37	0 20	50
							F/2g405	29	1 43	0 50	50
							F/2q462	Oct. 5	1 40	1 00	100
					Section III						
37202....	+21°908	ζ Tauri	$5^h31^m.7$	+21°05′	B3e	3.0	CQ 216	1939, Sept. 9	10^h02^m	0^h15^m	40 A/mm
							267	24	9 26	0 05	40
10516....	+49 444	φ Persei	1 37.4	+50 11	Bone	4.2	215	9	9 26	0 30	40
							264	24	8 01	0 10	40
5394....	+60 144	γ Cassiopeiae	0 50.7	+60 11	Bop	2.2	G 22	1940, Mar. 17	2 24	0 21	26
							G 23	17	3 01	0 33	26

TABLE 1—*Continued*

HD	BD	Name	α 1900	δ 1900	Sp.	Mag.	Plate	Date	Mid. Exp. U.T.	Exp.	Dispersion at λ 3933
	Section III—*Continued*										
190073	+ 5°4393		19h58m1	+ 5°28′	A0ep	7.9	CQ 238	1939, Sept. 11	7h59m	1h23m	40 A/mm
							270	25	2 50	2 00	40
186568	+33 3572		19 40.1	+33 55	A0	6.0	222	10	4 00	0 30	40
							234	11	4 52	0 30	40
160529	−33 12361		17 35.3	−33 27	A4se	6.7	221	10	3 00	1 00	40
							233	11	2 10	0 30	40
.....	.....	MtW 143	4 11.6	+55 46	Bep	11.5	F/2g361	14	11 12	1 24	50
							F/2q491	Oct. 6	9 03	1 00	100
218393	+49 4045	MWC 397	23 2.6	+49 40	Ave	6.8	CQ 214	Sept. 9	8 18	1 13	40
42474	+23 1243	WY Geminorum	6 5.8	+23 14	M3ep	7.4–7.9	F/2q366	21	11 15	1 00	100
							F/2q367	21	11 54	0 10	100
							CQ 269	24	11 02	1 45	40
							F/2g423	30	10 03	0 40	50
							F/2g424	30	10 31	0 05	50
							CQ 282	Dec. 1	7 50	4 00	40
							285	3	6 28	4 03	40
							289	4	5 59	4 03	40
214369	+57 2568	W Cephei	22 32.6	+57 54	K5e	8.6–9.3	F/2g412	Sept. 29	5 11	0 20	50
							F/2g413	29	5 28	0 05	50
							F/2g431	Oct. 1	6 23	0 01½	50
							F/2g432	1	6 34	0 02½	50
							F/2q458	4	6 55	0 10	100
							F/2q472	5	5 51	1 00	100
							F/2q589	Dec. 4	2 35	2 08	100

TABLE 1—*Continued*

HD	BD	Name	α 1900	δ 1900	Sp.	Mag.	Plate	Date	Mid. Exp. U.T.	Exp.	Dispersion at λ 3933
					Section III—*Continued*						
60414 60415	−14°1971	Boss 1985	$7^h29^m.2$	−14°18′	M2ep	5.2	F/2g426	1939, Sept. 30	11^h03^m	$0^h01\frac{1}{2}^m$	50 A/mm
							F/2q494	Oct. 6	12 05	0 05	100
							CQ 280	Nov. 14	11 20	2 00	40
							286	Dec. 3	9 38	2 00	40
203338 203339	+58 2249	Boss 5481	21 16.5	+58 13	K0+A0	5.6	F/2g407	Sept. 29	3 36	0 05	50
							F/2g408	Sept. 29	3 42	0 01	50
							F/2q454	Oct. 4	6 04	0 05	100
							F/2q455	Oct. 4	6 12	0 01	100
45677	−12 1500	.....	6 23.7	−13 00	B2e	7.2	CQ 275	Nov. 7	12 12	3 45	40
							CQ 283	Dec. 2	10 01	3 33	40
					Section IV						
221650	+48°4093	Z Andromedae	$23^h28^m.8$	+48°16′	.....	8.3–11.4	F/2g360	1939, Sept. 14	9^h18^m	1^h35^m	50 A/mm
							CQ 252	16	8 15	5 30	40
							F/2q471	Oct. 5	4 59	0 30	100
							F/2q489	6	7 54	0 11	100
							F/2q490	6	8 13	0 20	100
							F/2q501	12	7 50	0 08	100
							F/2q502	12	8 01	0 03	100
							CQ 271	18	4 33	3 15	40
							CQ 290	Dec. 5	3 00	2 00	40

TABLE 1—*Continued*

HD	BD	Name	α 1900	δ 1900	Sp.	Mag.	Plate	Date	Mid. Exp. U.T.	Exp.	Dispersion at λ 3933
	Section IV—*Continued*										
.....	.....	AX Persei	$1^h30^m.0$	$+53°45'$	.....	11.0	F/2q363	1939, Sept. 18	11^h00^m	1^h46^m	100 A/mm
							F/2q365	21	9 00	3 00	100
							F/2g415	29	6 58	1 02	50
							F/2q757	1940, Feb. 5	3 12	1 04	100
.....	.....	CI Cygni	19 46.5	$+35$ 26	.....	11.0	F/2g429	1939, Oct. 1	5 06	1 30	50
							F/2q453	4	5 03	1 30	100
222800....	$-15°6352$	R Aquarii	23 38.6	-15 50	Md	5.8–10.8	F/2g359	Sept. 14	6 59	2 31	50
							CQ 257	18	5 59	2 32	40
							F/2q362	18	8 30	2 00	100
							F/2g414	29	5 55	0 30	50
							F/2g433	Oct. 1	6 57	0 10	50
							F/2g595	Dec. 6	1 06	0 12	50

lines of the P Cygni type stars were not corrected for the velocity of expansion, except in Table 15, where they were also adjusted to correspond with the laboratory values.

I. ABSORPTION O STARS WITH EMISSION LINES

These stars are intermediate between Wolf-Rayet stars and P Cygni stars. The purpose of our work was to investigate the ultraviolet region of the spectrum, which has not formerly been described, and to discuss the spectral features of the photographic and the visual regions in the light of recent work on the spectra of highly ionized light atoms.

Former investigations by W. H. Wright[1] and by H. H. Plaskett[2] were largely devoted to the O stars: 9 Sagittae, BD+35°3930 N., 29 Canis Majoris, and the nucleus of the planetary nebula NGC 2392. Besides the bright *He* II line at λ 4686, these authors mention two bright *N* III lines at λ 4634 and λ 4640. The occurrence in emission of these particular *N* III lines seems at first very strange;[3] in early B stars and in pure absorption O stars, the lines λ 4097 and λ 4103 are always much stronger than λ 4634 and λ 4640; but in the four stars just mentioned, only the lines λ 4634 and λ 4640 appear in emission, whereas λ 4097 and λ 4103 are strong absorption lines.

C. H. Payne[4] examined the spectra of several southern stars of class O, taken with an objective prism and covering the photographic region. Among these objects, nine may be considered as essentially absorption O stars. All of them show *He* II 4686 and *N* III 4634 and 4640 in emission. In one case (HD 152408) these bright lines show an absorption companion on the violet side; in the same star *Hβ*, *Hγ*, *Hδ*, *Si* IV 4116, *He* I 4471, and *Mg* II 4481 show both absorption and emission.

We shall discuss the spectra of 9 Sagittae, of BD+35°3930 N., and of the nucleus of NGC 2392, using spectrograms obtained at the Cassegrain focus of the 82-inch McDonald reflector. The spectrograms extend from λ 3327 to λ 6678. For comparison we have also

[1] *Pub. Lick Obs.*, **13**, 206, 1918.

[2] *Pub. Dom. Ap. Obs., Victoria*, **1**, 325, 1922.

[3] Dr. W. H. Wright has called our attention to this peculiar behavior of *N* III.

[4] *Harvard Bull.*, Nos. 842, 843, 844, 1927.

examined two other O stars, HD 34656 and HD 190864, which at certain times have been observed to possess *N* III emission at λ 4634 and λ 4640. However, on our plates, taken on September 10 and September 12, 1939, there is no trace of emission. The fact that the *N* III emission is not permanent is of interest.

1. 9 SAGITTAE

This star is often considered as an absorption O-type star showing vestiges of Wolf-Rayet character. It was classified as O7w by C. H. Payne.[5] Three spectrograms have been measured, one on a Process plate and two others on Agfa Superpan Press film. The list of wave lengths and their identifications are given in Table 2. The scale of stellar intensities ranges from 0 (trace) to 10. The letter "s" designates a sharp line; "n," a nebulous line. The strong interstellar *Ti* II line λ 3384 was not included. Plaskett's list[2] contained the twenty-six strongest lines between *Ca* II K and *Hβ*.

Hydrogen.—The Balmer series may be followed to H_{24}. *Hα* appears as a line of the P Cygni type.[6] *Hβ* is an undisplaced absorption line; the weak emission on the violet wing is probably not due to *Hβ*.

He I.—The triplets are much stronger than the singlets, as compared with the laboratory intensities. The series $2p^1P^0 - nd^1D$ appears only for $n \leqslant 7$; whereas $2p^3P^0 - nd^3D$ is still present for $n = 14$. All these lines appear in the star itself; there seems to be some slight departure from thermodynamic equilibrium in the stellar reversing layer, but this matter will not be discussed here, since the much more extreme case of P Cygni has been investigated recently by Struve and Roach.[7] The line $2p^3P^0 - 3d^3D$ at λ 5875.62 is displaced toward the violet and shows possibly a weak emission at the normal wave length. This absorption line would thus originate in an expanding shell of the P Cygni type. The line $2p^1P^0 - 3d^1D$ at λ 6678 seems to have a similar structure.

The two absorption lines λ 3613.64 ($2s^1S - 5p^1P^0$) and λ 3888.65 ($2s^3S - 3p^3P^0$), whose lower levels are metastable, seem to be accom-

[5] *Stars of High Luminosity*, p. 67 (*Harvard Obs. Mono.*, No. 3, 1930).

[6] Merrill records (*Lick Obs. Bull.*, **8**, 24, 1913) that in 1913 *Hα* was not present in emission.

[7] *Ap. J.*, **90**, 727, 1939.

PLATE X

THE SPECTRUM OF 9 SAGITTAE

UNIV. OF MICH.

TABLE 2

LINES IN 9 SAGITTAE

λ	Int.	Identification			Note
		Elem.	λ	Int.	
3327.2	0				
3340.89	4	O III	3340.74	6	
		O IV	3348.08	2	
3348.2	0	O IV	3349.11	3	
		O III	3348.05	2	
		N III	3354.29	7	
		N III	3353.78	6	
		O III	3355.92	3	
3354.56	3	O IV	3353.70	2	
		He I	3354.52	1	
3360.54	2s				
3367.58	3	N III	3367.36	7	
		Ca III	3367.81	5	
		N III	3374.06	6	
3373.95	2	Ca III	3372.68	8	
		O III	3384.95	4	
3384.66	1	O III	3383.85	2	
3386.2	1	O IV	3385.55	6	
3390.0	1	O II	3390.25	8	
3390.9	1				
3397.41	2n				
3401.53	1s				
3411.42	1	O IV	3411.76	4	
3430.47	1	O III	3430.60	4	
3433.13	1				
3440.50	1	O III	3440.39	4	
3444.20	1	O III	3444.10	5	
3447.71	1	He I	3447.59	2	
3463.9	0	N IV	3463.4	1	
3468.0	0				
3471.88	2	He I	3471.78		1
3478.66	5	N IV	3478.69	7	
3480.42	0				2
3482.50	2	N IV	3482.98	5	
3487.8	0	He I	3487.72		
3498.62	1	He I	3498.63	1	
3530.48	1	He I	3530.50	1	
3554.67	2n	He I	3554.5	1	
3563.8	0n	O IV	3563.36	2	
3567.2	0n				
3583.80	1s				
3587.0	2n	He I	3587.4	1	
3600.41	1	(Fe III	3600.93	10)	
3604.03	1	(Fe III	3603.88	9)	
3609.79	1s	C III	3609.40	5	
3611.36	1s	He I	3613.64	3	3
3613.62	2	He I	3613.64	3	
3623.68	1s				
3634.35	5	He I	3634.3	2	
3638.77	0	O III	3638.70	3	
3643.41	2				
3653.36	1				
3663.82	0	Ne II	3664.09	9	
		H_{24}	3671.48		
3672.23	1n	H_{23}	3673.76		
3676.4	1	H_{22}	3676.36		
3679.4	1	H_{21}	3679.35		
3682.46	1	H_{20}	3682.81		
3686.58	1	H_{19}	3686.83		
3691.89	1	H_{18}	3691.56		
		Ne II	3694.22	10	
3694.43	2s	(O III	3695.37	4)	
3696.83	1	H_{17}	3697.15		
3699.05	2	O III	3698.70	5	
		H_{16}	3703.85		
		He I	3705.00	3	
3704.45	4n	O III	3702.75	5	
		O III	3703.37	5	
		O III	3704.73	3	
3707.50	1	O III	3707.24	6	
3709.66	1	Ne II	3709.64	7	
		(O III	3709.52	2)	
3711.90	3	H_{15}	3711.97		
3715.03	3	O III	3715.08	6	
3721.77	4	H_{14}	3721.94		
3725.6	0	O III	3725.30	3	
		O IV	3725.81	2	
3727.8	0	Ne II	3727.08	9	
		O II	3727.33	8	
3730.8	0				
3734.43	4	H_{13}	3734.37		
3738.92	1				
3744.2	0	O IV?	3744.73		
		N III	3747.66		
3748.23	1	N IV	3747.7	0	
		S III	3747.90	5	
3750.40	4	H_{12}	3750.15		
3753.03	1				
3754.70	2	O III	3754.67	7	
		N III	3754.62	6	
3757.17	3	O III	3757.21	5	
		O IV	3756.9		
3759.85	5	O III	3759.87	9	
		Ca III	3761.62	6	
3761.89	1	O II	3762.63	5	
		Si IV	3762.41	4	
3769.7	1	He II	3769.3		
		H_{11}	3770.63		
3770.60	5	N III	3771.08	7	
3774.47	1	O III	3774.00	6	
3777.0	0n	Ne II	3777.16	8	
3781.74	1	He II	3781.71		
3787.5	0				
3791.16	4	O III	3791.26	6	
3794.1	0	(S III	3794.69	6)	
3796.8	2	He II	3796.36		
3798.05	6	H_{10}	3797.90		
3803.30	1	(O II	3803.14	6)	
3808.0	1				
3810.59	1	O III	3810.96	2	
3813.54	2	He II	3813.53		
3819.51	5	He I	3819.61	4	
3824.23	0	N IV	3824		
3834.49	2	He II	3833.83		
3835.58	6	H_9	3835.39		
3847.79	1				
3858.30	2	He II	3858.10		
3862.5	0				
3867.18	1	He I	3867.46	2	
3882.13	1	O II	3882.19	7	
3886.33	1s	He I	3888.65	10	3
3887.70	2	He II	3887.47		
3889.17	6	H_8	3889.05		
		He I	3888.65	10	
3896.74	1				
3900.33	1	(A II	3900.63	5)	
		(Al II	3900.68	10)	
3905.59	1				
3909.55	1				
3919.50	1	O II	3919.28	6	
3923.76	3	He II	3923.51		
3927.96	1				
3929.8	1				
3961.96	3	O III	3961.59	8	
3964.52	2	He I	3964.73	4	
		Ca II	3968.49		4
3968.20	7	He II	3968.47		
		$H\epsilon$	3970.08		
3970.20	7				
3998.15	1	N III	3998.69	3	
4003.87	1	N III	4003.64	4	

TABLE 2—*Continued*

λ	Int.	Identification			Note
		Elem.	λ	Int.	
4005.4	0				
4009.8	1	(*He* I	4009.27	1)	
4020.22	1				
4026.09	7	*He* I	4026.19	5	
		He II	4025.64		
4030.93	1				
4051.1	0				
4057.74	2	*N* IV	4057.80	2	
4062.64	1				
4067.3	1	*C* III	4067.87	6	
4068.9	1	*C* III	4068.94	7	
4070.5	1	*C* III	4070.43	8	
4081.3	0	*O* III	4081.10	1	
		Ca III	4081.74	5	
4088.89	6	*Si* IV	4088.86	10	
4092.11	2				
4094.28	2				
4097.14	6	*N* III	4097.31	10	
4100.5	2	*He* II	4100.08	2	
4101.7	7	*Hδ*	4101.74		
4103.7	6	*N* III	4103.37	9	
4108.11	1				
4116.34	3	*Si* IV	4116.10	8	
4120.87	2	*He* I	4120.81	3	
4143.64	2	*He* I	4143.77	2	
4156.21	2				
4168.84	0	*He* I	4168.97	1	
4186.30	1	*C* III	4187.05	10	
		O II	4185.45	8	
4195.56	2	*N* III	4195.70	5	
4199.93	5	*N* III	4200.02	6	
		He II	4199.87	2	
4207.4	0	*Ca* III	4207.26	10	
		Ti III	4207.54	3	
4212.77	1	*Si* IV	4212.44	3	
		Ca III	4213.15	5	
4215.67	1	*N* III	4215.69	3	
		Ti III	4215.55	5	
4234.65	1				
4267.5	1	*C* II	4267.27	20	
		C II	4267.02	19	
4325.15	1	*C* III	4325.70	8	
4338.29	2	*He* II	4338.71	3	
4340.43	10	*Hγ*	4340.47		
4350.1	0				
4356.8	0				
4368.8	1				
4379.15	2	*N* III	4379.09	10	
4387.87	2	*He* I	4387.93	3	
4403.8	0	(*Ti* IV	4403.54	2)	
4420.1	0	(*Fe* III	4419.61	10)	
4448.0	0				
4463.17	2				
4471.43	8	*He* I	4471.48	6	
4476.1	0				
4479.9	2	(*N* IV	4479	...)	
4482.8	3				5
4485.43	2E				5
4489.74	3				
4494.13	2	(*N* IV	4495	...)	
4500.3	3				3
(4504.0	2E)				3
4510.4	2	*N* III	4510.92	6	
4515.1	2	*N* III	4514.89	7	
4524.12	2	*N* III	4523.60	4	6
4534.94	2	*N* III	4534.57	3	
		N III	4535.11	2	6
4541.57	8	*He* II	4541.63	5	
4630.97	4	*N* III	4634.16	9	7
4634.13	5E				
4638.42	5	*N* III	4640.64	10	7
4641.22	6E	*N* III	4641.90	3	
4647.53	2	*C* III	4647.40	10	
		C IV	4646.5		
		Ti IV	4647	3	
4654.3	1	*Si* IV	4654.14	4n	
4675.8	2				5, 10
4679.3	2E				5, 10
4682.8	2	*He* II	4685.81	300	8
4685.9	2E				8
4705.0	2				9, 10
4708.6	2E				9, 10
4713.3	2	*He* I	4713.14	3	
4736.1	0	*A* II	4735.93	15	
4848.6	2				
4853.2	2				10
4855.9	3E				
4859.2	3	*He* II	4859.36	7	
4861.0	7	*Hβ*	4861.34		
4921.7	2	*He* I	4921.93	4	
5015.8	3	*He* I	5015.67	6	
5136.1	2				
5411.5	7	*He* II	5411.57	50	
5426.9	0				
5592.4	2	*O* III	5592.37	6	
5695.8	3E	*C* III	5696.0	5	8
5872.2	4	*He* I	5875.62	10	11
5893.0	3				12
6077.5	2				
6280.6	on				13
6555.6	3	*Hα*	6562.82		8
6563.0	5E	*He* II	6560.16		8
6678.	2	*He* I	6678.15	6	

NOTES TO TABLE 2

The unblended interstellar lines of *Ca* II and *Ti* II are not included in the table.

1. *He* I is only a weak contributor.
2. Unidentified line, present in the B-type stars; see O. Struve, *Ap. J.*, **90**, 699, 1939.
3. Line presumably due to the expanding shell; somewhat uncertain.
4. Interstellar.
5. Unidentified lines of P Cygni character, originating in the shell.
6. Another contributor probable.
7. These *N* III lines of the P Cygni type are due to the shell.
8. Lines originating in the shell.
9. Lines originating in the shell, but bright component uncertain.
10. Very difficult region; measures uncertain.
11. Possibly weak emission on red side of the absorption line. This absorption is due to both the star and the shell.
12. Probably interstellar (D lines of *Na*).
13. Possibly interstellar.

panied by very weak absorption lines measured at λ 3611.36 and λ 3886.33. These two companions are sharper; if they are real, they are probably due to absorption in the expanding shell.[8]

He II.—H. H. Plaskett's work has shown that *He* II is strong in 9 Sagittae. He observed the series $4f^2F^o - ng^2G$ from $n = 9$ (λ 4541.63) to $n = 12$ (λ 4100.08, close to $H\delta$). On our plates this series may be observed from $n = 7$ (λ 5411.57, intensity 7) as far as $n = 22$. The even values of n give lines close to the Balmer lines, and these have been separated on our Process plate as far as H_{11}.

The series $3d^2D - nf^2F^o$ is especially interesting. The line λ 4685.81 ($n = 4$), which is the strongest *He* II line in the laboratory and in ordinary stellar spectra, appears as a very weak emission line with a weak absorption companion displaced toward the violet. On the other hand, Dr. A. B. Wyse[9] has called our attention to the fact that the line λ 3203 ($n = 5$), which is outside the wave-length range covered by our plates, is a strong absorption line. It is obvious that the "stellar" absorption line at λ 4686 must also be strong and that it has been covered by emission produced in the outer shell, whereas the stellar line λ 3203 has not been filled up by emission in the shell. A tentative interpretation of this different behavior of $3d^2D - 4f^2F^o$ and $3d^2D - 5f^2F^o$ may be found in the fairly close agreement of the line L_α (λ 1215.66) and of the *He* II line at λ 1215.13, which is the transition between the quantum levels $n = 2$ and $n = 4$. Since the $2s^2S$ level of *He* II is metastable, atoms of the shell which are in that level may absorb the Lyman α radiation emitted by the whole shell. That Lyman α is an emission line seems extremely probable, because $H\alpha$ is bright. By absorption of L_α from $2s^2S$, the *He* II atoms are brought to quantum number 4, whence they can fall down to $n = 3$, emitting λ 4686. The difference in wave lengths is compensated by the widths of the emission and absorption lines. There is no such process for λ 3203, which can, therefore, appear only as an absorption line. Lyman β (λ 1025.72) is close to the *He* II line λ 1025.27, connecting the quantum levels $n = 2$ and $n = 6$. But it is probable that the effect of L_β must be small compared with that of L_α. The

[8] The line λ 3965 ($2s^1S - 4p^1P^o$) yields no information on this point, because a fairly strong *O* III line falls at λ 3961.59.

[9] Private communication.

effect should be largest for the $4f\,^2F^o - 6g\,^2G$ transition at λ 6560.16, but this is blended with *Hα*. These circumstances are illustrated in Figure 1. A similar behavior was observed in Nova Aquilae by Wyse.

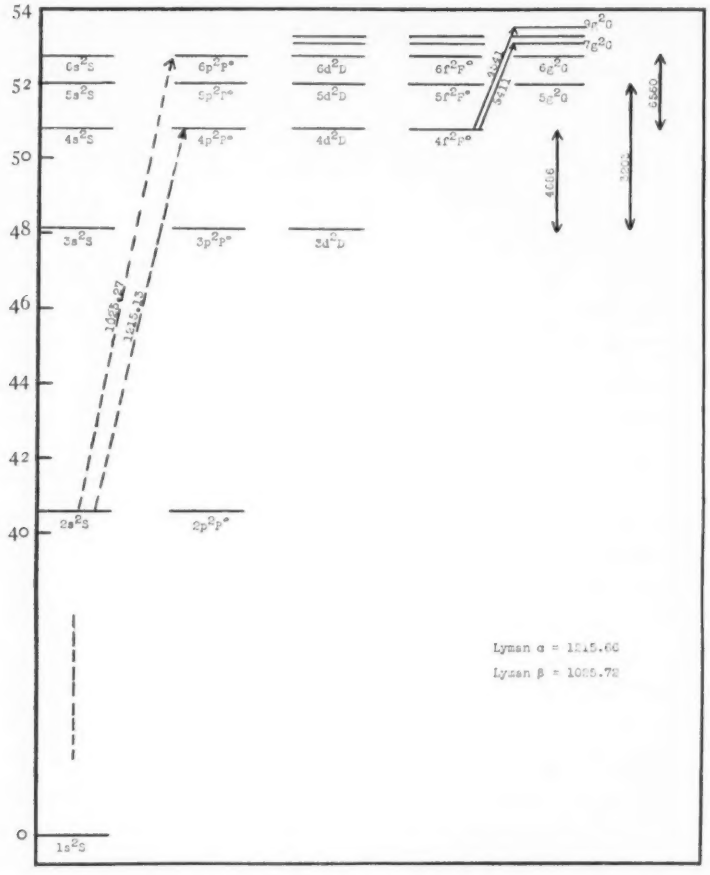

FIG. 1.—*He* II lines in 9 Sagittae

O II.—Extremely weak, no line being stronger than intensity 1 on our scale.

O III.—Strongly represented: twenty-four lines were measured, thirteen of them being free from blends. The strongest multiplets[10] are shown in Table 3.

[10] Dr. Wyse (private communication) has observed several strong absorption lines of *O* III in the ultraviolet region, below our limit, λ 3327.

The fact that *O III* appears only in absorption and with normal intensities is of importance. For example, the presence of λ 3759.87

TABLE 3

STRONGEST ABSORPTION LINES OF *O* III IN 9 SAGITTAE

TRANSITION		λ LAB.	INTENSITY	
			Star	Lab.
$3s^3P^o-3p^3D$.....	1–2	3754.67	2	7
(Excitation potential,	0–1	3757.21	3bl	5
33.0–36.3 v.)	2–3	3759.87	5	9
	1–1	3774.00	1	6
	2–2	3791.26	4	6
	2–1	3810.96	1	2
$3s^3P^o-3p^3S_1$.....	2–1	3340.74	4	6
(33.0–36.7 v.)				
$3p^3P-3d^3D^o$.....	0–1	3702.75	bl	5
(37.1–40.4 v.)	1–2	3707.24	1	6
	2–3	3715.08	3	6
	2–2	3725.30	0	3
$3s^1P^o-3p^1S$.....	1–0	3961.59	2	8
(33.7–36.8 v.)				
$3s^1P^o-3p^1D$.....	1–2	5592.37	2	6
(33.7–35.9 v.)				

TABLE 4

STRONGEST UNBLENDED LINES OF *N* IV IN 9 SAGITTAE

TRANSITION		λ LAB.	INTENSITY	
			Star	Lab.
$3s^3S-3p^3P^o$.....	1–2	3478.69	5	7
(46.5–50.1 v.)	1–1	3482.98	2	5
$3p^1P^o-3d^1D$.....	1–2	4057.80	2	2
(49.9–53.0 v.)				
$3s'^3P^o-3p'^3S$	0–1	4479	2	Predicted
(57.4–60.1 v.)	1–1	4495	2	Predicted

as a strong absorption line shows that Bowen's mechanism of excitation of the *O* III atoms by *He* II 304 does not play a role here.

O IV.—The presence of *O* IV may be considered as certain, one of its lines, λ 3385.55 (lab. int. 6), being of intensity 3. The other line, λ 3411.76 (lab. int. 4), is also present in 9 Sagittae (int. 1).

TABLE 5

LINES OF *N* III IN 9 SAGITTAE

TRANSITION		λ LAB.	INTENSITY	
			Star	Lab.
	Doublets			
$4d^2D-5f^2F^o$ (39.2–42.3 v.)	$1\frac{1}{2}-2\frac{1}{2}$	3998.69	1	3
	$2\frac{1}{2}-3\frac{1}{2}$	4003.64	1	4
$3s^2S-3p^2P^o$ (27.3–30.3 v.)	$\frac{1}{2}-1\frac{1}{2}$	4097.31	6	10
	$\frac{1}{2}-\frac{1}{2}$	4103.37	6	9
$4p^2P^o-5s^2S$ (38.5–41.4 v.)	$\frac{1}{2}-\frac{1}{2}$	4195.70	2	5
	$1\frac{1}{2}-\frac{1}{2}$	4200.02	5 bl	6
$3s'^2P-3p'^2D^o$ (36.7–39.6 v.)	$1\frac{1}{2}-1\frac{1}{2}$	4215.69	1 bl	3
$4f^2F^o-5g^2G$ (39.7–42.4 v.)	$3\frac{1}{2}-4\frac{1}{2}$	4379.09	2	10
$3p^2P^o-3d^2D$ (30.3–33.0 v.)	$\frac{1}{2}-1\frac{1}{2}$	4634.16	4A–4E	9
	$1\frac{1}{2}-2\frac{1}{2}$	4640.64	5A–5E	10
	$1\frac{1}{2}-1\frac{1}{2}$	4641.90		3
	Quartets*			
$3s^4P^o-3p^4P$ (35.5–39.1 v.)	$\frac{1}{2}-1\frac{1}{2}$	3353.78	3 bl	6
	$1\frac{1}{2}-2\frac{1}{2}$	3354.29		7
	$2\frac{1}{2}-2\frac{1}{2}$	3367.36	3	7
	$2\frac{1}{2}-1\frac{1}{2}$	3374.06	2	6
$3s^4P^o-3p^4D$ (35.5–38.2 v.)	$1\frac{1}{2}-2\frac{1}{2}$	4510.92	2	6
	$2\frac{1}{2}-3\frac{1}{2}$	4514.89	2	7
	$1\frac{1}{2}-1\frac{1}{2}$	4523.60	2	4
	$2\frac{1}{2}-2\frac{1}{2}$	4534.57	2	3
$3p^4S-3d^4P^o$ (38.7–41.5 v.)	$\frac{1}{2}-1\frac{1}{2}$	4535.11		2

*The multiplet $3s^4P^o-3p^4P$ has also been observed by Dr. Wyse (private communication).

Nitrogen.—*N* II is extremely weak or absent. *N* IV shows several lines, the strongest of which are listed in Table 4. The best criteria for *N* IV are $3s^3S - 3p^3P^o$ and $3p^1P^o - 3d^1D$. *N* V is possibly present as an extremely weak line at λ 4603. *N* III is very abundant, as is shown in Table 5.

The reproduction in Plate X shows that the *N* III lines at λ 4634 and λ 4641 have a P Cygni character, which has not been mentioned, as far as we know, by previous investigators.

TABLE 6

P CYGNI CHARACTER OF *N* III 4634–4641

Int.	Mean λ	Edges	Widths	
			In Angstroms	In Kilometers per Second
4A.....	4630.97	4630.10–4631.71	1.61	104
5E.....	4634.13	4632.18–4636.42	4.24	275
5A.....	4638.42	4637.71–4639.12	1.41	91
6E.....	4641.22	4639.67–4645.49	5.82	376

The best values for the widths are: for the absorption component, 1.61 A, or 104 km/sec; for the emission line, 5.82 A, or 376 km/sec.

The velocity of ejection in the shell giving rise to the absorption and emission line[11] is of the order of 200 km/sec. The computed values are slightly different, depending upon whether we assume that the broadening of the P Cygni absorption line is due to mechanical causes. If not, we should take the distance between the centers of the emission and absorption lines as: for 4634:

$$\Delta\lambda = 3.16 \text{ A or } V = 205 \text{ km/sec},$$

and for 4641:

$$\Delta\lambda = 2.80 \text{ A or } V = 181 \text{ km/sec}.$$

[11] It is reasonable to assume that the absorption and emission components of P Cyg type lines originate at the same distance from the star.

The most reliable value is 205 km/sec. If, on the other hand, we assume that the width of the absorption line is mainly due to the angular range in ejection velocity, we shall obtain the correct value of that velocity by taking the distance between the center of the bright line and the violet edge of the absorption line:

$$\Delta\lambda = 4.03\ \text{A} \qquad \text{or} \qquad V = 261\ \text{km/sec}\ .$$

All the lines of Table 5, except λ 4634 and λ 4641, originate essentially in the star itself. The absorptions and emissions at λ 4634 and

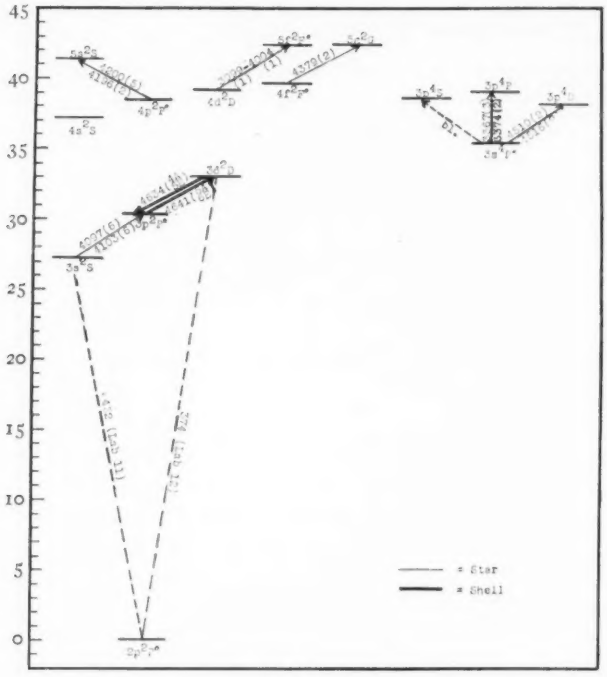

FIG. 2.—*N* III lines in 9 Sagittae

λ 4641 are due to the shell surrounding the central star. This is illustrated in Figure 2, where the heavy lines correspond to the shell and the lighter lines to the central star. In HD 34656, HD 190864, and 10 Lacertae—all pure absorption O stars—the absorption lines λ 4097 and λ 4103 are much stronger than λ 4634 and λ 4641, and the higher-level line λ 4379 is approximately of the same intensity

as λ 4604. In 9 Sagittae the relative intensities of λ 4379 and of λλ 4097 – 4103 are quite normal, in contrast to the appearance of λλ 4634 – 4641.

The following conclusions may be drawn from the observations:

a) We are certainly not dealing with a pure recombination spectrum, because λ 4379 and also λ 4097 and λ 4103 are in absorption.

b) The *N* III lines are not excited by the fluorescence mechanism which prevails in the nebulae. The absence of bright *O* III lines

TABLE 7

C III LINES IN 9 SAGITTAE

TRANSITION		λ LAB.	INTENSITY	
			Star	Lab.
$4f\,^3F^o - 5g\,^3G$	2–3	4067.87	1	6
(39.7–42.8 v.)	3–4	4068.94	1	7
	4–5	4070.43	1	8
$4f\,^1F^o - 5g\,^1G$	3–4	4187.05	1 bl	10
(39.8–42.8 v.)				
$3s'\,^1P^o - 3p'\,^1D$	1–2	4325.70	1	8
(38.3–41.1 v.)				
$3s\,^3S - 3p\,^3P^o$	1–2	4647.40	2	20
(29.4–32.1 v.)				
$3p\,^1P^o - 3d\,^1D$	1–2	5696.0	3E	5
(32.0–34.1 v.)				

shows that this process does not play a role. In the nebulae the groups λ 4097 and λ 4103, and λ 4634 and λ 4641, have normal intensities.

c) No high-level line appears in emission.

Carbon.—*C* II is extremely weak, the strongest transition $3d\,^2D - 4f\,^2F^o$ at λ 4267 being only of intensity 1. *C* IV is absent. *C* III is weak.

The behavior of *C* III is illustrated in Figure 3 and is somewhat similar to that of *N* III. In the singlets the transition $3s\,^1S - 3p\,^1P^o$ is in the unobservable infrared. In the triplets the transition

$3p^3P^o - 3d^3D$ is in the unobservable ultraviolet. We note the following:

a) The notations of the emission and absorption lines are similar in *C* III and *N* III.

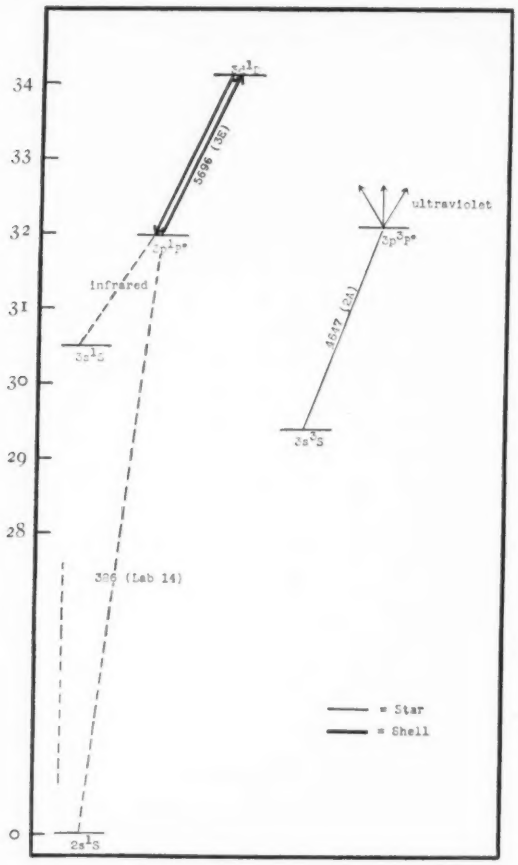

FIG. 3.—*C* III lines in 9 Sagittae

b) Contrary to the case of *N* III, the $3d^1D$ level requires two absorption processes from the ground level.

c) Again, as in *N* III, the highest levels do not give emission lines.

The carbon lines are weak, compared with the nitrogen lines. The star 9 Sagittae is apparently more closely related to the Wolf-

Rayet nitrogen sequence than to the carbon sequence, but carbon is not completely absent, and even *C* III shows an emission line.

The analysis of the spectrum of P Cygni[12] has shown that this star is also related to the nitrogen sequence, as the carbon lines are abnormally weak, compared with the nitrogen lines. The two stars HD 190864 and HD 34656, which at times have shown *N* III in emission, are also extremely poor in carbon lines. We have found no trace of *C* II and *C* IV and have only suspected a weak trace of *C* III. In the laboratory, λ 4647.4 is by far the strongest *C* III line in the astronomical region. The same is true in the carbon Wolf-Rayet stars.

TABLE 8

Si IV LINES IN 9 SAGITTAE

TRANSITION		λ LAB.	INTENSITY	
			Star	Lab.
$4s^2S-4p^2P^o$	$\frac{1}{2}-1\frac{1}{2}$	4088.86	6	10
(24.0–27.0 v.)	$\frac{1}{2}-\frac{1}{2}$	4116.34	3	8
$5g^2G-6h^2H^o$	$4\frac{1}{2}-5\frac{1}{2}$	4654.14	1	4n
(36.3–38.9 v.)				

Other atoms.—*Ca* III may be present but gives only very weak lines. The identifications of *Ne* II and *Ar* II are tentative and give only very weak lines. *Fe* III and *Ti* III may also be present as very weak lines.

Si II and *Si* III are absent. But *Si* IV is fairly strong, the unblended lines being given in Table 8.

Several bright lines are still unidentified, the two strongest being λ 4485.4 (2) and λ 4855.9 (3).

The expanding shell of 9 Sagittae.—The widths of the displaced *N* III absorptions at λ 4634 and λ 4641 are 1.61 A, corresponding to $\Delta V = 104$ km/sec. The widths of ten stellar absorption lines have been measured, and the mean width is $\Delta V_{st} = 200$ km/sec, which corresponds roughly to a stellar axial rotation of the order of 100 km/sec. At the mean position of the P Cygni layer, the velocity of

[12] Struve, *Ap. J.*, **81**, 66, 1935.

ejection is either 205 km/sec (3.16 A) or 261 km/sec (4.03 A). These values are in fair agreement with the width of the emission line at λ 4641, which is 5.82 A, or 376 km/sec.

The wave lengths of the centers of the emission lines, after correction for the stellar radial velocity, are in agreement with the laboratory values.[13] Hence, there is no strong occultation effect, and the emitting layer cannot be very close to the surface of the star. Let us suppose that the broadening of the displaced *N* III lines is due to one of the following mechanical causes: (*a*) the range in ejection velocity within the thickness of the P Cygni layer; (*b*) the range in the component of the ejection along the line of sight, inside the star's cylinder of sight; (*c*) the range in the component of axial rotation along the line of sight. We are unable to estimate the factor (*a*), but we may assume that the shell is rather thin and neglect this factor. A minimum value of *r* will be obtained with this procedure.

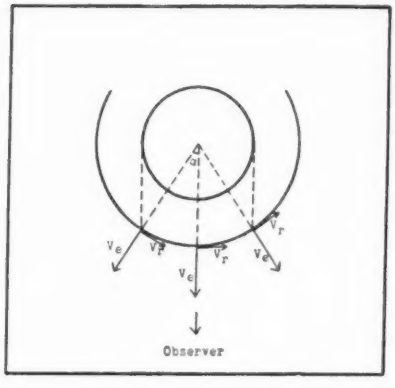

FIG. 4

Let us use the following terms: V_e, for the velocity of ejection at distance r (shell); V_r, for the velocity of axial rotation at distance r; V_R, for the velocity of axial rotation at the surface of the star; and α, for the angle shown in Figure 4.

The width of the absorption line is

$$\Delta V = V_e(1 - \cos \alpha) + 2V_r \sin \alpha .$$

As a working hypothesis, we shall assume that V_r is inversely proportional to r. We then obtain

$$\Delta V = V_e\left(1 - \sqrt{1 - \frac{R^2}{r^2}}\right) + 2V_r\left(\frac{R}{r}\right)^2 .$$

[13] The peculiar displacement of emission lines which is present in the spectroscopic binary 29 Can Maj (Luyten and Ebbighausen; Struve) is not observed in 9 Sag.

UNIV. OF MICH.

PLATE XI

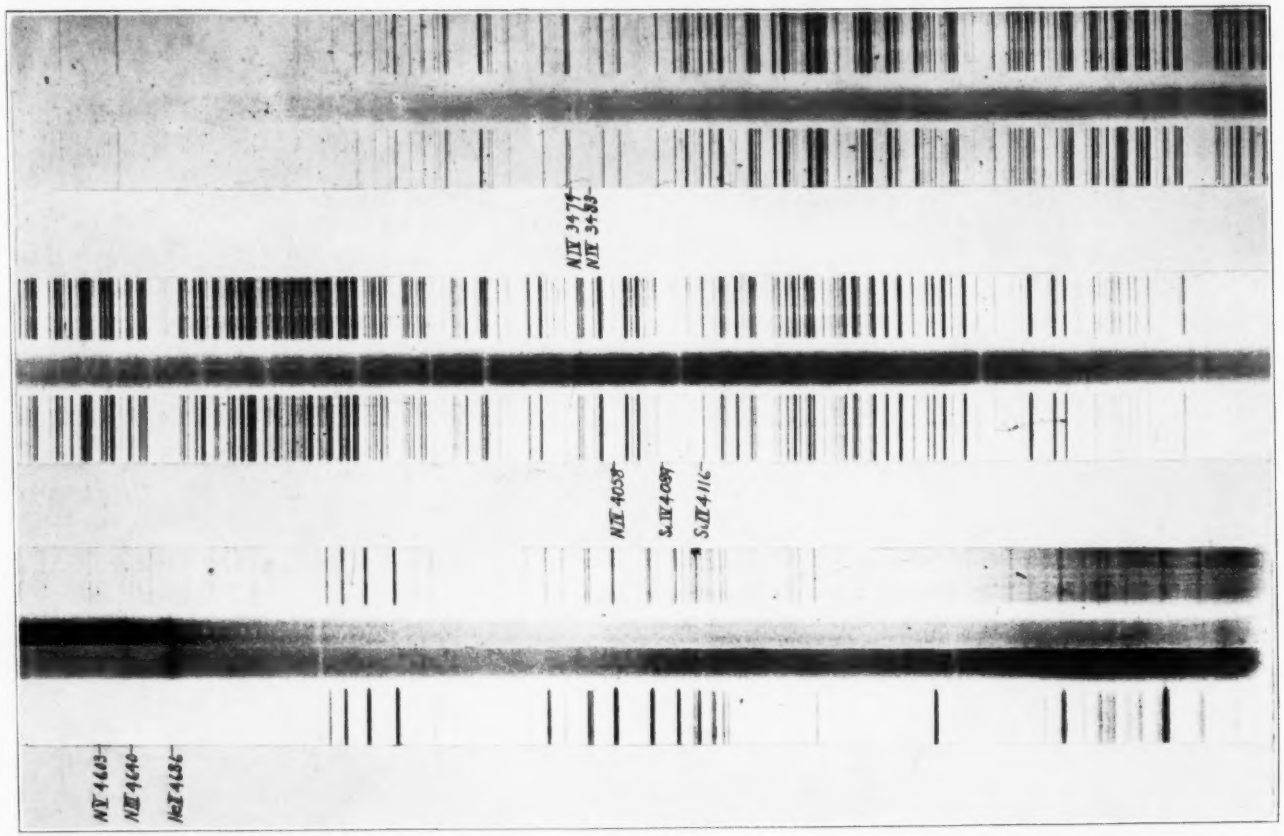

THE SPECTRUM OF BD+35°3930 N.

If we adopt $V_e = 205$ km/sec, we find $R^2/r^2 \sim 0.31$ or $R/r \sim 0.56$; this corresponds to a dilution factor of $W \sim 0.08$. In other words, the distance of the P Cygni layer from the star would be at least equal to the stellar radius. If we assume $V_e \sim 260$ km/sec, we find $R/r = 0.4$, or $r = 2.5R$. The P Cygni layer would then be at a distance of $1.5R$ from the stellar reversing layer.

2. BD + 35° 3930 N.

This star is the northern component of Σ 2624 (separation 2″). It was classified as O5w by C. H. Payne.[5] The absorption spectrum shows a stage of ionization much higher than that of 9 Sagittae. *N* IV is much stronger; *N* III shows λ 4634 and λ 4641 strongly in emission, whereas λ 4097 and λ 4103 have practically disappeared. *He* I is much weaker, and D_3 shows the P Cygni character. *He* II is of about the same intensity in both stars, but now λ 4686 is extremely strong in emission and is very broad (about 14 A). This may be due to the fact that *H* is now weaker. *Hα* again is a bright line, and *Hβ* has the P Cygni character (with $\Delta\lambda = 5.17$ A or $\Delta V = 319$ km/sec). *O* III is weaker. *C* II, *C* III, and *C* IV are absent. It is probable that BD+35°3930 N. is also related to the WN stars.

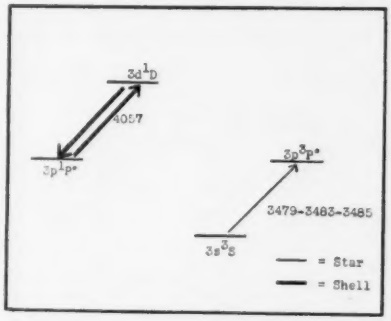

FIG. 5.—*N* IV lines in BD+35°3930 N.

The most interesting features in this star are the emission lines of *N* III, *N* IV, *N* V, and *Si* IV. Except for *N* III, these lines had not been previously observed.

N III.—The only difference from 9 Sagittae is that the absorption lines λ 4097 and λ 4103 have practically disappeared; there may even be faint emissions in their places.

N IV.—The multiplet $3s^3S - 3p^3P^o$ is very strong in absorption; in fact, λ 3478.7 (1–2) and λ 3483.0 (1–1) to λ 3484.90 (1–0) are the strongest ultraviolet lines below λ 3800. On the other hand, λ 4057.80 ($3p^1P^o - 3d^1D$) appears in emission (int. 2E) with a displaced absorption component (int. 1A; $\Delta\lambda = 2.46$ A, or 182 km/sec). The

level diagram (Fig. 5) is quite similar to that of the isoelectronic ion *C* III. The laboratory intensity of λ 4057.80 (2) is much lower than those of λλ 3478.7 (7), 3483.0 (5), and 3484.90 (3).

N V.—The multiplet $3s^2S - 3p^2P^o$ appears in emission:

$$3s^2S_{\frac{1}{2}} - 3p^2P^o_{1\frac{1}{2}}\ 4603.2\ (1A\text{–}1E),$$
$$^2S_{\frac{1}{2}} - \ ^2P^o_{\frac{1}{2}}\ 4619.4\ (0A\text{–}0E).$$

Here we encounter a type of transition (Fig. 6) with notations quite different from the cases of *N* III, *N* IV, and *C* III. The transi-

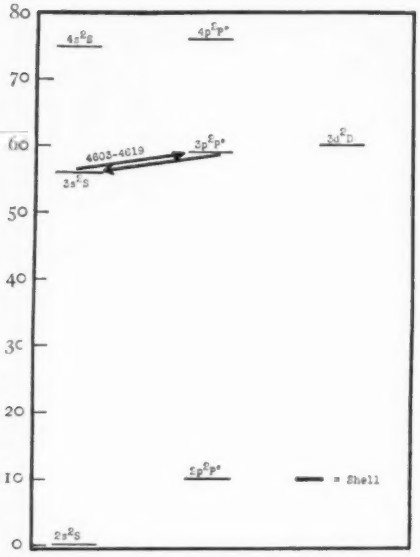

FIG. 6.—*N* V lines in BD+35°3930 N.

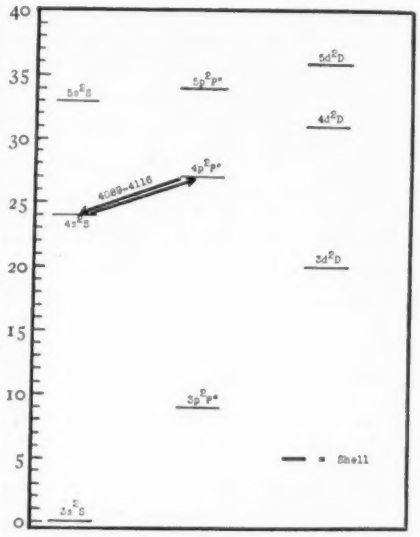

FIG. 7.—*Si* IV lines in BD+35°3930 N.

tions between $3p^2P^o$ and $3d^2D$ are in the unobservable infrared region. The observed lines are the strongest to be expected in the observable region. They have been predicted by Edlén from his laboratory investigations. The ejection velocity of *N* V is $\Delta\lambda = 2.59$ A, or $\Delta V = 169$ km/sec.

Si IV.—The multiplet $4s^2S - 4p^2P^o$ appears in emission, λ 4088.9 and λ 4116.1 having the intensities 1A and 2E, and 1A and 3E, respectively. The ejection velocity is $\Delta V = 161$ km/sec, corresponding to $\Delta\lambda = 2.20$ A. The type of transition is similar to that of *N* V (Fig. 7).

Unidentified lines of P Cygni character.—Three unidentified lines appear in the red region, the bright centers being near λλ 6215 (2), 6289 (2), and 6387 (2). All three show absorption on the violet side; the ejection velocity is of the order of 400 km/sec. The line λ 6387 is near $3s^1S - 3p^1P^o$ of *N* IV (λ 6383).

3. Nucleus of NGC 2392

The region λ 3930 to λ 4860 of this spectrum has been investigated by W. H. Wright,[14] who has shown that the nucleus of this planetary nebula is a typical O star, with *He* II 4686 and *N* III 4634 and 4641 in emission. We have obtained spectrograms of this object extending from λ 3400 to λ 6700. The absorption spectrum is typical of the early O stars. $H\gamma$ is present only in absorption, whereas $H\beta$ presents the P Cygni character.

Besides the bright lines observed by Wright, our spectrograms reveal also the strongest *N* V emission line at λ 4603. There is no trace of the *C* III line observed in emission in 9 Sagittae. The presence of a bright *N* IV line at λ 4057 is not conclusive.

This star is quite similar to BD+35°3930 N. Incidentally, it should be noted that the spectrum of the surrounding nebula (double-ring planetary in Gemini) contains the forbidden [*N* II] lines at λ 6548 and λ 6584;[15] these lines are very weak in comparison with *Hα*.

4. Summary of P Cygni Type Lines in 9 Sagittae and in BD+35°3930 N.

Table 9 lists the P Cygni type lines in 9 Sagittae and BD+35°3930 N. Even aside from *H* and *He*, there is a wide range in excitation potential. This is especially true for BD+35°3930 N., which shows in emission both *Si* IV (exc. pot. 24.0–27.0 v.) and *N* V (exc. pot. 56.3–59.0 v.). This, combined with the absence of emission corresponding to transitions between the highest states, excludes the pure process of recombination of ions and electrons. Any kind of "superexcitation" or "underexcitation" favoring either the higher or the lower levels is also excluded. On the other hand, these elements have no metastable levels. Hence, no dilution effect of the ordinary type

[14] *Lick Obs. Pub.*, **13**, 204, 1918.

[15] This region was not covered by Wright's spectrograms.

is to be expected. But it is not impossible that dilution influences different excited levels in different ways.

A similar effect has been observed by Struve and Roach in the *Si* III lines of P Cygni. The lines $4s^{1,3}S - 4p^{1,3}P^{o}$ appear in absorption, whereas $4p^{1,3}P^{o} - 4d^{1,3}D$ are emission lines. In this case, the excitation potentials are

$4s^{1}S$, 19.6 v.; $4s^{3}S$, 18.9 v.,
$4p^{1}P^{o}$, 21.8 v.; $4p^{3}P^{o}$, 21.6 v.,
$4d^{1}D$, 25.2 v.; $4d^{3}D$, 24.9 v.

Struve and Roach have pointed out that the lowest triplet level of *Si* III can be reached from state $^{3}P^{o}$ only in two steps. The same is true for *N* III, but not for *C* III.

TABLE 9

EMISSION LINES OF P CYGNI TYPE

Element	Wave Lengths	Notations	Excitation Potentials (Volts)
N III	4634.2–4640.6	$3p^{2}P^{o}-3d^{2}D$	30.3–33.0
N IV	4057.8	$3p^{1}P^{o}-3d^{1}D$	49.9–53.0
N V	4603–4619 (predicted)	$3s^{2}S-3p^{2}P^{o}$	56.3–59.0
C III	5696	$3p^{1}P^{o}-3d^{1}D$	32.0–34.1
Si IV	4089–4116	$4s^{2}S-4p^{2}P^{o}$	24.0–27.0
Hα, *Hβ*	6563–4861	$2p^{2}P^{o}-3, 4d^{2}D$	10.2–12.0 10.2–12.7
He I	5876	$2p^{3}P^{o}-3d^{3}D$	20.9–23.0
He II	4686	$3d^{2}D-4f^{2}F^{o}$	48.2–50.8

We have already shown that Bowen's fluorescence mechanism does not produce the excitation of the *N* III lines, but we have not found other plausible cases of fluorescence excitation.

According to Table 9, the emission lines are either of the type pP – dD, in which case the absorption lines are sS – pP, or they are of the type sS – pP, in which case the nature of pP – dD is unobservable. Hence, even the spectral notation of the transition is not conclusive. There is as yet no satisfactory explanation for the strong selection shown by the emission lines.

The emitting shells of HD 34656 and HD 190864 are not perma-

nent features. This may also be true for 9 Sagittae and BD+35°3930 N. In the case of BD+35°3930 N., H. H. Plaskett observed only absorption lines at λ 4603, while we find a fairly strong emission line of *N* V. No emission lines of *N* IV (λ 4058) and *Si* IV (λ 4089 and λ 4116) are mentioned by Plaskett, although it is impossible to miss them on our spectrograms. *Hα* was absent in 9 Sagittae in 1913, according to Merrill. Perhaps we should refrain from applying to such stars our usual ideas based upon permanent or equilibrium conditions.

Both stars are related to the WN sequence. Although 9 Sagittae is not free of carbon, we observe the continuous ejection of nitrogen. This reminds us of Campbell's hydrogen-envelope star.[16] The strong red character of the envelope which was thought to be due to *Hα* is largely produced by the forbidden doublet $2p^2\ {}^3P_{1,2} - 2p^2\ {}^1D$ of [*N* II] at λ 6548.4 and λ 6583.9; these two lines are roughly of the same intensity as *Hα*.[17] On the other hand, the nucleus is a typical carbon Wolf-Rayet star, classified as WC8 by Beals. We do not know whether carbon is absent from the nebular envelope, because the carbon ions have no forbidden lines; but at least we do know that nitrogen is not abundant in the nucleus. It is tempting to think that the entire supply of nitrogen of the atmosphere of the nucleus has been ejected in a manner similar to that which we actually observe in 9 Sagittae.

II. STARS OF THE P CYGNI TYPE

1. The Visual Spectrum of P Cygni

The ultraviolet and the photographic regions of P Cygni have been investigated by Struve and Roach,[18] by Struve,[19] and by Beals.[20] The region of wave lengths above *Hβ* has been considered only in a preliminary manner by Beals,[20] Kharadze,[21] and Struve.[19] We have obtained several good spectrograms of P Cygni in the visible region, using a normal incidence grating spectrograph at the Cassegrain

[16] BD+30°3639 = HD 184738; α 19^h31^m, δ +30°18′.

[17] P. W. Merrill, *Pub. A.S.P.*, **44**, 123, 1932.

[18] *Ap. J.*, **90**, 727, 1939.

[19] *Ap. J.*, **81**, 66, 1935.

[20] *M.N.*, **95**, 581, 1935.

[21] *Zs. f. Ap.*, **11**, 304, 1935.

focus of the 82-inch reflector. The measured lines are listed in Table 10.[22]

Fe III.—The multiplet $a^5D - z^5P^o$ is very strong, although it is not especially outstanding in laboratory sources; this is due to the metastable character of a^5D. The dilution effect is shown in Table 11. In the comparison star, γ Pegasi, the *Fe* III absorption lines have normal intensities. The great strength in P Cygni of *Fe* III lines originating from metastable levels confirms the results by Struve and Roach.[18]

N II.—Has no metastable levels involved in the production of permitted lines in the observable region. Figures 8 and 9 summarize the observed results for the singlets and for the triplets. There is some selection in the emission lines similar to that observed in the shells of O-type stars. Struve's observation[19] that the low levels are privileged is confirmed. For example, all the transitions $3s^1P^o - 3p^1S$, ^1P, ^1D and $3s^3P^o - 3p^3S$, ^3P, ^3D are very strong; high-level lines which have similar intensities in the laboratory are much weaker; the strong laboratory line λ 4447 is relatively weak in P Cygni. Among the singlets, the absence or extreme weakness of the low-level line λ 4895 ($2p'\ ^1D^o - 3p^1P$; lab. int. 4) is puzzling, but the spectral notation of this line is somewhat doubtful.

Carbon.—Struve[19] has noticed the surprising faintness of the *C* II and *C* III lines. Effects similar to those observed in *N* II appear also in *C* II. The low-level doublet λ 6578 and λ 6583, $3s^2S - 3p^2P^o$ (lab. int. 10 and 8; exc. pot. 14.4–16.3 v.), appears in emission, but the line λ 4267.20, $3d^2D - 4f^2F$ (exc. pot. 18.0–20.9 v.), which is much stronger in the laboratory, appears as a weak absorption and emission. It would be interesting to observe the behavior of the $3p^2P^o - 3d^2D$ transition ($\lambda\lambda$ 7231–7236; lab. int. 6 and 8) which connects the

[22] The following corrections and additions should be made in the paper by Struve and Roach (*Ap. J.*, **90**, 727, 1939):

a) In the list of lines, p. 735, the *Fe* III lines, λ 3329.89 and λ 3396.71, are $b^3G_3 - z^3H^o_4$ and $b^3G_5 - z^3H^o_6$. The line $b^3G_4 - z^3H^o_5$ at λ 3347.7 is also present in emission.

b) λ 3324.85 attributed to *S* III on p. 751 is blended with *Fe* III.

c) λ 3919 of *N* II is present.

d) λ 3437 of *N* II has a weak absorption component.

e) λ 3856 of *Si* II is present in emission.

TABLE 10

LINES IN P CYGNI

(Region $H\beta$–λ 6678)

λ	Int.	Identification			Note	λ	Int.	Identification			Note
		Elem.	λ	Int.				Elem.	λ	Int.	
4858.04	10A	*Hβ*	4861.34	....		5762.51	1A	.....	.....	....	
4861.04	20E					5765.52	1A	*N* II?	5767.43	3	
4919.61	6A	*He* I	4921.93	4	1	5833.46	0E	*Fe* III	5834.0	10	7
4921.72	3E					5872.07	10A	*He* I	5875.62	10	1, 4
5006.40	1E	*N* II	5005.14	10	2	5875.45	20E				
			5007.32	7		5886.49	1A	*C* II	5889.97	5	
5013.20	8A	*He* I	5015.67	6	1, 3	5889.94	10	*Na* I	5889.95	....	8
5015.76	8E					5895.90	8	*Na* I	5895.92	....	8
5040.65	1E	*Si* II	5041.13	8	4	5920.15	1En	*Fe* III	5919.3	7	
5043.09	2A	*N* II	5045.10	8		5928.34	1E	*Fe* III	5929.5	5	9, 10
5047.15	0E	*He* I	5047.74	2	3, 4	5931.22	1E	*N* II?	5931.79	7	4, 12
5055.65	1E	*Si* II	5056.17	10	1, 3, 5	5952.93	1E	*Fe* III	5953.6	6	5
5071.69	1A	*Fe* III	5073.78	3	3, 6	5978.49	3E	*Fe* III	5978.1	5	5
5077.32	1A	*Fe* III?	5078.93	4				*Si* II	5978.97	7	1
5084.55	1A	*Fe* III	5086.69	3	3, 6	5998.73	3E	*Fe* III	5999.4	5	5
5095.18	1A	.....	.....	....	3	6031.90	3E	*Fe* III	6031.1	7	5
5125.37	6A	*Fe* III	5127.32	6	3	6172.47	1E	.....	.....	....	
5127.89	3E					6220.54	1E	*Fe* III?	6220.6	3	
5154.09	6A	*Fe* III	5155.97	4	3	6241.37	1E	*N* II	6242.52	5	
5156.12	2E					6244.15	1E	*Al* II?	6243.35	10	
5191.84	1A	*Fe* III	5193.89	4		6277.74	2A	.....	.....	....	
5193.92	1E		5194.43	4		6283.46	1A	*N* II	6284.30	3	
5235.37	0E	*Fe* III	5235.30	5		6306.60	1A	.....	.....	....	
5243.38	1E	*Fe* III	5243.26	10		6340.08	1E	*N* II?	6340.67	4	
5552.58	0A	.....	.....	....		6344.14	1E	.....	.....	....	
5568.20	1A	.....	.....	....		6346.63	3E	*Si* II	6347.10	10	1
5571.21	1A	*Fe* III?	5573.3	4		6355.62	1E	.....	.....	....	
5664.22	6A	*N* II	5666.64	8	1, 4	6361.40	1E	.....	.....	....	
5666.32	4E					6369.88	2E	*Si* II?	6371.36	8	1, 11, 13
5671.73	1E	.....	.....	....		6374.74	2E	.....	.....	....	
5673.56	3A	*N* II	5676.02	6		6377.80	1A	*N* II	6379.63	5	4
5675.57	2E					6379.67	1E				
5677.47	7A	*N* II	5679.56	10	1, 4	6480.24	4A	*N* II	6482.07	8	1, 4
5679.17	5E					6482.04	3E				
5684.34	2A	*N* II	5686.21	6	1	6497.05	1A	.....	.....	....	
5686.12	2E					6499.99	1A	.....	.....	....	
5694.83	0A	*C* III	5695.8	5	1	6534.59	1A	.....	.....	....	
5696.17	0E	*Al* III	5696.47	8		6558.10	20A	*Hα*	6562.82	....	1, 4, 14
5708.71	2A	*N* II	5710.76	6	1, 4	6562.83	100E				
5710.54	2E					6570.75	1E	*Fe* III?	6570.4	1	
5720.97	1A	*Al* III	5722.65	6		6572.92	0E	.....	.....	....	
5737.85	3A	*Si* III	5739.76	8	1, 4	6577.76	2E	*C* II	6578.03	10	
5739.8	0E					6582.37	1E	*C* II	6582.85	8	
5744.96	0A	*N* II	5747.29	4	6	6611.02	2E	*N* II	6610.58	6	
5749.35	1A	.....	.....	....	6	6674.82	8An	*He* I	6678.15	6	1, 4
						6677.98	5E				

NOTES TO TABLE 10

1. Identified also by Beals, *M.N.*, **95**, 580, 1935.
2. The emission character is somewhat uncertain; may be two absorption lines.
3. Observed also by Struve, *Ap. J.*, **81**, 66, 1935.
4. Identified also by Kharadze, *Zs. f. Ap.*, **11**, 304, 1936.
5. Has extremely weak absorption on violet edge.
6. Very weak emission perhaps present.
7. Observed by King in strong spark in air.
8. Interstellar.
9. Separation from λ 5931.22 difficult.
10. Attributed to *N* II by Kharadze.
11. Separation from λ 6374.74 difficult.
12. Absence of λ 5941.7 (8) of same multiplet makes identification doubtful.
13. Double?
14. Emission extends from λ 6559.02 to λ 6567.29. The width measured by Beals is 8.8 A.

upper level of λ 6578 and λ 6583 (16.3 v.) and the lower level of λ 4267. Another transition similar to λ 7231 and λ 7236 is $3p^2P^o - 4s^2S$ (exc. pot. 16.3–19.4 v. λ 3918.98 and λ 3920.68); this seems to be absent in P Cygni.[23]

C III behaves as it does in 9 Sagittae. The $3p^1P^o - 3d^1D$ line at λ 5695.8 appears both in absorption and emission,[24] while the $3s^3S - 3p^3P^o$ group λλ 4651, 4650, and 4647, which is much stronger in the laboratory, is extremely weak in absorption.

Silicon.—The *Si* II lines λ 4128 and λ 4131, $3d^2D - 4f^2F^o$ (lab. int. 8–10; exc. pot. 9.79–12.78 v.) are absent, whereas λ 5041 and

TABLE 11

COMPARISON OF THE TWO TYPES OF *Fe* III LINES IN LABORATORY SOURCES, P CYGNI AND γ PEGASI

λ	Transition	Lab. Int.	Intensity in P Cygni		Intensity in γ Pegasi
			Abs.	Em.	
5127	$a^5D - z^5P^o$	6	6	3	Absent
5156	$a^5D - z^5P^o$	4	6	2	Absent
5243	$4d^7D_3 - 5p^7P^o_4$	10	.....	1	1
5834	$5s^7S_3 - 5p^7P^o_4$	10	.....	1	1

λ 5056, $4p^2P^o - 4d^2D$ (lab. int. 8–10; exc. pot. 10.02–12.47 v.) are present. This puzzling behavior was first noticed by Beals.[20] It is typical for P Cygni type stars. In the red region we observe the low-level lines λ 6347 and λ 6371, $4s^2S - 4p^2P^o$. The ultraviolet line λ 3856 is definitely present.

Si III has already been discussed by Struve and Roach.[18] In the visual region, λ 5739 is present almost entirely in absorption. Hence, the *Si* III triplets show exactly the same behavior as the singlets: the $sS - pP^o$ transitions appear in absorption and the $pP - dD$ transitions in emission. This is the same phenomenon which we recorded for *N* III in 9 Sagittae.

[23] The very weak line near λ 3919 is presumably *N* II 3919; it does not show duplicity.

[24] The blending by *Al* III will not affect the emission line, because the other component of the *Al* III doublet, λ 5722.65, appears only in absorption.

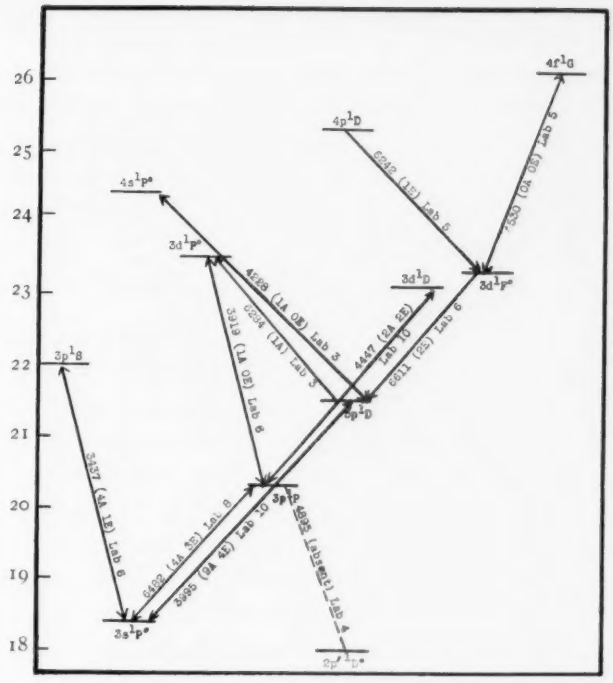

FIG. 8.—*N* II singlet transitions observed in P Cygni

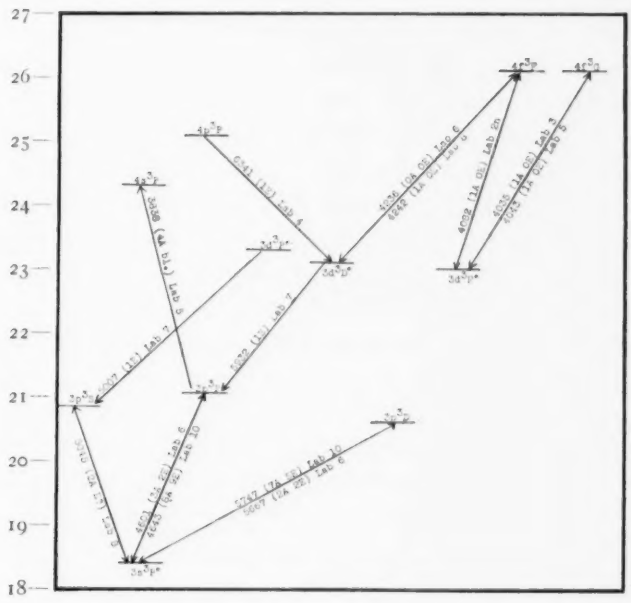

FIG. 9.—*N* II triplet transitions observed in P Cygni

The peculiar selectivity of the emission lines is the most outstanding unsolved problem of P Cygni. It is incorrect to assume, as some investigators have done, that the lines have normal intensities. The usual effect of dilution does not explain these observations, although its presence has been demonstrated by Struve and Roach's discussion of the *He* I and *Fe* III lines.

2. Z Canis Majoris

This is a variable star listed by C. Payne-Gaposchkin and S. Gaposchkin among the objects of the R Coronae type[25] (m = 8.4–11.5). Merrill has described the spectrum near maximum brightness ($m \sim$ 9).[26] It was of the P Cygni type, the main features of the spectrum being bright *H* and *Fe* II lines with broad dark components on their violet sides. A spectrogram taken by Merrill at about the same magnitude, but 15 months later, showed conspicuous differences in the relative intensities of the absorption and emission lines of *Fe* II and *Ti* II. According to Merrill, the behavior of the spectrum in a measure resembles that of the "iron star" XX Ophiuchi.

Four spectrograms were taken near minimum brightness ($m \sim$ 11.5) with the McDonald quartz and glass spectrographs and the F/2 Schmidt camera. The spectrum resembles that observed by Merrill. *H* is very strong in absorption, except in the case of *Hα*, which is seen on our plates only as a strong emission line. The emission components of *Hβ*, *Hγ*, and *Hδ* are relatively weak. *Ca* II shows a strong emission line and a very strong absorption line. *Na* I (D_1 and D_2 blended) is present as a very strong absorption line, without emission. The strongest lines of *Fe* II are present in emission and, rather faintly, in absorption. There is a suspicion[27] of forbidden [*Fe* II] 4359 and 4287. A fairly strong emission line, without absorption, at λ 6296 may be identical with [*O* I] 6300.

The radial velocities measured on December 21, 1939, are given

[25] *Variable Stars*, p. 290 (*Harvard Obs. Mono.*, No. 5, 1938).

[26] *Ap. J.*, **65**, 291, 1927.

[27] Merrill listed no forbidden [*Fe* II]. The Gaposchkins (their Table XI, II, p. 311) state that [*Fe* II] is present but attribute this to Vorontsov-Velyaminov (*New Stars and Galactic Nebulae*, p. 271, Moscow, 1935). This is probably based upon a misunderstanding. Vorontsov-Velyaminov does not actually state that [*Fe* II] is present, and he remarks that his data are essentially those of Merrill.

in Table 12. The violet displacements of the *H* absorption lines are somewhat larger than those recorded by Merrill. The blended line of *Na* I shows a large violet displacement; the measured wave length is 5885.6.

TABLE 12

RADIAL VELOCITIES OF Z CANIS MAJORIS

Line	Absorption	Emission	Line	Absorption	Emission
	km/sec	km/sec		km/sec	km/sec
Ca II K	−122	+95	*Fe* II 4549		+ 36
Hδ	−424	+48	*Fe* II 4556		+108
Hγ	−451	+58	*Fe* II 4584		+ 46
Hβ	−438	+36	*Fe* II 4924		+130
Fe II 4233		+56	*Fe* II 5018	−256	+130
Fe II 4352	−170	+55	*Fe* II 5169	−297	+ 90
Fe II 4523		+31			

3. BD+47°3487

This star was announced by Merrill[28] as belonging to the class of P Cygni. Its spectral type is B3eq.[29] No other description of the spectrum is known to us. The *H* lines show the P Cygni character conspicuously. Emission is present as far as *Hε*. The higher members of the Balmer lines are sharp absorption lines and can be traced on low-dispersion plates to H_{20}. There are several moderately strong P Cygni lines of *Fe* II, especially the conspicuous multiplet $a^6S - z^6P^o$ (λλ 4924, 5018, and 5169). On the other hand, the *Fe* II multiplet $b^4P - z^4D^o$, which includes λ 4233 and λ 4352, is weak. This may not be abnormal. *Ca* II K is a strong absorption line, without emission, which is displaced toward the violet and, therefore, originates in the expanding shell. There are a number of weak, diffuse *He* I lines, having normal intensities and small displacements. These lines probably originate in a stationary reversing layer. The *H* lines also show traces of broad wings, of the Stark-effect type, on the red sides of the emission lines. Thus, the spectrum of the star itself is B3, with considerable rotation and Stark effect, while the shell with *Fe* II and *Ca* II is characteristic of much lower ionization. This differ-

[28] *Ap. J.*, **76**, 182, 1932 (Star No. 212).

[29] *Ibid.*, **78**, 99, 1933 (Star MWC 374).

ence in the spectra of reversing layer and shell is typical for most stars of the P Cygni type in which the reversing layer can be seen through the shell. BD+47°3487 is in this latter respect similar to such stars as 17 Leporis and HD 190073, which show the spectrum of the reversing layer conspicuously, and it differs materially from P Cygni itself, which shows only the spectrum of the expanding shell. One plate shows a sharp line at λ 3959.0. This may be *He* I 3965, which arises from the metastable level 2^1S, and may therefore occur in the shell. But the violet displacement is excessive. The radial velocities are given in Table 13. The normal velocity of the *He* I lines and the large velocity of expansion of the shell are conspicuous. The star should be useful for the study of dilution effects in the shell.

TABLE 13

RADIAL VELOCITIES OF BD+47°3487

Line	Absorption	Emission	Line	Absorption	Emission
	km/sec	km/sec		km/sec	km/sec
Ca II K	−110	.....	*Fe* II 4924	−124	+52
He	−159	+21	*Fe* II 5018	−272	+19
Hδ	−175	+11	*Fe* II 5169	−237	+11
Hγ	−164	−26	*He* I 4026	− 22	.....
Hβ	.....	+24	*He* I 4144	− 24	.....
Fe II 4233	−181	−20	*He* I 4388	(+ 92)	.....
Fe II 4352	.....	+41			

4. BD+11°4673

This remarkable spectrum has been investigated by Merrill in the photographic and visual regions.[30] Our results (Table 14) extend the list of lines into the ultraviolet region. Since the spectrum has somewhat changed from that described by Merrill, we have extended the measurements to cover the entire photographic region. The forbidden lines of [*Fe* II] are very weak on our plate, and it is probable that the permitted lines of *Fe* II are also weaker than on Merrill's plates. *N* III is strong on our plate, both in absorption and in emission. It was absent on Merrill's plates. *He* II 4686 was present in emission in 1939, although it was absent on Merrill's plates. *Si* III 4567 was an emission line in 1939, as was also *Si* III 4552, although

[30] *Ibid.*, **69**, 330, 1929; **75**, 413, 1932.

PLATE XII

THE SPECTRUM OF BD+11°4673

(The line λ 4416 belongs to *Fe* III, not to [*Fe* III])

UNIV. OF MICH.

TABLE 14

LINES IN BD+11°4673

λ	Int.	Identification			Note
		Elem.	λ	Int.	
3368.4	0E	Ca III?	3367.81	5	
		Cr II?	3368.05	150	
		N III	3367.36	7	
3379.6	1E	Cr II	3379.82	60	
3392.0	1A	Cr II?	3393.00	25	
3392.74	1E				
3439.7	1A	Fe I?	3440.63	150	
3440.38	1E		3441.02	75	
3486.78	1A	Si III	3486.93	6	
3487.6	0E				
3529.41	2A	He I	3530.50	1	
3530.24	1E	V II?	3530.76	500	
3553.24	2A	He I	3554.57	1	
3554.18	1E				
3570.52	1E	Fe I?	3570.14	100	
3586.2	1A	He I	3587.28	2	
3587.22	1E	Al II	3586.55	9	
			3587.06	8	
			3587.44	7	
3589.99	2E	Si III	3590.46	8	
		V II?	3589.74	1000	
3599.70	0A	Al III	3601.62	6	
3601.28	3E	Fe III?	3600.93	10	
3611.52	1E	Al III	3612.35	4	
3613.32	1E	He I	3613.64	3	
		Sc II?	3613.84	100	
3633.09	4A	He I	3634.24	2	
3634.32	2E				
3654.50	0E	Al II	3655.00	8	
3660.62	1E				
3666.08	0E	H_{27}	3666.10		
3667.86	0E	H_{26}	3667.68		
3669.35	1E	H_{25}	3669.47		
3671.32	1E	H_{24}	3671.48		
3673.66	2E	H_{23}	3673.76		
3676.31	2E	H_{22}	3676.36		
3679.70	2E	H_{21}	3679.35		
3682.85	2E	H_{20}	3682.81		
3686.65	2E	H_{19}	3686.83		
3691.44	3E	H_{18}	3691.56		
3692.35	1E				
3694.33	1E	Ne II	3694.23	10	
3697.07	3E	H_{17}	3697.15		1
3703.99	3E	H_{16}	3703.85		
3705.44	3E	He I	3705.1		
3707.31	0E				
3708.92	0E	Ne II?	3709.64	7	
		Fe I?	3709.26	75	
3712.02	3E	H_{15}	3711.97		
3713.15	2E	O II	3712.75	7	
		Ne II	3713.09	10	
3719.78	1E	Fe I?	3719.95	250	
3721.98	4E	H_{14}	3721.94		
3727.32	1E	O II	3727.33	8	
		Ne II	3727.08	9	2
		V II?	3727.35	1000	
3734.48	5E	H_{13}	3734.37		
3737.18	1E	Fe I?	3737.14	150	
3750.27	5E	H_{12}	3750.15		
		O II	3749.49	9	
3754.79	0E	N III	3754.62	6	
3757.71	0E	Fe I?	3758.25	150	
3770.65	5E	H_{11}	3770.63		
		N III	3771.08	7	
3797.70	6E	H_{10}	3797.90		
3798.52	0E				

λ	Int.	Identification			Note
		Elem.	λ	Int.	
3805.74	2E	He I	3805.75	1	3
3806.60	2E	Si III	3806.56	5	
3818.19	4A	He I	3819.61	4	
3819.56	3E				
3823.35	0A				
3824.22	0E				
3829.09	1E	Mg I	3829.37	40	
3832.06	1E	Mg I	3832.31	80	
3834.15	1A	H_9	3835.39		
3835.33	6E				
3838.06	2E	He I	3838.09	1	
		N II	3838.39	5	
		Mg I	3838.30	100	
3840.72	0E	Fe I?	3840.45	80	
			3841.06	80	
3855.55	2E	Si II	3856.03	8	
3862.32	1E	Si II	3862.59	6	
3872.36	1E	He I	3871.80	1	
		Fe I?	3872.51	60	
3878.04	0E	He I	3878.18	1	
		Fe I?	3878.58	100	
3886.87	3A	He I	3888.65	10	
3888.42	8E				
3888.96	6E	H_8	3889.05		
3900.41	0E	Al II	3900.66	10	
3905.45	2E	Si I	3905.53	10	
3910.55	0E				
3914.41	0E	V II?	3914.33	250	
3918.56	1En	N II	3919.00	6	
3926.62	0E	He I	3926.53	1	
3933.78	2Es	Ca II	3933.66	40	
3937.96	2Es	N III?	3938.52	4	
3963.00	4A	He I	3964.73	4	
3964.89	3E				
3967.95	1Es	Ca II	3968.49	35	
3969.89	7E	$H\epsilon$	3970.08		
3994.91	3E	N II	3994.99	10	
4007.60	1A	He I	4009.27	1	
4009.27	2E				
4024.48	3A	He I	4026.19	5	
4026.25	4E				
4087.76	2A	Si IV	4088.86	10	
4089.26	1E				
4096.17	3A	N III	4097.31	10	
4097.67	2E				
4101.85	10E	$H\delta$	4101.74		
4114.81	1A	Si IV	4116.10	8	
4115.92	1E				
4119.84	1A	He I	4120.81	3	
4121.85	2E				
4141.89	1A	He I	4143.77	2	
4143.84	3E				
4163.12	0En				
4173.12	1E	Fe II	4173.48	8	
4175.94	0E	[Fe II]?	4177.22		
4178.97	2E	Fe II	4178.87	8	
4197.80	1A	N III	4200.02	6	
4199.99	0E	He II	4199.87		
4226.61	0E	Ca I	4226.74	500	
4230.51	1A	Fe II	4233.16	11	
4233.21	3E				
4258.37	1E	Fe II	4258.16	3	
4290.87	1E	Ti II	4290.23	50	
4296.75	1E	Fe II	4296.56	6	
4302.33	1E	Ti II	4301.93	15	

TABLE 14—*Continued*

λ	Int.	Identification			Note	λ	Int.	Identification			Note
		Elem.	λ	Int.				Elem.	λ	Int.	
4313.66	0E	*Sc* II?	4314.08	30		4548.42	1E	*Fe* II	4549.48	10	
4340.43	20E	$H\gamma$	4340.47	.....		4554.19	1E	*Fe* II	4555.90	8	
4351.13	2E	*Fe* II	4351.77	9		4567.63	2E	*Si* III	4567.87	7	
4379.39	1E	*N* III	4379.09	10		4576.02	2E	*Fe* II	4576.31	4	
4384.82	1E	*Fe* II	4385.39	7		4583.53	3E	*Fe* II	4583.84	11	
4388.19	5E	*He* I	4387.93	3		4590.61	1E	.....	.....	.....	
4416.06	2nn	[*Fe* II]	4416.28	.....		4601.78	1E	*N* II	4601.49	8	
4427.84	1E	*N* II?	4427.21	2		4607.55	1E	*N* II	4607.17	7	
4431.92	1E	*N* II	4432.71	.....		4610.68	1E	*N* II?	4609.60	0	
4442.99	0E	*Ti* II	4443.80	50		4620.29	0En	*N* II?	4621.40	7	
4447.16	3E	*N* II	4447.04	10		4629.29	3E	*Fe* II	4629.33	7	
4459.27	0E	[*Fe* II]?	4457.96	.....		4634.15	3E	*N* III	4634.16	8	
4469.41	1A	*He* I	4471.48	6		4640.51	4E	*N* III	4640.64	10	
4471.78	1E					4658.39	0E	[*Fe* III]	4658.18	.....	
4507.68	1E	*Fe* II	4508.29	8		4665.06	0E	*Fe* II?	4666.75	2	
4515.43	1E	*Fe* II	4515.34	7		4685.06	4E	*He* II	4685.81	.....	
4520.69	1E	*Fe* II	4520.24	7		4700.12	1E	[*Fe* III]	4701.54	.....	
4527.69	0E	.....	.....	.....		4713.60	3E	*He* I	4713.14	3	
4534.96	0En	*Fe* II	4534.17	2							

NOTES TO TABLE 14

1. Double?
2. Possibly with 0A.
3. Separation from λ 3806.60 difficult.

the latter was blended with two *Fe* II lines. *Si* III 4575, although not measured, is almost certainly present as a very weak emission line.

In the ultraviolet region the Balmer emission lines can be followed to H_{27}. The Balmer emission continuum is fairly strong. *N* II is fairly strong. *C* II is very weak or absent. Silicon is present in four consecutive stages of ionization: *Si* I, II, III, and IV. *Si* II shows the same behavior as in P Cygni: the lines λ 4128 and λ 4131 ($3d^2D - 4f^2F^o$; lab. int. 8–10), which are strong in A and B stars, are absent, whereas λ 5055 ($4p^2P^o - 4d^2D$) and λ 5958 and λ 5979 ($4p^2P^o - 5s^2S$) are present. The presence of *Mg* I and *Ca* I is fairly certain. *Fe* I is doubtful. *O* II and *O* III are uncertain.

The unusually large range of ionization represented in the spectrum of BD+11°4673 is very interesting. It suggests that there is considerable stratification in the emitting shell.

The radial velocities of the emission lines give, in the mean, −1.6 km/sec. The absorption lines of *He* I, *N* III, and *Si* IV give −123 km/sec.

5. RY Scuti

This object occupies a special place among the P Cygni stars. Merrill[31] has shown that RY Scuti has *Hβ*, *Hγ*, and *He* I 4472 in emission, *Hγ* and λ 4472 being accompanied by weak absorptions on the violet side. Besides these three lines, Merrill observed a group of fairly strong bright lines at λλ 4658 (int. 4), 4701 (2), 4734(1^+), 4755 (1), and 4770 (1). The strongest lines of this group had also been found in other objects—for example, in Nova Serpentis, where they are very intense, in Z Andromedae, BD+11°4673, etc. Their identification with the forbidden transitions of *Fe* III, $3d^6\ ^5D - 3d^6\ ^3F$, has recently been announced by Edlén and Swings.[32] On a spectrogram taken on May 11, 1938, in the visual region, P. W. Merrill[33] has also found the forbidden lines of [*N* II] at λλ 5755, 6548, and 6584, together with *He* I 5876 and *Hα*. There is some absorption on the violet side of D_3, and D_1 and D_2 of *Na* appear as stationary lines.

RY Scuti may be considered as representing a definite stage in the evolution of certain novae. These objects often pass through the *η* Carinae stage characterized by strong [*Fe* II] lines; the next stage may well be characterized by [*Fe* III]. This is one of the reasons why RY Scuti deserves careful attention. Our present knowledge concerning the spectral type was summarized by C. and S. Gaposchkin[34] as follows: "As there are almost no absorption lines in the spectrum, its spectral classification is difficult; it may be described as a bright-line spectrum of high excitation."

Seven spectrograms were obtained at the McDonald Observatory, on September 9, 14, 22, 23, 24, 29, and October 5, 1939; two of them were taken with the quartz prisms and the F/2 Schmidt camera, one with the quartz prisms and the 500-mm camera, and four with the glass prisms and the F/2 Schmidt camera. The star is greatly reddened; hence, different exposures are required for the different spectral regions. The results of the measures are collected in Tables 15 and 16.

[31] *Ibid.*, **67**, 179, 1928.

[32] *Observatory*, **62**, 234, 1939.

[33] Private communication.

[34] *Variable Stars*, p. 91 (*Harvard Obs. Mono.*, No. 5, 1938).

TABLE 15

ABSORPTION LINES IN RY SCUTI

λ	Int.	Identification			Note	λ	Int.	Identification			Note
		Elem.	λ	Int.				Elem.	λ	Int.	
3341.....	1	*O* III	3340.74	6		3996.3.....	1	*N* II	3995.00	10	
3407.8.....	0	*O* II	3407.38	7		4010.3.....	1	*He* I	4009.27	1	
3428.6.....	1	*O* III?	3428.67	3		4017.5.....	1	.....	.....	.....	
3473.6.....	1	*He* I	3471.78	.....		4025.5.....	2	*He* I	4026.19	5	
3531.5.....	0	*He* I	3530.50	.....		4028.8.....	1	*S* II	4028.74	7	
3555.5.....	1	*He* I	3554.50	1				*O* II	4069.90	7	
3569.3.....	0	.....	.....	.....		4070.4.....	1	*C* III	4068.94	10	5
3574.1.....	0	.....	.....	.....				*C* III	4070.43	8	
3587.3.....	1	*He* I	3587.33	2				*Si* IV	4088.86	10	
3606.6.....	0	.....	.....	.....		4090.3.....	2	*O* II	4089.29	7	
3636.2.....	0	*He* I	3634.28	2		4097.0.....	1	*N* III	4097.31	10	
3652.6.....	0	*He* I	3652.06	1		4101.4.....	3	*Hδ*	4101.74	.....	
3661.7.....	0	*S* III	3662.0	5		4104.3.....	2	*N* III	4103.37	9	
3674.2.....	0	H_{23}	3673.76	.....		4115.3.....	1n	*Si* IV	4116.10	8	
3679.8.....	0	H_{22}	3679.36	.....				*He* I	4143.82	2	
3686.4.....	0	H_{19}	3686.83	.....		4144.4.....	2	*S* II	4142.24	8	
		O III	3695.37	4				*S* II	4145.05	8	
3694.6.....	0	*Ne* II	3694.22	10				*C* III	4162.80	4	
		H_{16}	3703.86	.....	1	4162.0.....	1	*S* II	4162.64	10	5
3704.6.....	0	*He* I	3705.07	3		4187.0.....	1	*C* III	4187.05	10	
		H_{15}	3711.97	.....		4190.6.....	0	*O* II	4189.79	8	5
3712.2.....	0	*O* II	3712.75	7		4211.0.....	0	*Si* IV?	4212.44	4	
		H_{14}	3721.94	.....	2	4267.....	0	*C* II	4267.02	19	5
3721.0.....	0	*O* III	3720.86	3					4267.27	20	
3725.0.....	0	*O* II?	3727.3	8		4340.4.....	3	$H\gamma$	4340.48	.....	
3734.6.....	1	H_{13}	3734.37	.....		4354.9.....	1n	.....	.....	.....	
3743.2.....	0	*O* IV?	3744.73	.....		4366.9.....	1n	*O* II?	4366.90	5	5
		H_{12}	3750.15	.....				*C* III?	4368.14	4	
3749.4.....	1	*O* II	3749.49	9		4387.8.....	4	*He* I	4387.93	3	
3758.5.....	0	*O* III	3759.87	9		4416.5.....	0	*O* II	4414.89	10	
3770.3.....	1	H_{11}	3770.63	.....					4416.97	8	
3782.9.....	0	.....	.....	.....		4430.....	.....	.....	.....	.....	6
3797.6.....	1	H_{10}	3796.22	.....	3	4471.7.....	3	*He* I	4471.48	6	
3800.0.....	1	.....	.....	.....		4480.0.....	1	*Mg* II	4481.2	100	5
3820.2.....	2	*He* I	3819.61	4				*Al* III	4479.97	4	
3835.9.....	3	H_9	3835.39	.....		4504.2.....	1	.....	.....	.....	
3870.8.....	1	*He* I	3871.82	1		4513.....	1	*N* III	4514.89	7	
		He I	3888.64	10		4552.....	1	*Si* III?	4552.61	9	5,7
3888.6.....	4	H_8	3889.05	.....				*N* III?	4858.74	2	
						4857.....	0	*N* III?	4858.88	3	
3902.5.....	1	*S* III?	3901.55	7		4922.0.....	4	*He* I	4921.93	4	
3911.5.....	0	*O* II	3911.95	10		5446.....	1	.....	.....	.....	
		Si III	3924.44	4		5664.....	1	.....	.....	.....	
3925.1.....	0	*He* I	3926.53	1		6202.....	2n	.....	.....	.....	8
3933.9.....	3	*Ca* II	3933.68	.....	4	6287.....	3n	.....	.....	.....	9
3942.9.....	1	.....	.....	.....		6395.....	2n	.....	.....	.....	
3964.9.....	1	*He* I	3964.73	4		6459.....	1n	*N* III?	6453.95	3	
		Ca II	3968.49	.....	4						
3969.8.....	4	*He*	3970.08								

NOTES TO TABLE 15

1. Double?
2. Separation from λ 3725.0 difficult.
3. Separation from λ 3800.0 difficult.
4. Interstellar.
5. Line uncertain.
6. Broad interstellar band from λ 4415 to λ 4445.
7. There may be some emission at λ 4557.6.
8. Interstellar (Merrill λ 6203.0).
9. Interstellar (Merrill λ 6284).

General discussion.—The absorption spectrum is fairly rich in the ultraviolet region and is typical of an early type—say, late O or Bo. The elements represented are *H*, *He* I, *N* III and *N* II, *O* III and *O* II, weak C III and *C* II; probably also *S* III and *S* II, *Si* IV and *Si* III, and *Mg* II. The stationary lines H, K, and $D_{1,2}$, and the interstellar bands λλ 4415–4445, 6284, and 6203 are strong.

TABLE 16

EMISSION LINES IN RY SCUTI

λ	Int.	N*	Identification		Note	λ	Int.	N*	Identification		Note
			Elem.	λ					Elem.	λ	
4340.5	3	4	*Hγ*	4340.48		5007.6	1	3	[*O* III]	5007.6	
4471.5	2	3	*He* I	4471.48		5010.5	1	3	[*Fe* III]	5010.86	
4574.7	0	2	[*Fe* III]	4573.29	1	5032.2	0	1	[*Fe* III]	5032.93	1
4606.4	0	1	[*Fe* III]	4607.01		5040.1	1	2	.....	.....	2
4623.....	1	3	.....	.....		5058.....	0	1	[*Fe* III]	5060.06	1
4635.4	0	4	*N* III	4634.16		5117.2	1	1	[*Fe* III]?	5116.4	1
4641.5	0	1	*N* III	4640.64		5136.....	1	2	[*Fe* III]?	5135.2	1
4658.2	5	4	[*Fe* III]	4658.18		5270.2	5	3	[*Fe* III]	5270.30	
4670.....	0	2	[*Fe* III]	4667.10		5698.....	1	1	*C* III	5695.8	
4686.4	2n	4	*He* II	4685.81		5713.....	1	1	[*Cr* III]?	5712.7	
4701.5	3	4	[*Fe* III]	4701.54		5732.....	2	1	.....	.....	
4733.8	1	4	[*Fe* III]	4733.82		5755.....	3	2	[*N* II]	5755.0	
4756.3	1	1	[*Fe* III]	4754.87		5787.5	1	2	.....	.....	
4769.3	1	3	[*Fe* III]	4769.34		5834.....	1	2	.....	.....	
4777.6	1	2	[*Fe* III]	4777.71	1	5853.....	1	1	.....	.....	
4861.5	10	4	*Hβ*	4861.34		5876.....	6	2	*He* I	5875.6	
4895.4	1	1	.....	.....		5904.....	2	1	.....	.....	
4958.....	0	1	[*O* III]	4958.9		6548.....	3	2	[*N* II]	6548.4	
4985.6	1	2	[*Fe* III] / [*Fe* III]	4985.99 / 4985.99		6563.....	10	2	*Hα*	6562.8	
						6584.....	6	2	[*N* II]	6583.9	

* *N* designates the number of spectrograms on which the lines were measured.

NOTES TO TABLE 16

1. Line uncertain.
2. Present in NGC 7027 (int. 5), NGC 6572 (int. 1), and AX Persei. May be [*Fe* IV].

The emission spectrum shows *Hγ*, *Hβ*, *Hα*, *He* I 4471 and 5876, *He* II 4686, [*N* II], [*O* III], and *N* III 4634 and 4641. All the other strong emission lines are due to [*Fe* III]. This should be compared with the case of P Cygni, where the permitted *Fe* III lines are so outstanding. There is no trace of permitted *Fe* II or *Fe* III, or of forbidden [*Fe* II], in RY Scuti.

The only bright *He* I lines are λ 4472 ($2p^3P^o - 4d^3D$) and λ 5876 ($2p^3P^o - 3d^3D$), whereas the very strong transition $2s^3S - 3p^3P^o$ at λ 3888 does not appear in emission. The lines λ 4635.4 and

λ 4641.5 are the *N* III lines which appear so characteristically in emission in 9 Sagittae and similar stars (Sec. I). The line at λ 5698 may be *C* III 5696.

The bright-line spectrum is due to an ejected nebulosity surrounding the star and is very rich in forbidden [*Fe* III].

Forbidden lines of [*Fe III*].—According to the analysis of the *Fe* III spectrum by Edlén and Swings,[35] the ground level is $3d^6\ {}^5D$, and

TABLE 17

FORBIDDEN LINES OF [*Fe* III] IN RY SCUTI

Transition	λ Predicted	λ and Intensity in RY Scuti
$^5D-{}^3F$ 4–4	4658.18	4658.2 (5)
4–3	4607.01	4606.4 (0)
4–2	4573.29	4574.7 (0)*
3–4	4754.87	4756.3 (1)
3–3	4701.54	4701.5 (3)
3–2	4667.10	4670. (0)
2–3	4769.34	4769.3 (1)
2–2	4733.82	4733.8 (1)
1–2	4777.71	4777.6 (0)*
$^5D-{}^3P$ 3–2	5270.30	5270.2 (5)
2–1	5010.86	5010.5 (1)
1–1	5060.06	5058. (0)*
$^5D-{}^3H$ 4–6	4985.99	4985.6 (1)
3–5	5032.93	5032.2 (0)

* Line somewhat uncertain.

several metastable terms are based on the configurations $3d^6$ and $3d^54s$. The final term values are somewhat different from the ones used in the preliminary note.[32] The forbidden multiplet $^5D - {}^3F$ forms a prominent group of lines, the leading line being $^5D_4 - {}^3F_4$ at λ 4658.18; besides the five components observed by Merrill, four others have now been found.

The forbidden multiplet $^5D - {}^3P$ may also be expected, and three components have been found in RY Scuti, the leading line being $^5D_3 - {}^3P_2$ at λ 5270; this line is as strong as λ 4658. Hence, the two principal lines upon which an identification of forbidden [*Fe* III]

[35] Unpublished.

should be based are $^5D_4 - {}^3F_4$ at λ 4658.18 and $^5D_3 - {}^3P_2$ at λ 5270.30; next come $^5D_3 - {}^3F_3$ at λ 4701.54 and $^5D_2 - {}^3P_1$ at λ 5010.86.

The multiplet $^5D - {}^3H$ also appears in RY Scuti, with $^5D_4 - {}^3H_6$ (λ 4985.99) and $^5D_3 - {}^3H_5$ (λ 5032.93).

Several other very weak emission lines are present and may belong to other forbidden multiplets, but a complete discussion of these very weak lines would require additional material. The observed lines are listed in Table 17.

Summarizing, we may say that [*Fe* III] shows only two very privileged transitions. $^5D_4 - {}^3F_4$ at λ 4658.18 and $^5D_3 - {}^3P_2$ at λ 5270.30. This is fortunate, because it permits [*Fe* III] to appear fairly easily when the excitation conditions are fulfilled, because the excitation energy is distributed among a small number of lines.

It is quite certain that [*Fe* III] must be present in many novae at a certain stage; but its detection may be difficult when the bright bands are wide, because of blending:

[*Fe* III]	Neighboring Lines
4658.18.....	*N* III 4634–4641; *C* III 4650; *C* IV 4659; *O* II 4649
4701.54.....	*O* II 4699
4733.82.....	[*Fe* II] 4728; [*A* IV] 4740
5010.86.....	[*O* III] 5007; *He* I 5016; *Fe* II 5018
5270.30	[*Fe* II] 5273; *Fe* II 5276; [*Fe* VII] 5276

Remark concerning the forbidden lines of [*Fe* IV].—The spectrum of *Fe* IV has not yet been classified. But the analysis of *Fe* III makes it possible to locate approximately the centers of gravity of the metastable states of *Fe* IV:[36]

Fe III		*Fe* IV	
$3d^5$ (^6S) 4s	0 cm^{-1}	$3d^5$ (^6S)	0 cm^{-1}
(^4G) 4s	31,548	(^4G)	~ 32,000
(^4P) 4s	34,605	(^4P)	~ 35,100
(^4D) 4s	37,861	(^4D)	~ 38,500
(^4F) 4s	51,313	(^4F)	~ 52,100

The only transition in the observable region is $^4G - {}^4F$, requiring an excitation energy greater than 6 v.; it seems, therefore, that [*Fe* IV] should be weak. Several very weak emission lines appear in the

[36] See Edlén's report to the Paris meeting of 1939.

region around λ 5000; λ 5040.1 is also observed in AX Persei (see Sec. IV) and in NGC 7027, and may possibly be due to [*Fe* IV].

Variations in the spectrum.—In the Mount Wilson series, taken between 1921 and 1927, no appreciable changes[31] occurred in the spectrum. S. Gaposchkin[37] considers RY Scuti an eclipsing variable resembling β Lyrae. The radial velocities determined by Merrill from the emission lines show little variation. But this is no proof against the binary nature of this star.

TABLE 18

OBSERVATIONS OF RY SCUTI

Date 1939	Phase in Days	Velocity of λ 4472 in Kilometers per Second		Description of Spectrum
		Abs.	Em.	
Sept. 9.12.....	1.04	−162	.....	Absorptions very strong. No emission at *He* I 4472
Sept. 23.10.....	3.89	−170	− 1	Absorptions moderately faint. Emission at *He* 4472 strong
Oct. 5.07.....	4.74	−183	.....	Absorptions faint
Sept. 24.07.....	4.86	−100	+39	Absorptions faint. Emission at *He* I 4472 present
Sept. 14.16.....	6.08	−128	.....	Absorptions strong. Emission at *He* I 4472 absent
Sept. 29.07.....	9.86	−135	+22	Absorptions faint, but λ 4472 is sharp. Emission at *He* I 4472 present

Our spectrograms show rather marked changes in the intensities and profiles of the lines. The material is not sufficient to prove conclusively that these changes follow Gaposchkin's period, $P = 11.124939$ days, but they certainly take place within intervals of a few days. Using the last published minimum confirmed by the observations of J. G. Baker,[37] min. = JD 2428413.21, we compute the phases in days (Table 18).

Since only one line was measured, the scatter is no larger than may be attributed to errors of measurement. The mean of the three emission-line velocities is +21 km/sec, which compares reasonably well with Merrill's result, +30 km/sec. The absorption lines show P Cygni character throughout the period of 11 days. It is perhaps sig-

[37] *Harvard Ann.*, **105**, 511, 1937.

nificant that these absorption lines are strongest immediately following the primary minimum determined by Gaposchkin. It will be recalled that in β Lyrae the B5 component is also strongest soon after primary minimum. This component is essentially a P Cygni line.[38] On the other hand, it is certain that RY Scuti has no such large range in velocity as that observed in β Lyrae, for which $2K = 367$ km/sec.

III. OBSERVATIONS OF Be STARS

1. ζ Tauri

Attention has recently been drawn toward early-type stars surrounded by extended shells;[39] a typical example is ζ Tauri, which shows at times conspicuously sharp *He* lines at λλ 3965[39] ($2s^1S - 4p^1P^o$), 5016[40] ($2s^1S - 3p^1P^o$), and 3889[40] ($2s^3S - 3p^3P^o$), whereas all the other observed *He* lines are greatly broadened. Struve and Wurm have shown that this is due to the metastability of the $2s^1S$ and $2s^3S$ levels and to the resulting much higher populations of these levels in the case of dilution of radiation. The lines of ionized metals also arise from the shell and are not constant in intensity.

Ultraviolet spectra of ζ Tauri have recently been secured with the McDonald reflector. The series $2p^3P^o - ns^3S$ (to $n = 9$), $2p^1P^o - ns^1S$ (to $n = 9$), $2p^1P^o - nd^1D$ (to $n = 14$), and $2p^3P^o - nd^3D$ (to $n = 10$) are represented by very broad lines of relatively high intensity. The broadening of both the $2pP^o - nsS$ and $2pP^o - nd\,D$ series is obviously in agreement with the hypothesis of rotational broadening of these stellar lines.

On the contrary, *He* I 3613.64 ($2s^1S - 5p^1P^o$) appears as a rather sharp line, which is in agreement with the metastability of the $2s^1S$ level.

Our Process plates do not show the double Balmer continuum observed by Barbier and Chalonge,[41] beginning around λ 3720 and λ 3660, respectively, which they attribute to the stellar reversing layer and to the shell. This presumably indicates that the continuous

[38] Struve, *Observatory*, **57**, 265, 1934.

[39] Struve and Wurm, *Ap. J.*, **88**, 84, 1938.

[40] Biermann and Hachenberg, *Zs. f. Ap.*, **18**, 89, 1939; Davis, *Pub. A.S.P.*, **52**, 147, 1940.

[41] *Ap. J.*, **90**, 627, 1939.

hydrogen absorption is also variable. Incidentally, it should be noticed that the presence of strong, broad absorption lines of *He* I may distort the continuous background.

The sharp Balmer series due to the shell is easily followed to H_{30}; the Balmer continuum is rather strong and weakens several stellar *He* I lines.

TABLE 19

METALLIC LINES OBSERVED IN THE ULTRAVIOLET SPECTRUM OF ζ TAURI

λ	Int.	Identification			Intensity in α Cygni*	λ	Int.	Identification			Intensity in α Cygni*
		Elem.	λ	Int.				Elem	λ	Int.	
3243.8	1	*Fe* II	3243.72	8	3	3434.3	2	*Cr* II?	3433.70	75	8
3247.3	2	*Fe* II	3247.17	9	5	3442.7	2	*Mn* II	3441.98	30	8
3255.7	1	*Fe* II	3255.88	8	4	3454.0	1	*Ni* II?	3454.17	5	2
3259.1	2	*Fe* II	3258.77	10	6	3460.3	1	*Mn* II	3460.33	20	6
		Fe II	3259.05	10		3468.8	1	*Fe* II	3468.68	8	4
3276.1	1	*V* II	3276.12	1500	3 bl	3474.2	1	*Mn* II	3474.06	8	6
3281.2	1	*Fe* II	3281.29	7	4			*Mn* II	3474.15	8	
3289.2	1	*Fe* II	3289.35	7	3	3482.9	0	*Mn* II	3482.91	12	6
3295.4	1	*Cr* II	3295.42	30	10	3488.3	0	*Mn* II	3488.68	10	5
		Fe II	3295.81	6		3493.2	2	*Fe* II	3493.47	10	8
3306.9	1	*Cr* II	3307.04	30	3	3510.9	1	*Ti* II	3510.85	60	4
3329.5	2	*Ti* II	3329.48	70	5	3513.9	1	*Ni* II	3513.94	8	5
3335.9	2	*Cr* II?	3335.28	30	6 bl	3556.9	1	*V* II	3556.80	1500	3
3341.6	1	*Ti* II	3341.84	100	5	3585.7	2	*Cr* II	3585.31	60	10
3342.5	1	*Cr* II	3342.51	50	5			*Cr* II	3585.54	40	
3349.7	1	*Ti* II	3349.42	125	10	3596.1	1	*Ti* II	3596.05	60	3
3358.7	1	*Cr* II	3358.50	75	5	3621.4	1	*Fe* II	3621.27	6	5
3367.6	1	*Cr* II	3368.05	150	7	3624.9	1	*Ti* II	3624.84	70	4
3372.6	1	*Ti* II	3372.82	100	7	3631.0	1	*Cr* II?	3631.49	50	8
3373.7	1	*Ni* II?	3373.98	4	3	3640.6	1	*Ti* II?	3641.34	100	4
3380.5	1	*Cr* II	3379.82	60	6 bl	3715.4	1	*Cr* II	3715.19	20	5
3383.8†	2	*Ti* II	3383.77	125	6			*Cr* II	3715.45	18	
3387.7	1	*Ti* II	3387.85	50	5	3759.6	2	*Ti* II	3759.30	200	6
3394.1	1	*Cr* II	3393.86	30	6			*Fe* II	3759.46	6	
		Cr II	3394.32	30		3762.4	1	*Ti* II?	3761.32	200	6
3403.4	1	*Cr* II	3403.32	100	6	3845.3	2	.....	.....	.....	3
3407.3	1	*Ni* II	3407.32	8	4	3853.3	1	*Si* II	3853.67	3	3
3409.4	1	*Cr* II	3408.77	150	6	3856.2	2	*Si* II	3856.03	8	5
3421.5	1	*Cr* II	3421.20	75	7	3862.9	2	*Si* II	3862.59	6	6
3422.7	2	*Cr* II	3422.74	125	7	3935.9	1	*Fe* II	3935.94	6	3

* O. Struve, *Ap. J.*, **90**, 699, 1939.

† May be partly interstellar.

The new Process plates reveal many metallic lines in the ultraviolet region which are much sharper than the *He* I lines and thus arise in the outer shell. Most of these lines are at the limit of visibility. The identified lines have been collected in Table 19. There is good evidence for the presence of *Si* II, *Fe* II, *Ni* II, *Cr* II, and *Mn* II; *Ti* II is probably present and the two strongest lines of *V* II are suspected. The unidentified line λ 3845 observed by Struve in the A-type stars[42] is also present. The *Si* II lines are appreciably broadened,

[42] *Ap. J.*, **90**, 699, 1939.

compared with the cores of the Balmer lines. The other metallic lines are sharp, although not as sharp as the Balmer cores. All the observed absorption lines, except the $sp^2\ ^2D - 4p^2P^o$ transition of *Si* II, arise from a lower metastable level, in good agreement with the theory.[43]

2. The Visual Region of γ Cassiopeiae in March, 1940

Struve and Elvey[44] have recently found that the absorption lines of *Fe* III were strong and sharp in γ Cassiopeiae during the first part

TABLE 20

Fe III Lines in the Visual Region of γ Cassiopeiae

γ Cassiopeiae		Laboratory		
λ	Int.	λ	Int.	Transition
5063.7	1	5063.4	2	0–1
5074.1	1	5073.8	3	1–1
5086.7	1	5086.7	3	2–1
5114.4	0	.....	Predicted	1–2
5127.7	4	5127.3	6	3–2 2–2
5156.1	4	5156.0	4	4–3
5194.0	2	5193.9	4	3–3 2–3

of 1940. We obtained two grating spectrograms on March 16, 1940, extending from *Hβ* to *He* I 6678. Besides strong *Hβ* (central absorption with emission borders at distances of 1.98 A), *Hα*, *He* I [4713 (3A), 4922 (4A), 5016 (6A), 5048 (1A), 5876 (6A, 3E), 6678 (5A)], weak *Si* II [6347 (1A, 1E), 6371 (1A, 1E)], and very weak *N* II and *O* II (?), the spectrum shows only the $a^5D - 4p^5P^o$ multiplet of *Fe* III. All the components of this multiplet are present (Table 20). The lower level a^5D is metastable. The situation is similar to the case of P Cygni, where $a^5D - 4p^5P^o$ is also outstanding in the visual region, five components having been observed; but since the intensity

[43] The ultraviolet region of φ Per also shows the sharp *He* I line λ 3613.64. The three *Si* II lines are present, as well as the unidentified line λ 3845.3. Sharp lines of *Ti* II and *Cr* II may be present, but the measurements are uncertain.

[44] *Pub. A.S.P.*, **52**, 140, 1940.

gradient in γ Cassiopeiae is not as steep as in P Cygni, the multiplet is more fully represented.

The observed *Fe* III multiplet is the only one classified in the visual region which starts from a metastable level. Because of the strong dilution effect, the lines starting from metastable levels are greatly enhanced; for example, λ 5243.26 ($4d^7D_5 - 5p^7P^o_4$; lab. int. 10) and 5833.65 ($5s^7S_3 - 5p^7P^o_4$; lab. int. 10), which start from ordinary excited levels, are both absent. There is no other *Fe* III line which may be identified with certainty in the visual region of γ Cassiopeiae.

3. MtW 143

This spectrum has not appreciably changed since Merrill's observations[45] in 1931 and 1932. In the visual region, *Hα* and *He* I D_3 are very strong emissions. In the ultraviolet region *Hζ* is extraordinarily strong—doubtless because it is blended with *He* I. The last Balmer line seen in emission is H_9. Beyond this line there is only a suspicion of bright *He* I 3820. The continuous spectrum on the violet side of λ 3820 shows no absorptions or emissions. The permitted lines of *Fe* II are fairly strong, but there are no forbidden lines. *Fe* III is absent. No absorption lines could be seen with certainty. The radial velocities from the best plate are summarized in Table 21. The agreement with Merrill's mean velocity of −46 km/sec is satisfactory. The absence of *Mg* II 4481 in emission is conspicuous, in view of the great strength of *He* I and *Fe* II.

TABLE 21

RADIAL VELOCITIES OF MtW 143

Element	No. of Lines	Velocity
		km/sec
H	4	−46
He I	6	40
Fe II	9	−52

4. HD 218393

This is a remarkable representative of the small group of stars having extended atmospheres in which dilution of radiation sup-

[45] *Ap. J.*, **77**, 49, 1933.

presses lines which do not originate from metastable levels or from the ground levels. The spectrum has been described[46] by Merrill and by Harper. $H\alpha$ is a strong emission line; $H\beta$ is a fairly strong, double, emission line with weak absorption borders. The other Balmer lines, up to H_{24}, are sharp and deep absorption lines. $H\gamma$, $H\delta$, and $H\epsilon$ show traces of the double emission lines, and all Balmer lines give evidence of very weak Stark-effect wings. These wings are much weaker and narrower than in 17 Leporis and HD 190073—in keeping with the earlier spectral type of the reversing layer. The *He* I lines are very broad, and rather faint. *Mg* II 4481 and *Si* II are weak and intermediate in width. Several lines of *Fe* II are very sharp and resemble the cores of the *H* lines. The whole spectrum bears a decided resemblance to that of ζ Tauri, but *Ca* II is very strong in the shell of HD 218393, while it is weak in ζ Tauri, and the former shows no sharp lines of *He* I arising from metastable levels. The shell of HD 218393 corresponds to a lower degree of excitation than that of ζ Tauri. The progression of line widths from *H* to *He* is, however, similar and suggests in both cases stratification of the extended atmosphere.

The variability of the sharp α Cygni lines has already been commented upon by Merrill. Our plate shows them faintly. Merrill assigns to HD 218393 spectral type Ave; Harper proposes B9p; and the *Henry Draper Catalogue* gives A5p. The discrepancies in these data are due to the variability of the spectrum, on one hand, and to the intrinsic peculiarity of the spectrum, on the other. Evidently the reversing layer is of type B3 or B5. The large variations recorded by Harper and Merrill in the velocities of the *He* I lines suggest that the star is a binary—perhaps like φ Persei[47] or ζ Tauri. The outer shell corresponds to a later type, but because of the effect of dilution it is futile to assign it to a definite class. The radial velocities from our plate are summarized in Table 22. The large negative value derived from *He* I agrees with Harper's result in 1931 and 1932. Merrill obtained positive velocities in 1923. The available material is insufficient to trace the variations in velocity.

[46] Merrill, *Ap. J.*, **72**, 109, 1930; **78**, 109, 1933 (Star MWC 397); Harper, *Pub. Victoria*, **7**, 94, 1937.

[47] Hynek, unpublished.

5. HD 186568

This is not a Be star. *Hα* is a strong absorption line, and there are no other emission lines. The star was placed on the observing program because Harper[48] had called attention to the fact that, while *He* I 4472 is broad and fuzzy, *He* I 4026 is sharp. Our plate shows that *Mg* II 4481, *Ca* II K, and *He* I 4009 are extremely sharp. The *Si* II lines are fairly sharp. *He* I 4472 is diffuse, and *He* I 3820 is very diffuse. On our plate, *He* I 4026 also looks slightly diffuse but perhaps less so than does *He* I 4472. The *H* lines are very strong and show large broadening by Stark effect. It is surprising that *He* I 4009 should be sharp, while *He* I 4388 does not show. The lines of *He* I

TABLE 22

RADIAL VELOCITIES OF HD 218393 ON SEPTEMBER 9, 1939

Element	No. of Lines	Velocity
		km/sec
Sharp *H* cores	19	−26.1
Diffuse *He* I	4	−99
Sharp *Fe* II	4	−44.6
Slightly diffuse *Si* II	5	− 8.1
Slightly diffuse *Mg* II	1	−59.4
Sharp *Ca* II	2	− 8.3

which become strengthened when the radiation is diluted are not present. Hence, there is no reason to suspect the existence of an extended atmosphere. The ultraviolet region of the spectrum is normal and shows weak indications of the strongest *Mn* II lines. There is no similarity to HD 218393 or ζ Tauri. The radial velocity from our plate is −18 km/sec. The mean from Harper's three plates is −12 km/sec.

6. HD 160529

This star, classified as Oe5 in the *Henry Draper Catalogue*, was found by Merrill, Humason, and Burwell[49] to possess a bright line at *Hα*, while "the dark *Hβ* line is weak as if partly neutralized by emission." The rest of the spectrum was similar to that of α Cygni. Our observation confirms the similarity to α Cygni, but *Hβ* is an

[48] *Pub. Victoria*, **7**, 79, 1937.

[49] *Ap. J.*, **76**, 159, 1932.

emission line of the P Cygni type. Several strong *Fe* II lines, especially the strongest members of the multiplet $a^6S - z^6P^o$, λλ 4924, 5018, and 5169, show weak emission lines with violet absorptions. The star is clearly a P Cygni type object and resembles 17 Leporis.[50] The latter has a strong emission line at *Hα*[51] and occasionally a very weak P Cygni type emission line at *Hβ*. The *Fe* II lines have often been suspected of having faint emission borders on their red sides, but this has not been proved.

In HD 160529 the strongest absorption lines are H and K of *Ca* II. They are broad and deep, suggesting a large amount of turbulence. The mean radial velocity derived from these two lines is −91 km/sec. There can be little doubt that they originate in an expanding shell. The *H* lines are remarkably weak. Were it not for the P Cygni character of *Hβ* we should be inclined to attribute this to low hydrogen content, as in υ Sagittarii.[52] Our plate does not extend to the limit of the Balmer series, and we have no record of the drop in the continuous spectrum. The velocities derived from the *H* lines show a considerable range. The strongest lines give:

Hδ	− 62.5 km/sec
Hγ	− 90.3
Hβ	−120.9

This apparent increase in the velocity of expansion as we pass from the weaker lines near the Balmer limit to the stronger lines showing P Cygni structure is common in the spectra of expanding shells. A similar effect is present in *Fe* II, the mean from all thirty absorption lines being −67 km/sec, while the members of multiplet $a^6S - z^6P^o$ give

λ 4924	−109.1 km/sec
5018	−133.9
5169	−136.7

Table 23 gives a summary of the radial velocities. *Mg* II 4481 is a fairly strong and sharp line. Since we know that dilution of the radiation tends to weaken this line, it is reasonable to suppose that it belongs to the reversing layer, not to the outer shell. The radial veloci-

[50] Struve, *Ap. J.*, **76**, 85, 1932. [51] *Ap. J.*, **90**, 727, 1939.

[52] Struve and Sherman, *Ap. J.*, **91**, 428, 1940; Greenstein, *Ap. J.*, **91**, 438, 1940.

ty of the reversing layer would then be −33 km/sec; and the maximum velocity of expansion, with respect to the reversing layer, would be of the order of −100 km/sec.

TABLE 23

RADIAL VELOCITIES OF HD 160529 ON SEPTEMBER 11, 1939

Element	No. of Lines	Velocity	Element	No. of Lines	Velocity
		km/sec			km/sec
H (absorption)	9	−49.2	*V* II (absorption)	2	−36.5
H (emission)	1	+39.0	*Cr* II (absorption)	15	−30.4
Fe II (absorption)	30	−67.1	*Ca* II (absorption)	2	−91.4
Fe II (emission)	4	+32.3	*Sc* II (absorption)	2	−19.5
Fe I (absorption)	9	−33.6	*Ni* II (absorption)	1	−45.2
Si II (absorption)	3	−37.2	*Mg* II (absorption)	1	−32.9
Ti II (absorption)	24	−42.3			

The *H* lines show no wings produced by Stark effect, and if our interpretation of *Mg* II 4481 is correct, the reversing layer is that of a supergiant, like *α* Cygni.

7. HD 190073

The remarkable structure of the *Ca* II lines and the presence of bright *Na* I $D_{1,2}$ was announced by Merrill.[53] The *H* lines were described by him and by Beals.[54] The spectrum has not changed much since 1928. The emission lines of *Ti* II and *Fe* II—all permitted—are fairly conspicuous on our plate. The strong *Fe* II lines λλ 4924, 5018, and 5169 show P Cygni structure, but the violet absorptions are weak, while the emissions are strong. Several other strong *Fe* II lines also suggest P Cygni structure. The emission lines of *H* are conspicuous as far as *Hδ*; they are quite broad and, in the case of *Hδ* and *Hγ*, may be centrally reversed. Otherwise, the *H* lines agree with Beals's description. *Hε* is complicated by *Ca* II H, but *Hζ* seems to show an exceedingly weak double emission line. The higher members of the Balmer series are in absorption only. These lines are unusually strong and give indication of large Stark effect. The wings of the higher members blend so that the background of the continuous spectrum rapidly declines toward the vio-

[53] *Ap. J.*, **77**, 51, 1933.

[54] *Pub. A.S.P.*, **51**, 219, 1939.

PLATE XIII

PLATE XIII

THE SPECTRUM OF HD 190073

UNIV. OF MICH.

let. The continuous spectrum on the violet side of λ 3647 is very weak. This feature permits several emission lines to stand out conspicuously against the faint continuous background. The emission lines, measured in the ultraviolet region and between the Balmer lines, are given in Table 24. These emission lines are fairly broad, suggesting a considerable dispersion in the motion of the shell.

In addition to the absorption lines described by Merrill, there are a number of faint but sharp absorption lines of *Si* II (λλ 3854, 3856, 3863, 4128, and 4132), of *Fe* II (violet borders of emission lines), and a few others, some of which have not been satisfactorily identified.

TABLE 24

EMISSION LINES IN HD 190073

Line	Intensity	Line	Intensity
Ti II 3535.41	1	*Cr* II 3677.86	1
Fe I 3581.21	0	*Ti* II 3685.20	10
Cr II 3585.31	1	*Ti* II 3706.22	1
Ti II 3596.06	2	*Ti* II 3741.65	1
Fe I 3608.87	0	*Ti* II 3759.30	12
Cr II 3613.21	1	*Ti* II 3761.32	12
Cr II 3631.49	3	*Fe* I 3859.92	2
Ti II 3641.34	0	*Ti* II 3900.54	2
Fe I 3647.85	0		

For example, a line at λ 3814 can hardly be the faint *Fe* II line 3814.12 or the *Ti* II line 3814.60.

The structure of the *Ca* II lines agrees with Merrill's description. The only difference is in the position of the faint narrow emission within the broad violet absorption component. On Merrill's plates this emission was unsymmetrically displaced toward the red from the middle of the absorption line.[55] On our plate the emission is clearly displaced toward the violet side of the middle of the absorption line. The radial velocities agree well with those published by Merrill.

The most significant fact about HD 190073 is the existence of an undisplaced reversing layer of high density in which the Stark wings of the *H* lines originate. Superposed over this spectrum is the P Cyg-

[55] See Merrill's Fig. 1, *Ap. J.*, **77**, 53, 1933.

ni type structure produced in the expanding shell. The similarity of this phenomenon to that observed in 17 Leporis has been discussed elsewhere.[56]

8. Stars with Forbidden [*Fe* II] Lines

Fe II has a large number of metastable levels of multiplicities 6, 4, and 2 based on the configurations $3d^64s$, $3d^7$, and $3d^54s^2$. In Dobbie's table,[57] all the 24 levels up to 38,215 cm^{-1} are metastable.

It is well known that Merrill[58] has identified several [*Fe* II] multiplets in η Carinae, and these lines have subsequently been found in many other stars. Heretofore, only the following transitions have been observed:[59]

a^6D-a^6S	a^4F-b^4F
$-b^4P$	$-a^4G$
$-b^4F$	$-b^4P$
	$-a^4H$

The two lowest metastable levels are a^6D and a^4F, the next one being a^4D. It is safe to expect the two multiplets $a^6D - b^4D$ and $a^4F - b^4D$. These groups of lines are in the observable ultraviolet region. We should also expect other transitions, such as $a^4D - b^2D$, which arrive in the higher level, a^4D. No transitions involving doublet terms have been found thus far, and several such multiplets may be expected.

In order to search for these lines, we selected a number of stars having strong [*Fe* II] lines. Our program included WY Geminorum, W Cephei, Boss 1985, Boss 5481, BD+11°4673, HD 45677, etc. Among these stars, WY Geminorum and Boss 1985 proved to be best suited for our purpose.

WY Geminorum (HD 42474, mag 7.4–7.9) varies irregularly and rather slowly. It was classified at Harvard as ordinary K5 and at Mount Wilson[60] as M3ep. It is most certainly a multiple object, the ultraviolet region being perfectly free from the late-type spectrum and showing broad Balmer lines, down to H_{23}, with sharp centers.

[56] Struve, *Proc. Nat. Acad.*, **26**, 117, 1940.

[57] *Ann. Solar Phys. Obs., Cambridge*, **5**, Part I, 1938.

[58] *Ap. J.*, **67**, 391, 1928. [59] I. S. Bowen, *Rev. Mod. Phys.*, **8**, 80, 1936.

[60] Adams and collaborators, *Ap. J.*, **81**, 220, 1935.

PLATE XIV

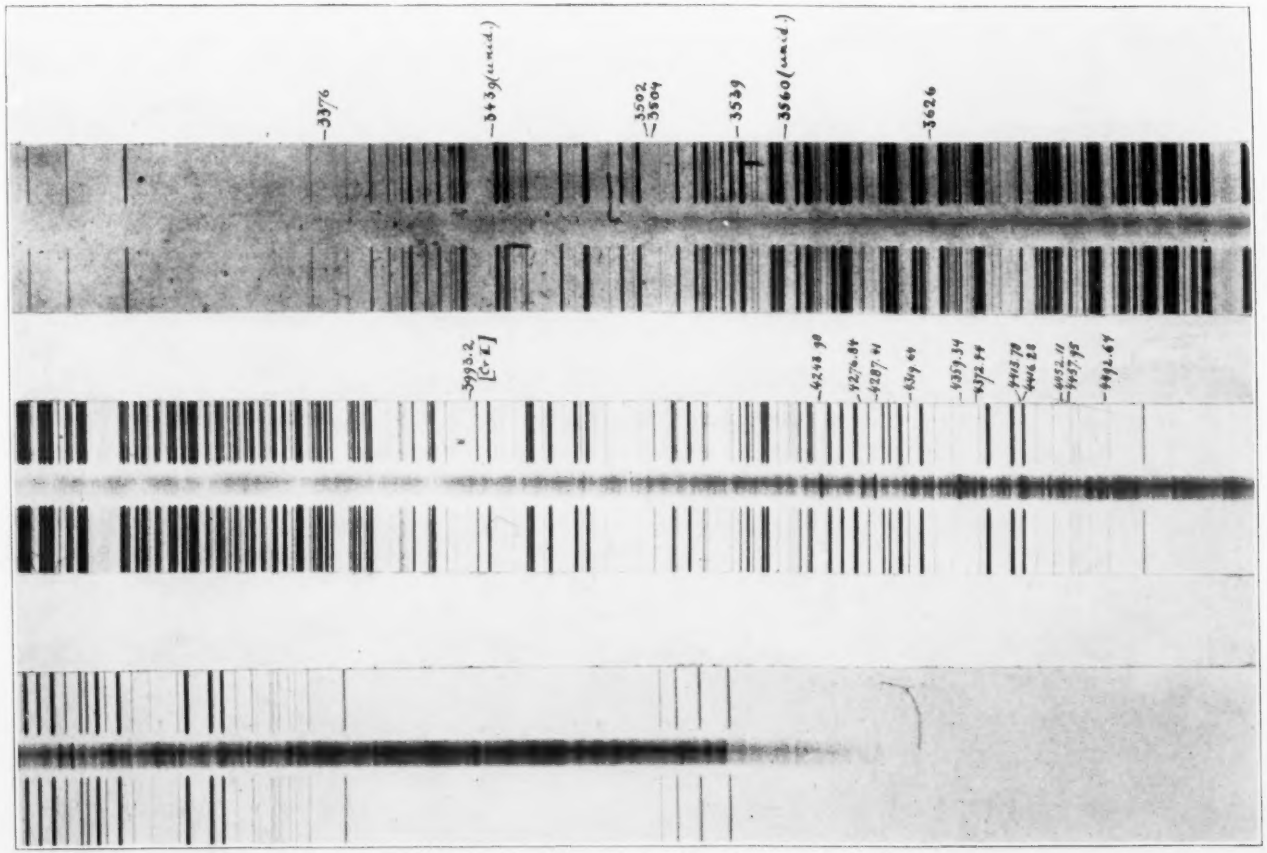

THE SPECTRUM OF WY GEMINORUM

Except for the unidentified lines λ 3439 and λ 3560 and the [*Cr* II] line χ 3992, only lines of [*Fe* II] have been indicated

UNIV. OF WICH.

There is a sharp and narrow line of *Ca* II K. A strong line at λ 3820 must be due to *He* I. The earlier component is of type B3. Redman[61] observed the photographic region of the spectrum with a dispersion of 92 A/mm at $H\gamma$ and found six emission lines, five of which had been identified as [*Fe* II]; the sixth line is λ 4068.8, which Redman believes is also due to [*Fe* II].

The star W Cephei is similar to WY Geminorum. It was classified as Kp at Harvard and as Mep at Mount Wilson, and it also shows [*Fe* II] lines, though they are weaker than in WY Geminorum. The continuous spectrum extends far into the ultraviolet, and there is a strong, but sharp, line at *Ca* II K. The Balmer lines are not clearly seen in the ultraviolet region, but there are several other absorption lines which we have not yet fully identified. The strongest is at λ 3708. This is probably not *Fe* I 3710, because the stronger laboratory line *Fe* I 3720 is not pronounced in the star. The spectrum is mostly continuous, but some of the weaker features may be due to *Fe* I. It is possible that the spectrum of a bright late-type star is combined with that of a relatively faint star of very early type—so early, in fact, that the Balmer absorption lines are no longer visible with the small dispersion which we have used for the ultraviolet region.

Boss 1985 (HD 60414–60415), classified as K5 + Be at Harvard and as M2ep at Mount Wilson, is also a double object, consisting of an M star and a Be star. It is known to possess [*Fe* II] lines. The structure of the H lines is remarkable. A bright line of appreciable width is flanked on the red side by a narrow, deep absorption line; and this structure is superposed over a broader line, having Stark-effect wings, especially on the violet side of the emission line. The emission line is strong in $H\epsilon$, $H\zeta$, and H_9. It can still be detected in H_{10}. The higher members of the Balmer lines are well visible, and their strength, as well as the intensity of *He* I 3820, suggest that the type of the earlier component is B3e. The blending with the late-type star renders it difficult to identify the absorption lines even in this region.

Boss 5481 (HD 203338-9) is a visual binary (Ko + Ao at Harvard; K5p at Mount Wilson); the [*Fe* II] lines are present but are

[61] *M.N.*, **92**, 118, 1932; *Pub. Victoria*, **6**, 34, 1931.

much weaker than in Boss 1985. On our plates the earlier component is clearly of type B2: the *He* I lines are strong, and there are lines of *O* II. This spectrum predominates on the violet side of $H\gamma$; but even $H\beta$, belonging to it, is still clearly visible. The forbidden [*Fe* II] lines are very weak, and it is probable that they originate in the outer atmosphere of the K star. The binary is listed by Aitken as No. 14864. The components have magnitudes 5.6 and 9.9; their separation is about 5″ in position angle 45°. It is doubtful that the light of the fainter visual component has entered the slit of the spectrograph. The brighter component must itself be composite, and the excitation of the gases in the K star by the B star is doubtless responsible for [*Fe* II] lines. The relatively great intensity of the B star is disadvantageous to the emission lines, and it is possible that they are intrinsically as strong as in other stars of this group.

BD+11°4673, already considered in Section II, and Z Andromedae, which will be discussed in Section IV, were poor in [*Fe* II] at the time of our observations.

HD 45677 was richer in [*Fe* II] and confirmed the results obtained from the other stars. The spectrum has not changed appreciably since the time of Merrill's observations.[62] This star is not composite in the sense that a late-type spectrum is superposed over that of an early type. The spectrum of the reversing layer shows fairly broad lines of *He* I and sharper lines of *O* II, *C* II, *N* II, and *Mg* II, together with very broad Stark-effect wings of *H;* it is of type B2. The shell is responsible for the emission lines of *Fe* II, [*Fe* II], [*O* I] 6300, etc., for the emission lines of $H\alpha$, $H\beta$, $H\gamma$, and $H\delta$ and for the exceedingly sharp central absorption lines of *H* which are followed to H_{29} or H_{30}. The radial velocities from the lines of the shell agree with those from the reversing layer. It is significant that the sharp component of $H\zeta$ is not greatly strengthened, and that *He* I 3965 is not visible as a strong, sharp line. Evidently *He* I is not excited in the shell; otherwise we should see those lines which arise from metastable levels. The *Ca* II K line is sharp and fairly strong. Its velocity agrees with that of the other lines.

Our investigation is based mainly on WY Geminorum and Boss 1985, and we decided to confine the present discussion to the region of wave lengths shorter than λ 4000, which is practically free from

[62] *Ap. J.*, **67**, 405, 1928.

PLATE XV

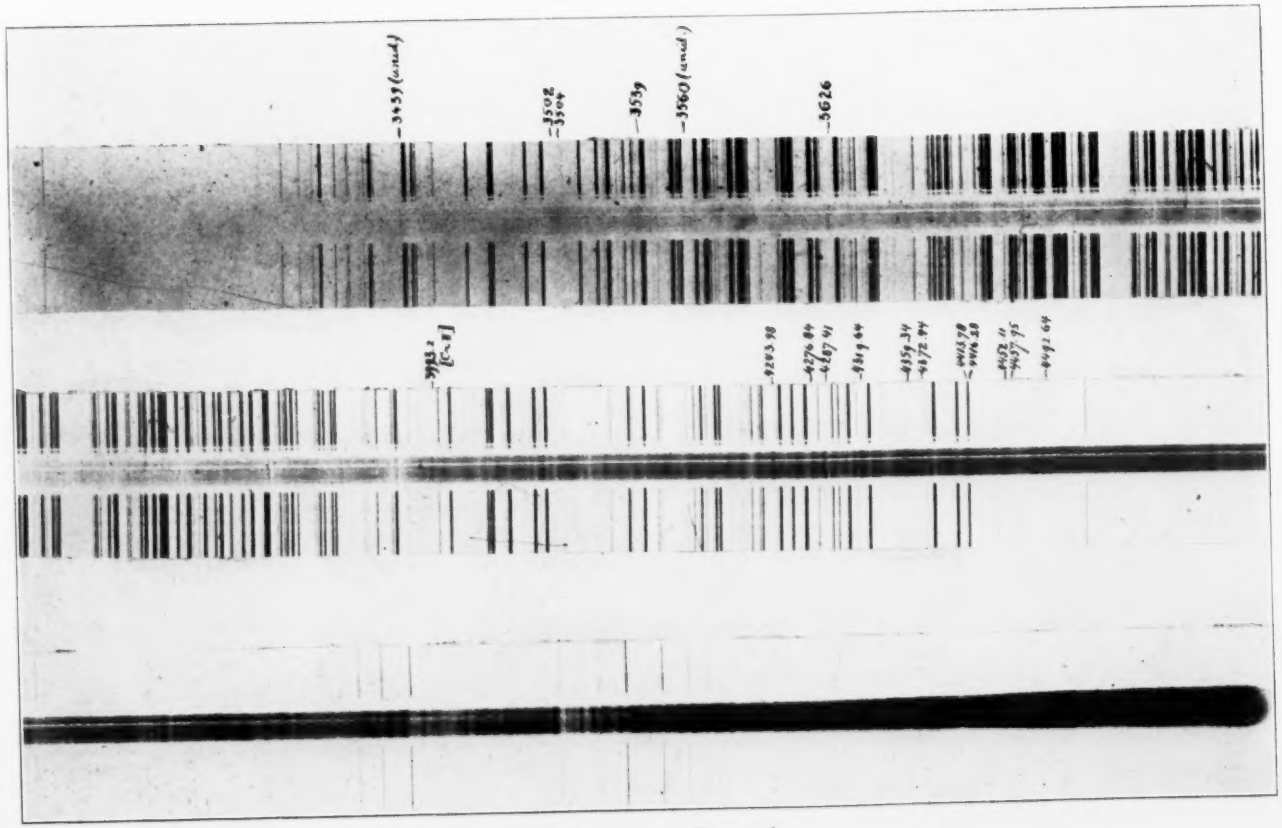

THE SPECTRUM OF BOSS 1985

Except for the unidentified lines λ 3439 and λ 3626 only lines of [*Fe* II] have been indicated

UNIV. OF MICH.

the spectrum of the late-type component. The permitted lines of *Fe* II are weak compared with the forbidden transitions. Our results for the newly observed forbidden multiplets are collected in Table 25.

TABLE 25

NEW FORBIDDEN TRANSITIONS OF [*Fe* II]

Transition	λ Predicted	λ Observed in WY Geminorum	λ Observed in B 1985
	Lower Level a^6D		
$a^6D_{\frac{1}{2}}-b^4D_{\frac{1}{2}}$	3289.5	3290 (2)	3289.4 (2)
$D_{\frac{1}{2}}\quad D_{1\frac{1}{2}}$	3289.9		
	Lower Level a^4F		
$a^4F_{4\frac{1}{2}}-b^4D_{3\frac{1}{2}}$	3376.2	3376.6 (2)	3376.2 (3)
$F_{4\frac{1}{2}}\quad D_{2\frac{1}{2}}$	3387.1	3387.8 (1)	3386.9 (1)
$F_{3\frac{1}{2}}\quad D_{3\frac{1}{2}}$	3441.0	3441.0 (1)	.....
$F_{3\frac{1}{2}}\quad D_{2\frac{1}{2}}$	3452.3	3452.2 (2)	3452.0 (1)
$F_{3\frac{1}{2}}\quad D_{1\frac{1}{2}}$	3455.1	3455.3 (1)	.....
$F_{2\frac{1}{2}}\quad D_{2\frac{1}{2}}$	3501.6	3502.1 (2 bl)	3501.5 (2 bl)
$F_{2\frac{1}{2}}\quad D_{1\frac{1}{2}}$	3504.5	3504.4 (4)	3504.2 (4)
$F_{2\frac{1}{2}}\quad D_{\frac{1}{2}}$	3504.0		
$F_{1\frac{1}{2}}\quad D_{3\frac{1}{2}}$	3524.4	3524.4 (0)	.....
$F_{1\frac{1}{2}}\quad D_{2\frac{1}{2}}$	3536.2	3536.2 (0)	.....
$F_{1\frac{1}{2}}\quad D_{1\frac{1}{2}}$	3537.2	3539.1 (3)	3538.8 (3)
$F_{1\frac{1}{2}}\quad D_{\frac{1}{2}}$	3538.7		
	Lower Level a^4D		
$a^4D_{1\frac{1}{2}}-a^2S_{\frac{1}{2}}$	3502.0	3502.1 (2 bl)	3501.5 (2 bl)
$D_{1\frac{1}{2}}-b^2D_{2\frac{1}{2}}$	3625.8	3626.5 (4)	3626.5 (5)
$D_{\frac{1}{2}}\quad D_{1\frac{1}{2}}$	3664.7	3665.7 (2)	.....
$D_{1\frac{1}{2}}-c^2D_{1\frac{1}{2}}$	3385.0	3385.0 (1)	3385.8 (1)
$D_{1\frac{1}{2}}\quad D_{2\frac{1}{2}}$	3390.7	3390.7 (0)	.....

The following conclusions have been derived:

1. The excitation potential reached is 4.72 v. instead of 3.2 v.

2. No [*Fe* II] transition has been observed between doublets and sextets. On the other hand, several forbidden lines connect metastable doublets and quartets.

3. In the $a^6D - b^4D$ multiplet, the spectral region observable

with our instrument permitted only the observation of the $\frac{1}{2}$–$\frac{1}{2}$ transition at λ 3289.5.

4. Forbidden lines arriving at the a^4D level are observed. Several new forbidden multiplets which should appear above λ 4000 may be expected, since the [*Fe* II] spectrum is so strong in these stars. But, owing to the presence of the late-type component, our present material is not sufficient for a systematic discussion of these multiplets, although it does show several new forbidden lines.[63]

5. In the $a^4F - b^4D$ multiplet the observations are roughly in agreement with the relative intensities computed from the formulae by A. Rubinowicz.[64]

TABLE 26

FORBIDDEN TRANSITIONS $a^6S - b^4D$ OF [*Cr* II]

Transition	λ Predicted	λ Observed
$2\frac{1}{2}-3\frac{1}{2}$	3993.2	3993.2 (3)
$2\frac{1}{2}-2\frac{1}{2}$	3992.9	
$2\frac{1}{2}-1\frac{1}{2}$	3991.8	
$2\frac{1}{2}-2\frac{1}{2}$	3991.1	

6. The spectra of WY Geminorum and Boss 1985 are so rich in [*Fe* II] that it is interesting to search for forbidden transitions of other singly ionized metals. A fairly strong line measured at λ 3993.2 agrees with the forbidden transitions $a^6S - b^4D$ of [*Cr* II], a^6S being the ground level of *Cr* II (Table 26).

7. Two strong unidentified lines appear at λ 3439.0 and λ 3559.6 (see Pl. V); they are also present in HD 45677.

IV. PECULIAR SYSTEMS SHOWING SIMULTANEOUSLY SPECTRAL FEATURES DUE TO VERY HIGH AND VERY LOW EXCITATION

Several recent discoveries have shown that systems consisting of a late-type giant and a hot companion are not infrequent.[65] This sec-

[63] New observations are planned in this connection. It would be interesting to find a pure Be star showing [*Fe* II] with the same degree of sharpness and completeness. The spectrum of HD 45677 shows that the presence of a late-type binary component is not necessary for the production of [*Fe* II].

[64] Rubinowicz and Blaton, *Erg. Ex. Naturwissenschaften*, **11**, 176, 1932.

[65] In Section III we have considered such objects as WY Gem and W Cep, which consist of a late-type star and of an early B star. Other examples are VV Cep, ζ Aur, ε Aur, etc.

MICH. UNIV.

PLATE XVI

THE SPECTRUM OF Z ANDROMEDAE

tion is devoted to the discussion of several objects of this type, showing simultaneously an M-type spectrum and forbidden lines of high excitation.

1. Z Andromedae

The spectrum of Z Andromedae has been described by H. H. Plaskett.[66] During the entire period of his observations, 1923–1926, it showed only emission lines. Hogg[67] found *TiO* bands in absorption, which increased in intensity while the star was fading in light. The recent outburst in the total light of the star[68]—was accompanied by a remarkable change in spectrum.[69] The star is now of the P Cygni type. The permitted emission lines of lower excitation (*Fe* II, *Ti* II, etc.) are present, and are fairly conspicuous. The forbidden lines of [*Fe* II] are much weaker than on Plaskett's plates. The strong emission lines attributed by Plaskett to the nebular part of Z Andromedae have disappeared.

It has been suggested[70] that the *TiO* spectrum comes from an M-type companion, while the emission lines of Plaskett's "nebula" are excited in a tenuous shell surrounding a very hot, small star. The emission lines of the "star" (*Fe* II, etc.) could perhaps come from

[66] *Pub. Victoria*, **4**, 119, 1928.

[67] *Pub. A.S.P.*, **44**, 328, 1932; *Pub. A.A.S.*, **8**, 14, 1934.

[68] L. Campbell, *Pop. Astr.*, **47**, 571, 1939; K. Himpel, *Die Sterne*, **19**, 210, 1939, and **20**, 14, 1940.

[69] Struve and Elvey, *Pub. A.S.P.*, **51**, 297, 1939. [*Note added in proof:* According to L. Campbell, the visual magnitude of Z And was 8.2 when our first plate was taken—September 14, 1939. The star remained bright until December 5, 1939, when the last spectrogram of this series was obtained. Two spectrograms were secured after the star became again observable in the east—on May 12 and 15, 1940. The entire aspect of the spectrum has changed. It again resembles that described by Plaskett, but the "nebular" spectrum is more pronounced on our plates than on Plaskett's. The visual apparent magnitude was estimated to be 9.3. The spectrum shows almost only emission lines. The forbidden lines of [*O* III] are strong, with the auroral transition relatively strong—as in novae. There is some indication of the fluorescence lines of *O* III, but λ 3760 is weak or absent. [*Ne* III] and [*Ne* V] are very strong; *He* I is strong; *He* II 4686 is very strong. *N* III 4634–4640 is fairly strong. The *H* lines are visible in emission as far as H_{10}. The higher members are not clearly seen, but there is a suspicion of several P Cygni type lines at λλ 3687, 3693, etc. The continuous spectrum shows a marked drop near λ 3647, showing that the continuous Balmer absorption is not completely filled in by emission. Several permitted emission lines of *Fe* II are present, but the forbidden lines of [*Fe* II] have not with certainty been identified. The development of Z And bears strong resemblance to that of a nova.]

[70] Hogg, *Pub. A.A.S.*, **8**, 14, 1934.

the outer layers of the M star, excited by the radiation of the hot star.

The recent outburst permits us to clarify this picture. The spectrum of *TiO* has disappeared, together with the emission lines of *He* II, *N* III, *O* III, etc. The permitted emission lines of *H*, *Fe* II, *Ti* II, etc., have remained, but they now have violet absorption borders. The forbidden lines are weak. There can be little doubt that the outburst occurred in the hot star and that the light of the M star is lost in the increased brilliance of that object. The presence of emission *Fe* II, etc., suggests that these lines are produced in the shell which surrounds the hot star. The weakening of [*Fe* II] may well be caused by the decrease in dilution of radiation occasioned by the expansion of the photosphere. The disappearance of emission lines of *He* II, etc., may be due to the fact that the exciting radiation in the extreme ultraviolet has changed, or it may point to the possibility that these lines originate in the atmosphere of the M star and have been obliterated by the outburst. The latter hypothesis would require a strengthening of the emission lines because of the increased radiation of the hot star. But theoretical considerations suggest that there may be a lag of months or even years before the ionization of the extremely tenuous gas of the M star adjusts itself to the changes in radiation of the hot star. Whether the presence of emission lines of *He* II, etc., after the outburst[71] should be considered as evidence that their light was not suppressed is not certain at the present time.

The succession of events in Z Andromedae resembles those in T Coronae Borealis. This nova of 1866 was observed at several places during its recent rise in brightness.[72] Hachenberg and Wellmann have established the binary nature of this object.

Table 27 shows the intensities of the lines measured on our first and out last plates of Z Andromedae. In general, the absorption lines became more prominent and the emission lines slightly fainter. But the change was not conspicuous. The dilution of the exciting radiation could not have been very pronounced, because *Mg* II 4481 and several *Ti* II lines were present in absorption. This is interest-

[71] *Die Sterne*, **19**, 210, 1939.

[72] Hachenberg and Wellmann, *Zs. f. Ap.*, **17**, 246, 1939; Wellmann, *Zs. f. Ap.*, **19**, 16, 1939; Joy, *Pub. A.S.P.*, **50**, 300, 1938; Minkowski, *Pub. A.S.P.*, **51**, 54, 1939.

TABLE 27

INTENSITIES OF LINES IN Z ANDROMEDAE

λ	Absorption 1939		Emission 1939		λ	Absorption 1939		Emission 1939	
	Sept. 16	Dec. 5	Sept. 16	Dec. 5		Sept. 16	Dec. 5	Sept. 16	Dec. 5
Ti II					*Ti* II—*Cont.*				
3372.8	3	.....	0	.....	4572.0	0	1	1	0
3383.8	3	.....	0	.....	5336.8	0	0	2	1
3387.8	2	.....	0	.....					
3394.4	.....	2	.....	0	*Fe* II				
3444.3	1	.....	0	.....	3468.5	0	1	0	0
3456.4	.....	2	.....	0	3493.5	1	1	0	0
3465.7	1	1	0	0	3499.9	1n	.....	0	.....
3477.2	1	2	0	0	3507.4	1	1	0	0
3491.1	.....	1	.....	0	3564.5	1n	.....	0	.....
3504.9	1n	3	0	0	3621.3	2	1	1	0
3510.9	1	1	0	0	3634.9	.....	1	.....	0
3520.3	1	.....	0	.....	3764.1	.....	2	.....	0
3535.4	.....	1	.....	1	3814.1	1nn	.....	3nn	.....
3596.1	0	2	0	0	3824.9	.....	1	.....	0
3624.8	.....	2n	.....	0	3906.0	.....	0	.....	0
3641.3	0	1	0	0	3935.9	1	2	1	0
3650.8	0	3	0	0	3938.7	2	1	2	1
3662.2	1	1	0	0	3945.2	.....	0	.....	2
3685.2	3	4	0	0	3981.6	1nn	.....	1	.....
3741.7	1	5	0	0	4002.1	.....	0	.....	0
3757.7	.....	1	.....	0	4122.7	1	0	0	2
3759.3	4	4	1	0	4173.5	0	0	3	3
3761.3	3	4	2	0	4178.9	0	0	5	3
3776.1	.....	1	.....	0	4233.2	2	3	6	5
3900.5	1	2	1	1	4258.2	.....	0	.....	1
3913.5	1	4	3	2	[4287.4]	0	.....	1	.....
4012.4	1	0	4	1	4296.6	2	1	0	1
4028.4	1	.....	2	.....	4303.2	0	0	1	0
4053.8	0	0	1	1	4351.8	0	0	3	4
4161.5	1	1	2	1	[4359.4]	0	0	1	1
4163.7	0	2	3	1	4379.4	.....	0	.....	1
4171.9	1	.....	1	.....	4384.3	0	.....	3n	.....
4290.2	0	1	2	1	4385.4	.....	0	.....	1
4294.1	0	2	0	0	4416.8	0	0	3	1
4300.1	.....	3	.....	0	4455.3	.....	1	.....	0
4312.9	1n	1nn	1n	0	4489.2	.....	0	.....	1
4337.9	0	.....	1	.....	4491.4	0	0	2	1
4374.8	0	0	2n	1	4508.3	.....	1	.....	1
4395.0	1n	0	3	1	4515.3	0	1	2	2
4399.8	0	.....	2	.....	4520.2	0	.....	0	.....
4443.8	0	2	2	1	4522.6	0	0	1	1
4468.5	1	2	1	0	4534.2	.....	1	.....	1
4488.3	0	.....	1	.....	4541.5	0	0	1	1
4501.3	1	.....	1	.....	4549.5	1	3	3	3
4534.0	0	.....	1	.....	4555.9	0	1	2	1
4563.8	0	2	1	0	4576.3	.....	1	.....	1

TABLE 27—*Continued*

λ	Absorption 1939		Emission 1939	
	Sept. 16	Dec. 5	Sept. 16	Dec. 5
Fe II—*Cont.*				
4583.8	0	1	5	5
4629.3	0	0	4	2
4666.8	0	.....	1nn	.....
4731.5	0	0	1n	1
4923.9	3	1	3	4
5018.5	7	1	4	4
5169.1	2	2	4	3
5197.6	1	1	2	1
5234.6	1	1	1	1
5276.0	2	.....	1	.....
5284.1	0	.....	2	.....
5316.6	1	0	5	3
5362.9	1	1	3	2
5534.9	.....	0	.....	1
6149.3	.....	0	.....	3
Cr II				
3391.4	1	.....	0	.....
3394.4	.....	2	.....	0
3403.3	2	.....	0	.....
3408.8	3	2	0	0
3421.2	2	1	0	0
3422.7	2	2	0	0
3433.3	2	3	1	0
3585.3	3n	3	0	1
3603.8	1	2	1	0
3608.7	1	1	0	0
3613.2	1n	.....	0	.....
3631.5	2	3	3	1
3644.7	1	.....	0	.....
3677.8	2	3	0	0
3715.3	2	3	2	1
3727.4	2	2n	1	0
3754.6	.....	1	.....	0
3765.6	.....	1	.....	0
3905.6	1	.....	2	.....
3979.5	.....	1n	.....	0
4242.4	1	1	0	1
4261.9	1	.....	0	.....
4634.1	.....	1	.....	0
4848.3	.....	0	.....	1
H				
H_{28}	1	.....	0	.....
H_{27}	1	.....	0	.....
H_{26}	2	1	0	0
H_{25}	2	2	0	0
H—*Cont.*				
H_{24}	3	3	0	0
H_{23}	4	4	0	0
H_{22}	4	4	0	0
H_{21}	4	4	0	0
H_{20}	5	5	0	0
H_{19}	4	4	0	0
H_{18}	6	6	0	0
H_{17}	6	6	0	1
H_{16}	7	7	0	1
H_{15}	7	9	1	4
H_{14}	8	6	1	1
H_{13}	8	7	0	1
H_{12}	8	7	2	6
H_{11}	6	7	0	4
H_{10}	10	8	1	3
H_{9}	9	10	2	3
H_{8}	10	8	2	4
$H\epsilon$	9	8	4	7
$H\delta$	10	7	5	8
$H\gamma$	9	4	7	12
$H\beta$	6	0	10	10
Fe I				
3719.9	.....	0	.....	0
3737.0	1	1	3	1
3748.3	1	3	0	0
3763.8	2	.....	1	.....
3767.2	1n	1	0	0
3820.4	.....	1nn	.....	0
3827.8	.....	1	.....	0
3850.0	0	1	0	0
3860.0	.....	0	.....	1
3872.5	.....	0	.....	1
4005.3	0	.....	1	.....
4045.8	0	.....	0	.....
4143.9	0nn	.....	0	.....
4202.0	0	.....	1	.....
Mn II				
3439.0	0	.....	2	.....
3442.0	3	3	3	2
3460.3	2	1	1	0
3474.1	2	2	1	0
3482.9	1n	1n	0	0
3488.7	1	.....	0	.....
3495.8	1	.....	0	.....
3497.5	1	.....	0	.....

TABLE 27—*Continued*

λ	Absorption 1939		Emission 1939		λ	Absorption 1939		Emission 1939	
	Sept. 16	Dec. 5	Sept. 16	Dec. 5		Sept. 16	Dec. 5	Sept. 16	Dec. 5
V II					*Ca* II				
3517.3	2n	1n	0	0	3706.4	3	1	3	0
3556.8	1	.....	0	.....	3737.0	1	1	3	1
3589.7	2	1	0	0	3933.7	9	8	4	3
3592.0	.....	1	.....	0	3968.5	10	8	0	0
3593.3	.....	1	.....	1					
3727.4	2	2n	1	0	*Mg* I				
3745.8	1	1	0	0	3829.4	1	.....	0	.....
3847.3	.....	1	.....	0	3832.3	1	3	0	1
3896.2	.....	1nn	.....	1	3838.0	2	3	1	1
3903.3	.....	0	.....	0					
3973.6	.....	1	.....	0	*Mg* II				
3997.1	0	.....	0n	.....	4481.3	1	1	0	0
4005.7	.....	0	.....	0					
4035.6	0	.....	0	.....	*Si* II				
					3856.0	1	1	1	1
Ni II					3862.6	1n	1	0	0
3471.4	2n	1	0	0	4128.1	1	1	0	2
3513.9	4	3	1	1	4130.9	2	1	0	0
3576.8	2	3	2	1					
3769.5	3	5	0	0	*He* I				
4067.0	3	0	0	0	4471.5	1	.....	0	.....
4362.1	0	0	0	0					
Sc II									
3572.5	1	1	0	0					
3580.9	.....	1n	.....	0					
3613.8	.....	1nn	.....	0					
3642.8	1	.....	0	.....					
4325.0	0n	.....	0	.....					

ing, in view of the presence of weak forbidden [*Fe* II] lines. But it is possible that the forbidden lines originate in a distant shell which has not yet been engulfed by the expanding photosphere.

A very remarkable astrophysical phenomenon becomes apparent from an inspection of Table 27. The metallic lines (notably *Ti* II) tend to show pure absorption lines on the violet side of the Balmer limit (λ 3647) and emission lines on the red side. This phenomenon is the exact opposite of what we had described in HD 190073. We are not aware of other stars showing the same conspicuous discontinuity in the appearance of the metallic lines.

Figure 10 shows the transitions of *Ti* II. The effect is not connected with the excitation potentials of the levels involved; nor is it in any way correlated with the spectroscopic notations of the various

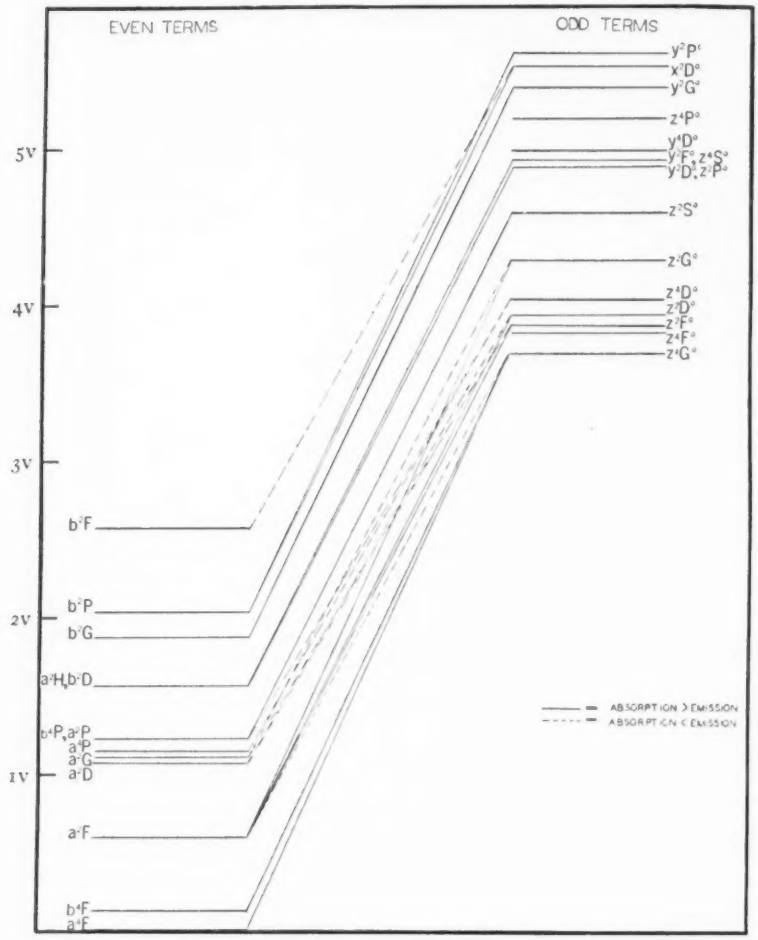

FIG. 10.—*Ti* II lines in Z Andromedae

terms. Moreover, other metals show the same discontinuity near λ 3647.

The following explanation suggests itself. The *H* absorption lines are strong, and they extend to H_{28}. The continuous spectrum shows

a marked step at λ 3647, and all evidence points toward a large continuous absorption coefficient, due to *H*, in the expanding shell.[73] At the Balmer limit the continuous absorption coefficient κ_ν experiences a sudden change. This produces a weakening of the absorption lines on the violet side of λ 3647 by a factor of $\gamma = \kappa_\nu''/\kappa_\nu'$.[74] The existence of this effect has been so abundantly proved in ordinary stars and even in shells[74] that we safely assume that it holds for Z Andromedae.

The emission lines originate in a tenuous ring formed by the outer layers of the shell. In reality, there must be a gradual transition from continuous spectrum to line emission as we pass from the center of the apparent disk of the star to the edge. But if we adopt Milne's picture of a hazy atmosphere for the expanding shell, we may well extend this picture and assume that line emission comes from those parts of the shell for which the total optical thickness $\tau < \tau_1$, where τ_1 is the level of the fictitious photosphere according to Milne (approximately $\tau_1 = 1/3$). If we assume, for simplicity, that the outer parts of the shell have a constant κ_ν, then τ_1 is proportional to the length of the chord, x, which separates the region of line emission from the region of continuous emission. The volume of the shell which gives rise to line emission is $V = \frac{1}{6}\pi x^3$. But $x \propto \kappa_\nu$. Accordingly, the intensities of the emission lines should vary as γ^3, and the ratio of emission intensity to equivalent breadth in absorption should vary as γ^2. A density gradient in the shell would only increase the effect. In ordinary A stars γ is of the order of 10. Hence, the ratio of emission to absorption should vary greatly when we pass from the violet side of the Balmer limit to the red side.

Table 28 gives the radial velocities measured for Z Andromedae on three plates.

2. AX Persei and CI Cygni

The spectra of these two stars have been investigated by Merrill[75] from spectrograms taken in 1931 and 1932. They showed bright lines of *H*, *He* I, *He* II, *N* III, [*O* III], and [*Ne* III], superimposed on an M-type spectrum. The variable character of the two stars has

[73] Struve, *Proc. Nat. Acad.*, **26**, 117, 1940.

[74] Struve and Sherman, *Ap. J.*, **91**, 428, 1940; Roach and Blitzer, *Ap. J.*, in press.

[75] *Ap. J.*, **77**, 44, 1933.

been discussed extensively. C. and S. Gaposchkin[76] state that "CI Cygni is another double (or triple) object: a red star, a blue star, and a nebula (which may possibly be the outer envelope of the red star)." In both cases the light curve shows similarity to Z Andromedae.

Several spectrograms of AX Persei and CI Cygni were obtained in the wave-length region λλ 3300–6700.

At first sight the spectrum of AX Persei appears to have changed greatly since 1931–1932. At the present time AX Persei and CI

TABLE 28

RADIAL VELOCITIES OF Z ANDROMEDAE

Elem.	Absorption 1939			Emission 1939		
	Sept. 16	Oct. 18	Dec. 5	Sept. 16	Oct. 18	Dec. 5
Ti II	−118.5	−65.4	−58.3	− 8.2	+28.1	+50.4
Fe II	−140.0	−62.9	−72.4	+ 3.1	+35.0	+42.4
H	− 80.9	−72.5	−54.7	+23.2	+60.5	+58.6
Cr II	− 88.3	−44.4	−58.6	+ 8.8	+13.5	+43.2
Fe I	−112.6	−63.6	−82.1	+ 0.9	.....	+22.6
Mn II	− 89.0	.....	−50.5	+14.4	.....	+46.5
Ni II	− 87.9	.....	−65.5	−10.2	.....	+25.4
V II	−105.0	.....	−61.4	− 8.2	+13.5	+49.6
Sc II	−126.7	.....	−39.0	+ 5.6	.....	.....
Ca II	− 68.5	−67.2	−41.2	− 3.2	+36.3	+28.1
Ca I	.....	.....	.....	−11.5	.....	+22.6
Mg I	− 70.6	−58.8	−46.9	− 4.1	.....	+41.6
Mg II	− 92.6	−20.0	−53.2	.....	.....	.....
Si II	− 82.5	−87.2	−42.9	+ 7.6	.....	+62.3
He I	−106.4	.....	.....	.....	.....	.....

Cygni are so similar that we combine their description in the same section.[77] In Table 29 we have collected the emission lines and their probable identifications.

Besides the weak continuous spectrum with M-type absorptions, our spectrograms show only emission lines.

Hydrogen.—The Balmer lines are observed from $H\alpha$ to H_{21}, and there is also a strong Balmer continuum in emission as far as λ 3470. This spectrum may be attributed essentially to the "nebular com-

[76] *Variable Stars*, pp. 315–316, 1938.

[77] Dr. G. P. Kuiper has found from low-dispersion spectrograms (340 A/mm at H_γ) that the spectral type of AX Per is gM3e and that of CI Cyg, gM4e.

TABLE 29

EMISSION LINES IN AX PERSEI AND CI CYGNI

AX PERSEI		CI CYGNI		IDENTIFICATION		EXCITATION POTENTIAL OF HIGHER LEVEL (VOLTS)	NOTES
λ	Int.	λ	Int.	Elem.	Lab. λ		
3340.7	1	3340.7	1	*O* III	3340.74	36.7	1
3346	4	3346	4	[*Ne* V]	3345.8	3.8	
3426	8	3425.6	8	[*Ne* V]	3425.8	3.8	
3443.8	4	3444.0	3	*O* III	3444.1	40.7	1
3586.4	3	3586.7	4	[*Fe* VII]	3587.2	3.6	
3678.5	1			H_{21}	3679.3	13.51	
3682.5	2	3682.0	1	H_{20}	3682.81	13.51	
3686.4	2	3685.9	1	H_{19}	3686.8	13.50	
3691.2	2	3691.4	1	H_{18}	3691.6	13.50	
3696.7	2	3697.0	1	H_{17}	3697.2	13.49	
3703.7	3	3703.6	1	H_{16}	3703.9	13.49	2
3705.0	1						
3712.1	3	3712.0	1	H_{15}	3712.0	13.48	
3714.8	1						
3721.8	3	3722.3	1	H_{14}	3721.9	13.47	
3727.8	on	3727	on	[*O* II]	3726.1 3728.6	3.3	
3734.5	4	3734.7	2	H_{13}	3734.4	13.46	3
3750.0	4	3750.7	2	H_{12}	3750.2	13.45	
3754.7	1			[*Fe* V]	3755.5	3.3	
3759.3	6n	3759.1	5	*O* III [*Fe* VII]	3759.9 3759.9	36.3 3.6	1, 4
3770.8	4	3770.6	2	H_{11}	3770.6	13.43	
3798.4	4	3798.1	2	H_{10}	3797.9	13.40	
3820.4	1	3820.0	1	[*Fe* V]	3820.2	3.3	
3826.9	on						
3835.5	5	3835.5	3	H_9	3835.4	13.37	
3840.8	0	3840	0	[*Fe* V]	3838.9	3.3	
3869.5	4	3869.3	1	[*Ne* III] [*Fe* XI]?	3868.7 3871.9	3.2 4.7	
3889.3	7	3888.8	3	H_8	3889.1	13.33	
3904.9	1	3905.4	0	*Si* I	3905.5	5.06	5
		3923.4	0	*He* II [*Ti* IX]	3923.51 3923	53.9 3.2	
3933.6	3	3933.9	1	*Ca* II	3933.7	3.1	
		3938.0	1				6
3964.8	1	3964.9	1	*He* I	3964.7	23.64	
3969.5	7n	3970.0	4n	[*Ne* III] $H\epsilon$	3967.5 3970.1	3.2 13.26	
		4010.6	1	*He* I	4009.3	24.2	
4026.4	2	4026.5	2	*He* I	4026.2	23.9	7
4071.1	0	4071	0	[*Fe* V]	4071.5	3.1	
4097.4	2	4097.4	2	*N* III	4097.3	30.3	1
4102.4	8	4101.9	5	$H\delta$ *N* III	4101.7 4103.4	13.16 30.3	1
		4122.0	0	*He* I [*K* V]	4120.8 4120±	23.9 3.0	

TABLE 29—*Continued*

AX Persei		CI Cygni		Identification		Excitation Potential of Higher Level (Volts)	Notes
λ	Int.	λ	Int.	Elem.	Lab. λ		
4144.6	1	4143.6	1	*He* I	4143.8	24.1	
.....	.....	4161.7	1	[*K* V]	4160±	3.0	
.....	.....	4173.4	0	*Fe* II	4173.4	5.53	
4178.6	on	4179.7	1	*Fe* II [*Fe* V]	4178.9 4181.4	5.52 3.0	
4233.7	1	4233.1	0	*Fe* II	4233.2	5.49	
.....	.....	4244.4	1	[*Fe* II]	4244.8	3.21	
4277.2	0	4277.5	0	.....	.....	.....	8
4286.2	0	4286.8	0	[*Fe* II]	4287.4	2.88	8
4296.4	0	4297.0	0	*Fe* II	4296.6	5.56	8
4303.6	0	4303.9	0	*Fe* II	4303.2	5.56	8
4316.3	0	.....	.....	.....	.....	.....	8
4340.2	10	4340.3	8	*Hγ*	4340.5	13.00	
4352.1	1	4351.6	1	*Fe* II	4351.8	5.53	
4359.3	1	.....	.....	[*Fe* II]	4359.3	2.88	
4364.1	5	4363.3	2	[*O* III]	4363.2	5.3	
4371.5	0	.....	.....	[*Fe* II]	4372.5	3.21	
4378.5	1	.....	.....	.....	.....	.....	
4387.9	1	4387.0	1	*He* I	4387.9	23.9	
.....	.....	4409.7	0	[*Cr* IX]	4408	3.8	
4472.4	2	4471.5	3	*He* I	4471.5	23.6	
.....	.....	4481.6	0	*Mg* II	4481.2	11.6	9
4491.7	1	4489.9	1	*Fe* II *Fe* II [*Fe* II] [*Fe* II]	4489.2 4491.4 4488.8 4492.6	5.56 5.59 2.83 2.79	
.....	.....	4516.2	1	*Fe* II	4515.3	5.56	
.....	.....	4523.6	0	*Fe* II	4522.6	5.56	
4541.5	0	4541.2	1	*He* II	4541.6	53.5	
4550	0	4549.8	1	*Fe* II *Ti* II	4549.5 4549.6	5.53 4.3	
4557.8	0	4555.3	1	*Fe* II	4555.9	5.52	
4571.7	0	4571.7	2	*Mg* I	4571.1	2.7	5
.....	.....	4576.6	1	*Fe* II	4576.3	5.53	
4584.0	1	4582.4	2	*Fe* II	4583.8	5.49	
.....	.....	4629.2	1	*Fe* II	4629.3	5.46	
4634.0	0	4633.0	1	*N* III	4634.2	33.0	1
4640.7	1	4640.2	1	*N* III	4640.6	33.0	1
.....	.....	4658.6	0	[*Fe* III]	4658.2	2.7	9
4684.6	8	4685.8	6	*He* II	4685.8	50.8	
4704.9	0	.....	.....	[*Ti* IX]? [*Fe* III]?	4700± 4701.5	2.7 2.7	
4713.4	3	.....	.....	*He* I [*A* IV]?	4713.1 4711.4	23.6 2.6	
4861.5	15	4861.3	10	*Hβ*	4861.3	12.69	
4923.2	1	4922.5	1	*He* I *Fe* II	4921.9 4923.92	23.64 5.38	
4944.7	1	4940.5 4949.5	1 1	[*Ca* VII] [*Fe* VII]	4941 4942.3±	2.7 2.5	10

TABLE 29—*Continued*

AX Persei		CI Cygni		Identification		Excitation Potential of Higher Level (Volts)	Notes
λ	Int.	λ	Int.	Elem.	Lab. λ		
5007.7	1	5008	0	[*O* III]	5007.6	2.5	
5016.6	0	.....	.....	*He* I	5015.7	23.0	
				Fe II	5018.4	5.34	
5041.3	1	.....	.....	.....	.....	.....	11
5160.8	3	5156.0	3	[*Fe* VII]	5158.3±	2.6	
5274.0	1	5274.1	2	[*Fe* VII]	5276.1±	2.6	
				[*Fe* III]	5270.5	2.6	
5309.2	1	.....	.....	[*Ca* V]	5308.9	2.3	
5337.5	1	.....	.....	[*Fe* VI]?	5336.4	2.5	12
5408.4	3n	.....	.....	*He* II	5411.6	53.1	
5581	0	.....	.....	[*O* I]?	5577.3	.....	9
.....	.....	5618.2	1	[*Ca* VII]	5619	2.7	
5719.9	2	5721.5	4s	[*Fe* VII]	5720.9	2.2	
.....	.....	5739.5	1	*Si* III?	5739.8	21.8	
5752	1	5752	1	[*N* II]	5755	4.0	9
5875.5	9	5876.8	5	*He* I	5875.6	23.0	
6090.0	8	6089.8	7	[*Fe* VII]	6085.5	2.2	
				[*Ca* V]	6085.9	2.3	
6349.7	1	.....	.....	[*K* V]	6349.5	4.9	
6371.0	1	6370.3	1	[*Fe* X]	6372±	1.9	
Hα	25	*Hα*	15	*Hα*	6562.8	12.04	

NOTES TO TABLE 29

1. These are the *O* III and *N* III lines excited by Bowen's fluorescence mechanism.
2. In AX Persei, H_{16} is abnormally broad and strong.
3. In AX Persei, H_{13} is broader than the other Balmer lines.
4. Both contributors are certainly present.
5. Characteristic lines of the long-period variables.
6. Also present in BD+11°4673.
7. There are possibly two weak emission lines in AX Persei between λ 4030 and λ 4070.
8. The measurement of this group of lines was very difficult.
9. Uncertain.
10. The line is possibly double in AX Persei.
11. Also present in NGC 7027, NGC 6572, and RY Scuti. May be [*Fe* IV].
12. Identification doubtful.

ponent" of the system, its intensity being too high for the "late-type component." There is no anomaly in the intensities of $H\epsilon$, $H\beta$, etc., like those present in late-type variables.

He I.—Many lines belong to the series $2p^3P^o - nd^3D$, $2p^1P^o - nd^1D$, $2p^3P^o - ns^3S$, and $2s^1S - np^1P^o$. The line λ 4713 seems to be abnormally strong, but this may be due to blending with [*A* IV] 4711.4.

He II.—Many lines are blended; but, aside from the strong line λ 4686, the following are unblended: λ 4541 ($4f^2F^o - 9g^2G$) and λ 5411 ($4f^2F^o - 7g^2G$).

O II.—The forbidden [*O* II] doublet at λ 3727 is extremely weak.

O III.—The lines excited by λ 303.780 of *He* II ($1s^2S - 2p^2P^o$) are very conspicuous (λλ 3341, 3444, and 3760). The forbidden lines have relative intensities similar to those found in planetaries of type Pd, such as IC 4997: the auroral transition λ 4363.2 ($2p^2\ ^1D - 2p^2\ ^1S$) is much stronger than the nebular transition N_1, λ 5007.6 ($2p^2\ ^3P_2 - 2p^2\ ^1D$). Such relative intensities are rare among galactic nebulae but have been observed also in Z Andromedae, RW Hydrae, and R Aquarii,[78] which are closely related to the present stars. This would seem to indicate a rather high electron pressure in those regions where [*O* III] 4363 originates.

N II.—The auroral line λ 5752 is faintly present.

N III.—The two doublets λλ 4097–4103 and λλ 4634–4640, excited by *O* III 374 (itself excited by *He* II, according to Bowen's mechanism), are present.

Ne III.—The nebular-type lines are present; the auroral transition at λ 3342.8 is absent.

Ne V.—The forbidden nebular lines λ 3346 and λ 3426 are very strong.

Ca II.—K λ 3933.7 is present.

Ca V.—There is some evidence of the presence of [*Ca* V]: the first component $3p^4\ ^3P_2 - 3p^4\ ^1D$ at λ 5309 is present in AX Persei, and the second is blended with [*Fe* VII] at λ 6088.

Ca VII.—Its presence is fairly certain in CI Cygni; λ 5618.2 ($3p^2\ ^3P_2 - 3p^2\ ^1D$) and λ 4941 ($^3P_1 - ^1D$) are both present.

Mg I.—λ 4571, which is typical of the long-period variables, is present.

Mg II.—The evidence for λ 4481 is inconclusive.

Si I.—λ 3905 is usually present in long-period variables.

Fe II.—Many permitted lines are observed, all of them coming from z^4D^o and z^4F^o (both 5.5 v.). The presence of [*Fe* II] is still uncertain.

[78] See end of this section.

Fe III.—The strongest forbidden line of [*Fe* III] at λ 4658 is faintly present in CI Cygni.

Fe IV.—We refer here to the discussion of the spectrum of RY Scuti in Section II. It is possible that λ 5041.3 is a forbidden [*Fe* IV] line.

Fe V.—Bowen has located the metastable levels of *Fe* V. Several forbidden lines have been tentatively identified by various investigators, in nebulae or novae; but all of these identifications were based only upon rough wave-length agreements. The results for [*Fe* III] in RY Scuti (see Sec. II) may bring some light, as *Fe* III and *Fe* V have complementary electronic configurations $3d^6$ and $3d^4$ with regard to the half-closed shell $3d^5$. We may, thus, assume for [*Fe* V] that the identification criteria are also

$$\left\{\begin{matrix} {}^5D_4-{}^3F_4\ (\lambda\ 3891) \\ {}^5D_3-{}^3F_3\ (\lambda\ 3839) \end{matrix}\right\} \quad \text{and} \quad \left\{\begin{matrix} {}^5D_3-{}^3P_2\ (\lambda\ 3896) \\ {}^5D_2-{}^3P_1\ (\lambda\ 4072) \end{matrix}\right\}.$$

The line ${}^5D_4 - {}^3F_4$ will usually be blended with the Balmer line *H*8, but ${}^5D_3 - {}^3F_3$ was actually observed in AX Persei and CI Cygni; the ${}^5D_3 - {}^3F_4$ component appears also at λ 3820.2. The line ${}^5D_2 - {}^3P_1$ was found at λ 4071 in both stars.

Fe VI.—There is no certain identification of [*Fe* VI], the only coincidence being λ 5337 (${}^4F_{\frac{9}{2}} - {}^4P_{\frac{5}{2}}$).

Fe VII.—The analysis of this spectrum by Bowen and Edlén permitted them to identify [*Fe* VII] in Nova Pictoris, where it produces the strongest lines. We have found the [*Fe* VII] transitions to be a prominent feature in AX Persei and CI Cygni. The measured wave lengths are given in Table 30, and these are probably better than the predicted values or than the wave lengths measured in Nova Pictoris, because the lines of AX Persei and CI Cygni are fairly sharp.

The prominence of [*Fe* VII] shows that AX Persei and CI Cygni are especially suitable for investigations of forbidden lines of highly ionized atoms.

Fe X.[79]—The ground level $3p^5\ {}^2P^0$ has become so widely separated that the forbidden transition between the two components falls near λ 6372, according to Edlén's analysis. We have observed an emission line at λ 6370.7 in AX Persei and CI Cygni, with no other

[79] The *Fe* VIII and *Fe* IX ions have no forbidden lines of low excitation potential.

good identification available.[80] The identification with [*Fe* X] seems plausible for the following reasons:

a) AX Persei and CI Cygni show high ionization.

b) This transition is the only forbidden line of *Fe* X which is possible for a low electronic excitation, and the intensity would, therefore, be concentrated in one line.

c) The ionization potential of *Fe* IX, which is somewhere around 230 v., is not much higher than that of *Fe* VI (around 150 v.?), and we know that *Fe* VII is very abundant in AX Persei.

The line λ 6372 is a transition between the two components of the ground level $^2P^o$: $3p^5\ ^2P^o_{1\frac{1}{2}} - 3p^5\ ^2P^o_{\frac{1}{2}}$ (exc. pot. 1.9 v.). The transition

TABLE 30

[*Fe* VII] LINES OBSERVED IN AX PERSEI AND CI CYGNI

λ	Transition	Intensity		Remarks
		AX Persei	CI Cygni	
3586.6	$^3F_3-{}^1G_4$	3	4	
3759.2	$^3F_4-{}^1G_4$	6	5	Blended with fluorescence line of *O* III
4945	$^3F_3-{}^3P_2$	1	1	Separation from [*Ca* VII] difficult
5158.0	$^3F_3-{}^3P_1$	3	3	
5274.1	$^3F_4-{}^3P_2$	1	2	
5721.5	$^3F_2-{}^1D_2$	2	4	
6089.9	$^3F_3-{}^1D_2$	8	7	Weakly blended by [*Ca* V]

probability of magnetic dipole radiation is[81] in this case 70 sec^{-1}, which is a normal value for a forbidden transition.

K V.—The predicted wave lengths of the $^4S - {}^2D$ forbidden transitions of [*K* V] are very uncertain. The following identifications are possible.

4161.7 : $3p^3\ ^4S - 3p^3\ ^2D_{1\frac{1}{2}}$
4122.0 : $3p^3\ ^4S - 3p^3\ ^2D_{2\frac{1}{2}}$ (blended with *He* I)
6349.7 : $3p^3\ ^2D_{1\frac{1}{2}} - 3p^3\ ^2P_{\frac{1}{2}}$

[80] *Si* II 6371.4 is excluded because all the transitions in other regions are absent. The effect of the superposed late-type spectrum has been considered.

[81] From Brinkman's formula, kindly communicated by Dr. G. Breit.

Cr IX.—All the intensity due to low electronic excitation would be concentrated in two lines: λ 3273.5 and λ 4407.9. A weak line measured at λ 4409 has no other identification.

Mn IV.—One of the two strongest expected lines of [*Mn* IV][82] is $^5D_3 - {}^3P_2$, near λ 4591; a weak line is present at λ 4594.8, but $^5D_4 - {}^3F_4$ being absent, this is probably not the correct identification.

Ti IX.—This ion has two forbidden lines around λ 3923 and λ 4700 ($^3P_{1,2} - {}^1D_2$). The first is blended with *He* II; but the observed line appears abnormally strong because the stronger line, $4f\,^2F^o - 11g\,^2G$ (λ 4199.9) of the same series, is absent. The second [*Ti* IX] line may be the line observed at λ 4704.9.

The spectrum of CI Cygni does not seem to have suffered important modifications since the time of Merrill's observations. But the matter is quite different in the case of AX Persei. It is evident at once that *He* I is now weaker, compared with *He* II, that [*Ne* III] has also decreased in intensity, and that [*O* III] 4363 is weaker than in 1932, although it is still fairly conspicuous. It is clear that the ionization has increased in the regions giving rise to forbidden lines.

Even if we compare spectrograms taken at such a short interval as from September 20, 1939, to February 4, 1940, we find a change in the direction of increased ionization. Compared with [*Fe* VII], *H* and *He* I decreased in intensity; *Ca* II has practically disappeared; *N* III has increased, which is due to an increase of *He* II causing the *N* III fluorescence. *Fe* II has not changed appreciably.

The complex character of AX Persei and CI Cygni is obvious. The late-type component is presumably a variable itself, the bright lines of *Si* I (λ 3905) and *Mg* I (λ 4571) being characteristic of late-type variables. There is also a nebula of very high excitation ([*Ne* V] and [*Fe* VII] being strong) and of density similar to that of the planetaries of type Pd (provided that [*O* III] 4363 originates in the nebula itself); we observe in the nebula the fluorescence of *O* III and *N* III excited by the *He* II line at λ 303.78. In this nebulosity the excitation increases, which means that the corresponding nucleus becomes hotter. Now the similarity with Nova Pictoris, which also shows strong [*Fe* VII] lines, suggests that this nucleus is a post-nova, the surrounding

[82] Derived from a comparison with [*Fe* V] and [*Fe* III].

nebulosity being the matter ejected at the time of the outbursts.[83] The present effective temperature of the nucleus must be very high, of the order of 150,000° or more, in order to produce six and probably nine ionizations of the iron atom. Accordingly, its maximum radiation is near λ 200, and the quantity of continuous radiation emitted in the observable range is an extremely small fraction of the total radiated energy. There is no difficulty in understanding why the spectrum of the nucleus has not been observed.

The *Fe* II lines appear much too strong to be attributed solely to the regular emission of a late-type variable. The spectrum shows strong [*Fe* VII], weak intermediate ionizations, including [*Fe* III], and then again fairly strong *Fe* II.[84] It is possible that the *Fe* II lines are excited in the outer part of the M star by the diluted radiation of the hot nucleus, which is itself surrounded by the [*Fe* VII] nebula.[85]

Besides the M spectrum, Merrill had observed in AX Persei an absorption spectrum of a type earlier than M3—say K0p. This does not appear now, but the change may perhaps be due to a change in the excitation of a certain region of the M star by the hot companion.

3. R Aquarii

The complex case of the spectrum of R Aquarii has been investigated by Merrill,[86] using Mount Wilson spectrograms extending over 15 years. In this section we present some additional spectroscopic data based on McDonald spectrograms taken between September 13 and December 12, 1939. Besides the nebular lines tabulated by Merrill, our spectrograms show the [*O* II] doublet fairly strongly; λ 4363 (auroral transition of [*O* III]) is now weak.[87] The relative intensities of N_1 and N_2 are quite irregular, N_2 being too weak when we consider its theoretical transition probability. Photometric measurements

[83] The velocity of expansion is very small at the present time, because the bright lines are sharp.

[84] Individually the *Fe* II lines are not strong; but the energy is distributed among many lines.

[85] But in Z And this hypothesis is not tenable.

[86] *Ap. J.*, **81**, 312, 1935.

[87] Relative to the nebular transitions, the auroral transition λ 4363 is much weaker in R Aqr than in AX Per and CI Cyg.

show that N_2 is 6.9 times weaker than N_1; whereas the theoretical ratio is 3. This behavior is presumably due to an occultation effect of the nebula by the *TiO* atmosphere of the late-type component, since N_2 falls very close to a strong *TiO* band head. N_1 also falls in a *TiO* band, but much farther from the head, and is consequently less reabsorbed. Such an occultation effect was discussed by Wright[88] in order to explain the absence of the [*Ne* III] line at λ 3968. The other component, λ 3869, of the nebular pair had been observed by J. H. Moore;[89] in this case the blanketing was due to the *Ca* II line H. This appears also on our spectrograms. The absorption of the nebular light by the *TiO* layer is much weaker than the absorption of the hydrogen lines and of the other bright lines. This appears from a comparison of plates taken in September and in December, 1939. $H\gamma$ falls in a region practically free from *TiO* absorption. The strength of the *TiO* bands at the wave length of $H\beta$ is appreciable, but it is still more at N_1 and much more at N_2. Between September and December, 1939, $H\gamma$ increased considerably in intensity; it was much weaker than N_1 in September and much stronger in December. But $H\beta$ remained weaker than N_1. An examination of the spectrograms shows that N_1 is not reduced by *TiO* to the same extent as $H\beta$, although the absorption band appears stronger at N_1 than at $H\beta$. This shows that [*O* III] does not originate in the same region as the Balmer lines.

At certain phases, the spectrum of R Aquarii is very rich in [*Fe* II] lines, and it is then very similar to WY Geminorum.

Merrill has observed at certain phases the forbidden transitions of [*Fe* III]; but these, as well as the permitted *Fe* III lines, were absent during our period of observation.

We shall not consider here the outer lenticular nebulosity discovered by C. O. Lampland,[90] although it is puzzling that no marked change has ever been noticed in its brightness. But continuous observations of this nebulosity are lacking, and there may be a consid-

[88] *Pub. A.S.P.*, **31**, 309, 1919.

[89] *Ibid.*

[90] *Pop. Astr.*, **30**, 619, 1922.

erable lag of time between the variation in excitation and the variation in nebular brightness.

The character of the long-period variable seems to be quite regular. In the light of Z Andromedae, AX Persei, and CI Cygni it seems most promising to try to explain the spectroscopic data by assuming the presence of two stars: one regular long-period variable and one of early type surrounded by nebular matter. This hypothesis, which has been considered on several occasions,[91] gains weight from the observations discussed in this section.

V. CONCLUSIONS

Two advances have recently been made in the interpretation of emission-line stars of early spectral type. The dilution of the exciting radiation from the hot star, caused by the distance between the source of continuous radiation and the gases responsible for the shell, produces marked changes in the spectrum and permits us to evaluate, under favorable conditions, the ratio, R/r, of the radius of the star to the radius of the shell. This, in most cases, is not excessively small, and we may estimate that in nearly all cases $0.1 < R/r < 1$. This is one important result, as it gives us the order of size of the nebulous shell.

The second advance consists in our recognition of the importance of the continuous absorption in the shell. The optical thickness of the shell may be very small (α Cygni) or very large (P Cygni). In those cases in which the optical thickness is small, we are able to see the spectrum of a deeper layer. In most cases the transition from the deep reversing layer to the shell is discontinuous, or, at least, very sudden; but in a few stars there are definite indications of stratification in the shell (P Cygni, ζ Tauri, and HD 218393). When the shell expands, the reversing layer usually has a small radial velocity. In a few cases (17 Leporis) it is certain that the shell covers the entire apparent disk presented by the reversing layer, and the phenomenon is not one of prominence action, with normal regions between expanding prominences.

[91] Merrill, *Ap. J.*, **81**, 331, 1935; C. and S. Gaposchkin, *Variable Stars*, p. 315, 1938.

The study of P Cygni type stars shows that expanding shells may be associated with reversing layers of the supergiant class (HD 160529, α Cygni, and β Orionis) or with reversing layers of main-sequence characteristics (HD 190073, 17 Leporis, and BD+47°3487). Rapid axial rotation of the reversing layer is not a necessary condition, even in the main-sequence reversing layers (17 Leporis and HD 190073), although in some stars the rotation does seem to be large (BD+47°3487).

It will be recalled here that in ordinary Be stars axial rotation plays an important role.[92] There can be no doubt that this is not the case in P Cygni type stars. It is almost certain that axial rotation acts as a trigger mechanism in the production of shells of Be stars. There is no evidence that these stars are, as a rule, binaries. But there is some evidence that Be stars are, on the average, more luminous than main-sequence stars without emission lines. They are definitely less luminous than the supergiants, but the latter do not, as a rule, have large rotational velocities.

We suggest that some mechanism other than axial rotation is responsible for P Cygni type emission. It is probable that high luminosity favors this process: a surprisingly large percentage of supergiants show weak P Cygni emission at *Hα* when they are examined with sufficient dispersion. But there are also normal main sequence stars with strong P Cygni characteristics. We must infer that luminosity is not alone to blame. Some of these stars (Z Andromedae, RY Scuti, and β Lyrae) are known binaries. It is at least probable that the binary nature of a star favors the origin of a shell. This hypothesis is supported by the peculiar class of composite spectra which we have discussed in Sections III and IV. Some of these objects have B-type spectra which are perfectly normal in all respects and which have no excessive rotation and no supergiant characteristics. Yet, when these normal stars are associated with an M star, as a binary, they give rise to strong emission spectra of [*Fe* II] (WY Geminorum, W Cephei, and Z Andromedae) or to emission spectra of higher excitation and ionization (AX Persei and CI Cygni). The

[92] Struve, *Ap. J.*, **73**, 94, 1931; *J. Appl. Phys.*, **10**, 802, 1939; Struve and Swings *Ap. J.*, **75**, 161, 1932; Merrill, *Pub. A.S.P.*, **45**, 49, 1933.

fact that a few related stars (HD 45677) are apparently not composite does not mean that they are not binaries. Z Andromedae in its present stage would also be interpreted as a single star. However, we know from the work of Hogg that an M-type spectrum was present when the brightness of the hot star was low.

There is all reason to believe that the binary nature of a star stimulates the process of shell formation. But there are many close spectroscopic binaries which show no tendency toward emission.

YERKES OBSERVATORY
AND
MCDONALD OBSERVATORY
March 1940

NOTES

COSMIC STATIC

Several papers[1] have been published which indicate that an electromagnetic disturbance in the frequency range 10–20 megacycles arrives approximately from the direction of the Milky Way. It has been shown[2] that black-body radiation from interstellar dust particles is not the source of this energy.

The antenna system shown in Figure 1 was constructed for the investigation of this phenomenon.[3] The receiver can be set at the desired declination by rotating along the meridian on the circular tracks at each side. Readings at a fixed declination are taken over an interval of several hours, the rotation of the earth providing the change in right ascension.

The drum at the focal point is an artificial black body described elsewhere.[4] The entire receiving system has an effective cone of acceptance approximately 3° in diameter.

The output is indicated by a microammeter so connected that any intercepted energy will cause the readings to decrease. A few typical records are shown in Figure 2, in which the individual points are omitted because they lie too close together. The magnitude of the dip in the curve gives a measure of the intensity of the received energy. Over a long period, as the apparatus warms up, the zero level will gradually rise. The dotted line indicates the run which would have been obtained had no radiation been captured.

The results of preliminary measures of the variation of the static

[1] K. G. Jansky, *Proc. I.R.E.*, **20**, 1920, December, 1932; **21**, 1387, October, 1933; **23**, 1158, October, 1935; **25**, 1517, December, 1937. H. T. Friis and C. B. Feldman, *Bell Tech. J.*, **16**, 337, July, 1937.

[2] Whipple and Greenstein, *Proc. Nat. Acad. Sci.*, **23**, 177, 1937.

[3] For details of the instrumental design and the method of reduction of the data see G. Reber, *Proc. I.R.E.*, **28**, 68, 1940.

[4] G. Reber, *Communications*, **18**, 5, December, 1938.

disturbance as a function of galactic longitude are shown in Figure 3, in which each point represents the central intensity of the dip on one

FIG. 1.—Antenna system viewed from the north. The resonance chamber can be seen supported at the focal point of the parabolic reflector.

night's record. The magnitude of the systematic error may be ± 50 per cent, but the general order of the disturbance is correct. The plane from which this energy arrives is tilted about 5° south of the plane of the galaxy in the vicinity of longitude 150°.

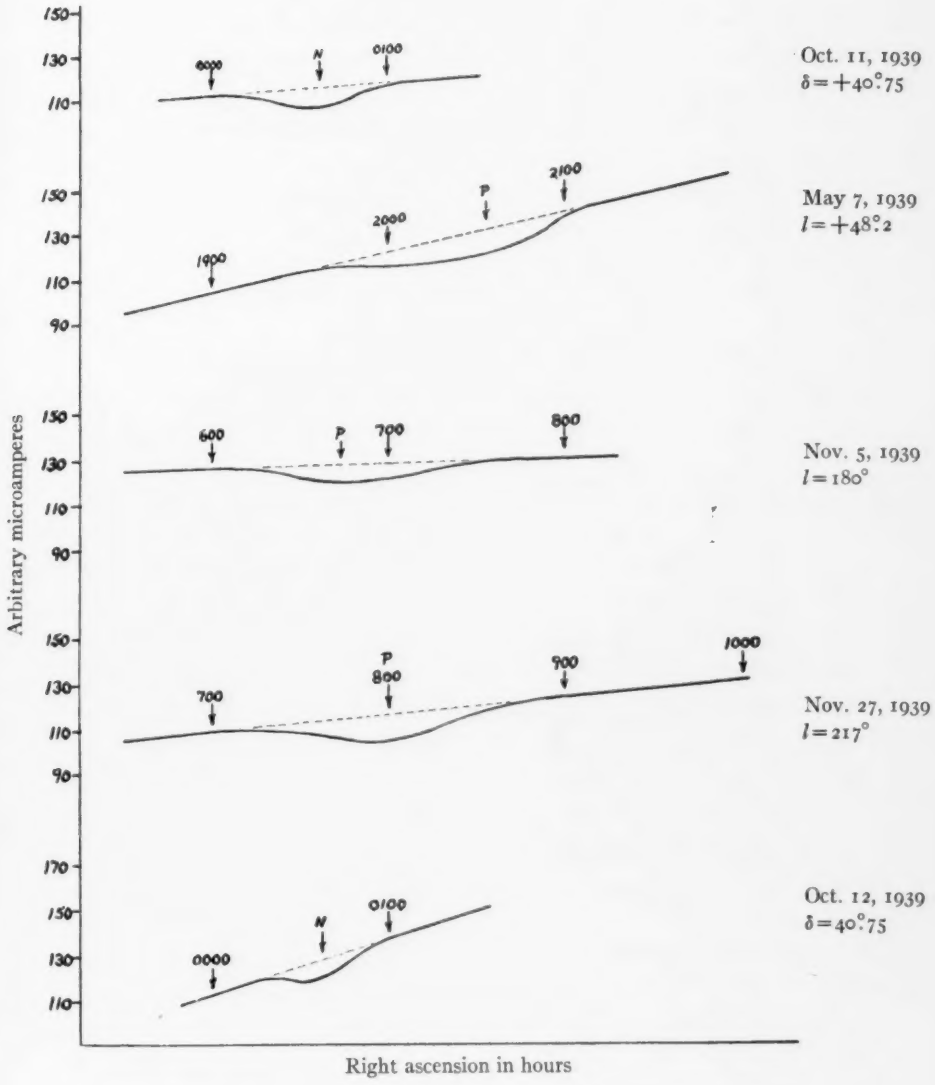

FIG. 2.—Typical records of observation. *P*—plane of Milky Way; *N*—center of Andromeda Nebula.

Since the theory of black-body radiation predicts an intensity proportional to the square of the frequency in this range, the first tests were made at 3300 megacycles. Nothing was found at the sensitivity limit of 10^{-20} watts per square centimeter per circular degree per kilocycle band width. Improved equipment for the frequency of 900 megacycles gave no results at the limit of 10^{-22} watts per square centimeter per circular degree per kilocycle band width. The data of Figures 2 and 3 were obtained at 162 megacycles.

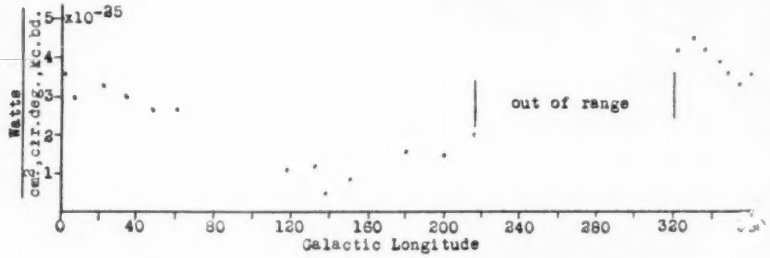

FIG. 3.—Intensity of maximum incident radiation as function of galactic longitude.

A few bright stars, such as Vega, Sirius, Antares, Deneb, and the Sun, gave negative results. Mars and the Orion nebula also gave no readable indication. If radiation is present from any of these objects, the intensity is below 10^{-25} watts per square centimeter per circular degree per kilocycle band width at 162 megacycles. The only other positive results are from the great nebula in Andromeda, with a mean of four readings, giving a maximum intensity of 8×10^{-26} watts per square centimeter per circular degree per kilocycle band width.

The foregoing observations confirm previous evidence that radiation in the radio spectrum is apparently coming from the direction of the Milky Way. The intensity is a function of galactic longitude.

GROTE REBER

212 WEST SEMINARY AVENUE
WHEATON, ILLINOIS
December 1939

INTERSTELLAR RADIATION FROM FREE ELECTRONS AND HYDROGEN ATOMS

ABSTRACT

The intensity of the radiation produced by electrons and hydrogen ions is considered. It is shown that for an electron temperature of 10,000° and a density of one electron per square centimeter we may expect from interstellar space an intensity of radiation at a wave length of 1.65 meters of 5.8×10^{-18} ergs per square centimeter per second per square degree per kilocycle band width. This is in excellent agreement with the observational value given by Reber. The computations have been extended over the range 10 meters to 4400 A.

In this note we wish to consider the possible contribution of atomic or ionic processes to the radiation in the radio region of the spectrum. The observations of Jansky[1] and of Reber[2] indicate that there exists radiation, in this region, of the order of 10^{-17} ergs per second per square centimeter per kilocycle coming from a square degree in the Milky Way. Whipple and Greenstein[3] attempted to explain this radiation in terms of the thermal emission by interstellar dust particles, with no success, since the maximum temperature which they could attribute to these particles was about 30°, leaving a discrepancy in intensity of the order of 10,000. Reber[4] proposed an explanation of the radiation in terms of the so-called free-free transitions of electron and proton systems in interstellar space. While his computations were very rough and did not allow for all possibilities, they did indicate that the order of magnitude approaches that of the actual observed intensity. This success may be ascribed principally to his use of an electron temperature of 10,000°, a value which is probably of the right order.

In addition to the free-free transitions we shall take account of the transitions between continuous and bound levels near the continuous limit in hydrogen. The transfer of radiation is governed also by electron and particle scattering. On the other hand, interactions between two free electrons will give rise only to quadrupole radiation, which can be neglected in the spectral range under consideration.

[1] *Proc. I.R.E.*, **20**, 1920, 1932; **25**, 1387, 1937.

[2] *Ap. J.*, **91**, 621, 1940.

[3] *Proc. Nat. Acad. Sci.*, **23**, 177, 1937.

[4] *Proc. I.R.E.*, **28**, 68, 1940.

To compute the contributions of each of these processes we must have some information concerning the velocity distribution in the electron gas. No adequate theory exists at the present time which predicts the nature of the distribution function, so that as a substitute we must make use of a Maxwellian one. While this is certainly not the exact function, it should predict the correct order of magnitude for the intensities of the light emitted and absorbed. There is only one possible source of serious error. One can allow for the stimulated emission, in the case of thermal equilibrium, by multiplying the true absorption coefficient by the correction factor

$$1 - e^{-h\nu/kt} .$$

In the far infrared the exponential is very nearly unity, and the correction factor is usually very small. It is evident that one has here a delicate balance of the two mechanisms that may be seriously disturbed if the condition of thermal equilibrium, or the condition of a Maxwellian velocity distribution in our case, is only approximately true.

The emission and absorption of radiation due to the free-free transitions progress according to the conditions of local thermodynamic equilibrium. If we denote the volume absorption coefficient by κ_ν, the emission is $\kappa_\nu B_\nu$. The bound-free transitions produce only emission, because of the high dilution of the exciting radiation, which may be written $\kappa'_\nu B_\nu - \mu'_\nu I_\nu$, where κ'_ν is the absorption coefficient that would obtain in thermal equilibrium and μ'_ν is the coefficient of stimulated emission. We have

$$\mu'_\nu = \kappa'_\nu \frac{1}{e^{h\nu/kt} - 1}$$

by virtue of the thermal distribution of the emitting particles. In addition we introduce σ, the coefficient of scattering by electrons. Since the density of radiation in space is low, we use σ only in computing the extinction and neglect its contribution to the *Ergiebigkeit*.

Under the conditions which we have outlined, the equation of transfer for a ray in the plane of the Milky Way becomes

$$-\frac{dI_\nu}{ds} = (\kappa_\nu + \sigma_\nu - \mu'_\nu)I_\nu - (\kappa_\nu + \kappa'_\nu)B_\nu . \qquad (1)$$

Putting

$$-d\tau_\nu = d(\kappa_\nu + \sigma_\nu - \mu_\nu'), \tag{2}$$

it follows that

$$\frac{dI_\nu}{d\tau_\nu} = I_\nu - \frac{\kappa_\nu + \kappa_\nu'}{\kappa_\nu + \sigma_\nu - \mu_\nu'} B_\nu . \tag{3}$$

If we suppose that the radiation finds its origin along the line of sight between the earth and a limiting optical depth τ_ν, we can deduce from (3) that

$$I_\nu = \int_0^{\tau_\nu} \frac{\kappa_\nu + \kappa_\nu'}{\kappa_\nu + \sigma_\nu - \mu_\nu'} B_\nu e^{-\tau_\nu} d\tau_\nu ,$$

or, replacing the *Ergiebigkeit* by a mean value,

$$I_\nu = \frac{\kappa_\nu + \kappa_\nu'}{\kappa_\nu + \sigma_\nu - \mu_\nu'} B_\nu (1 - e^{-\tau_\nu}) . \tag{4}$$

The wave-mechanical equations for the absorption coefficients given by Menzel and Pekeris[5] were used in carrying out the numerical computations. For each spectral region the appropriate expressions for the Gaunt correction factors were inserted in the integrals. The bound-free contributions were taken care of by means of the smoothed formula, and for this reason the resulting curve does not display the discontinuities at the heads of the various series. For electrons at 10,000° the intensity at the head of the Balmer series jumps by a factor of 17, while the Paschen discontinuity is 2.6; but it is only in the immediate vicinity of the series heads that the smoothed formula is seriously in error.

The value of 10,000° adopted for the electron temperature is certainly of the right order of magnitude, since the principal source of the ionizing radiation is found in the B-type stars. The optical depth, τ_ν, was computed on the assumption that the thickness of the emitting layer is about 16,000 parsecs, or 5×10^{22} cm.

The number of electrons per cubic centimeter may be estimated from three different lines of approach. Struve and Elvey[6] have ob-

[5] *M.N.*, **96**, 77, 1935.

[6] *Ap. J.*, **88**, 364, 1938.

served the intensity of *Hα* as produced in interstellar space in the directions of Cygnus and Cepheus. Their value for the absolute intensity of *Hα* may be used to determine $N_i N_e$, the product of the numbers of electrons and of hydrogen ions per cubic centimeter. Using the anaysis of the recombination of hydrogen given by Baker and Menzel[7] (their case B), we have computed that $N_i = N_e = 0.6$.

Struve[8] and Dunham[9] have estimated the electron density from the observed relative intensities of interstellar *Ca* I and *Ca* II absorption lines. They find 30/cc and 10/cc, respectively. Dunham points out that the density may well be a tenth of his determination because of the uncertainties of the problem.

The intensity of the recombination spectrum, both continuous and discrete, is proportional to $N_i N_e$ multiplied by the thickness of the emitting layer. This intensity in the photographic region, centered around $\lambda = 4400$ A and including the continuum and the lines *Hγ* and *Hδ*, must be less than the observed intensity of diffuse light in the Milky Way, since it is likely that the larger portion of this light arises from starlight scattered by interstellar dust. The observed intensity is about 60 tenth-magnitude stars per square degree.[10] Using a thickness of the emitting layer of 1600 parsecs and an electron temperature of 10,000°, we have computed that this intensity implies that

$$N_i = N_e < 1 .$$

This determination of an upper limit must be given considerable weight since it is based on observational material whose uncertainty lies in the possibility that the true intensity may be smaller than 60 but is certainly not larger by more than the photometric uncertainty of about 20 per cent. We have, therefore, adopted as an upper limit the rounded value

$$N_i = N_e = 1 ,$$

which is compatible with all the determinations.

[7] *Ap. J.*, **88**, 52, 1938.

[8] *Proc. Nat. Acad. Sci.*, **25**, 39, 1939.

[9] *Proc. Amer. Phil. Soc.*, **81**, 277, 1939.

[10] Henyey and Greenstein, unpublished.

The results of the computation are indicated in Figure 1. The broken line gives the trend of the black-body intensity in the long-wave region. The full curve shows the computed intensities for the various parts of the spectrum. In the photographic region the course

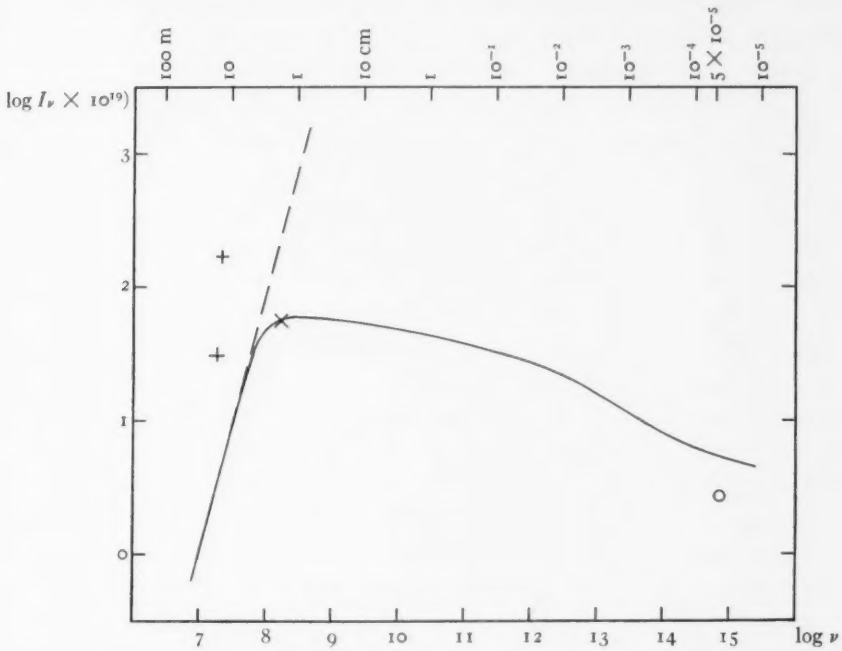

FIG. 1.—The full curve represents the total radiation from free electrons in the galaxy. Ordinates are $19 + \log_{10} I$, where the unit of I is ergs per cm² per sec per square degree per kc band width. Broken curve shows black-body radiation for 10,000°. Observational data are entered as follows:

o—Photographic intensity of diffuse light from Milky Way (Henyey and Greenstein)
+—Radio measures by Jansky (reduced by Reber)
×—Radio measures by Reber

of the curve is fixed essentially by the bound-free transitions, but to the red of 20μ they become negligible in comparison to the free-free processes. It can be seen that the two curves begin to deviate one from the other at a wave length of about 5 meters. This results from the fact that the value of τ_ν changes at this wave length from an amount much greater than unity to less than unity, or, physically,

at this wave length the radiating layer ceases to be opaque and becomes effectively transparent.

The crosses in the long-wave region represent the intensities measured on radio receivers by Jansky and by Reber. The predictions of the theory are in satisfactory agreement with Reber's observation, but in the case of Jansky's data the discrepancy is serious. A change in the value of τ_ν could, at most, lower the computed curve very slightly, since the layer is practically opaque at this wave length, but could never raise it above the black-body intensity. In order to produce the intensity observed by Jansky, it would be necessary to have a source at a temperature of the order of 150,000°.

The observation indicated in the photographic region is the one of relatively high precision discussed above.[10] It will be seen that this observation falls considerably below the computed curve. In reality, if we allow for the probable existence of scattered starlight, the curve should pass well below the point. This apparent discrepancy originates from the large thickness of emitting matter, 16,000 parsecs, which we have used. The high value of the absorption coefficient in the photographic region, amounting to 1 mag. per kiloparsec, means that we cannot receive light from an equivalent thickness much greater than 1500 parsecs. This requires that the intensity at λ 4400 must be cut by a factor of more than 10, in agreement with our previous conclusions.

We conclude that interaction between free electrons and ions in interstellar space probably produces radiation of observable intensity in the radio and possibly the visual region of the spectrum.

L. G. HENYEY
PHILIP C. KEENAN

YERKES OBSERVATORY
February 1940

INDEX TO VOLUME 91

INDEX TO SUBJECTS

PAGE

Atmospheric Absorption of Infrared Solar Radiation at the Lowell Observatory. II. The Spectral Interval: 5.5–8 μ. *Arthur Adel and C. O. Lampland* 1

Atmospheric Absorption of Infrared Solar Radiation at the Lowell Observatory. III and IV. The Spectral Intervals: 8.0–11.0 μ and 11.0–14.0 μ. *Arthur Adel and C. O. Lampland* 481

B stars, The Colors of 1332. *Joel Stebbins, C. M. Huffer, and A. E. Whitford*. 20

Balmer Absorption upon the Equivalent Widths of Stellar Absorption Lines, The Effect of Continuous. *Otto Struve and Frances Sherman* . 428

Balmer Lines in Early-Type Stars, On the Number of. *A. Unsöld and O. Struve* 365

Binary Stars, New White Dwarfs, Subdwarfs, and. *G. P. Kuiper* . . 269

CH Bands in Comet Spectra. *J. Dufay* 91

Cluster M 67, Proper Motions in the Galactic. *E. G. Ebbighausen* . . 244

Clusters, Galactic Star. *Robert J. Trumpler* 186

Clusters, Integrated Photographic Magnitudes of Sixty-eight Globular. *William H. Christie* 8

Comet Spectra, *CH* Bands in. *J. Dufay* 91

Comets, On the Evolution of. *Herbert Jehle* 473

Contraterrene Matter, The Hypothesis of the Existence of. *V. Rojansky* 257

Cosmic Static. *Grote Reber* 621

Cosmological Theories. *E. A. Milne* 129

Dreyer's Catalogues of Nebulae and Clusters, Some Corrections to. *Dorothy Carlson* 350

Erratum. *S. Chapman* 368

f-Values by the Method of Total Absorption, Absolute. *Robert B. King and Donald C. Stockbarger* 488

Galactic System and the Elliptical Nebulae NGC 3115 and 4494, Some Problems concerning the Structure and Dynamics of the. *J. H. Oort* 273

PAGE

$H\gamma$ in A-Type Stars, The Contours of. *C. J. Krieger* 476

Helium Levels, Metastability of Hydrogen and. *G. Breit and E. Teller* . 215

Helium in the Orion Nebula, Relative Populations of 2^1S and 2^3S States of. *O. C. Wilson* 360

Hydrogen and Helium Levels, Metastability of. *G. Breit and E. Teller* . 215

Interstellar Radiation from Free Electrons and Hydrogen Atoms. *L. G. Henyey and Philip C. Keenan* 625

Luminosities of Stars of Types G and K in Two Selected Fields, Spectroscopic. *Philip C. Keenan* 506

M—S Differentiation, On the Physical Significance of the. *Karl Wurm* . 103

Magnitudes of Sixty-eight Globular Clusters, Integrated Photographic. *William H. Christie* 8

Meteor Spectrum of High Excitation, A. *A. N. Vyssotsky* 264

Microfilm Sets of Periodicals 368

Moon, Radiation Measurements on the Eclipsed. *Edison Pettit* . . . 408

Nebulae. IX. On the Excitation of Fractional Multiplets by Electron Capture, Physical Processes in Gaseous. *George H. Shortley and Donald H. Menzel* 307

Nebulae and Clusters, Some Corrections to Dreyer's Catalogues of. *Dorothy Carlson* 350

Nebulae in Messier 101, Emission. *Carl K. Seyfert* 261

Nebulae NGC 3115 and 4494, Some Problems concerning the Structure and Dynamics of the Galactic System and the Elliptical. *J. H. Oort* . 273

Negative Hydrogen Ions, The Continuous Absorption of Light by. *H. S. W. Massey and D. R. Bates* 202

North Polar Sequence, Spectral Types of Stars of the. *Philip C. Keenan* 113

Novae, The Relation between Absorption Velocity and Rate of Decline for Galactic. *Dean B. McLaughlin* 369

Orion Nebula, Relative Populations of 2^1S and 2^3S States of Helium in the. *O. C. Wilson* 360

25 Orionis, 1933–1939, The Spectrum of. *Helen W. Dodson* 126

Parallaxes with the 60- and 100-Inch Reflectors. Seventeenth Series, The Photographic Determination of Stellar. *Adriaan van Maanen* . . . 503

Prominences, The Motion of Eruptive. *R. G. Giovanelli* 83

PAGE

Reviews:
Albright, John G. *Physical Meteorology* 368
Boyer, Carl B. *The Concepts of the Calculus* 368
Gatterer, A., and J. Junkes. *Atlas der Restlinien von 30 chemischen Elementen* (G. Abetti) 479
Kayser, H., and R. Ritschl. *Tabelle der Hauptlinien der Linienspektren aller Elemente* (O. Struve) 367
Stumpff, K. *Tafeln und Aufgaben zur harmonischen Analyse und Periodogrammrechnung* 367

Ross 22, Note on. *G. P. Kuiper* 366

Rowland Intensity Scale, An Investigation of the. *Donald H. Menzel, Leo Goldberg, and Edward M. Cook* 320

v Sagittarii, The Spectrum of. *Jesse L. Greenstein* 438

Solar Eclipse, The General Illumination during a Total. *John Q. Stewart and C. D. MacCracken* 51

Solar Eruptions. *R. G. Giovanelli* 334

Solar Radiation at the Lowell Observatory. II. The Spectral Interval: 5.5–8 μ, Atmospheric Absorption of the Infrared. *Arthur Adel and C. O. Lampland* 1

Solar Radiation at the Lowell Observatory. III and IV. The Spectral Intervals: 8.0–11.0 μ and 11.0–14.0 μ, Atmospheric Absorption of Infrared. *Arthur Adel and C. O. Lampland* 481

Solar Reversing Layer from *CN* (λ 3883), The Excitation Temperature of the. *Leon Blitzer* 421

Spectral Energy-Curve of the Sun in the Ultraviolet. *Edison Pettit* . . 159

Spectral Types of Stars of the North Polar Sequence. *Philip C. Keenan* 113

Spirals, The Distribution of Color in. *Carl K. Seyfert* 528

Stars of Large Proper Motion, Magnitudes and Colors of. *Carl K. Seyfert* 117

Stars, Spectrographic Observations of Peculiar. *P. Swings and O. Struve* 546

Stars of Types G and K in Two Selected Fields, Spectroscopic Luminosities of. *Philip C. Keenan* 506

Stellar Absorption Lines, The Effect of Continuous Balmer Absorption upon the Equivalent Widths of. *Otto Struve and Frances Sherman* . 428

Sun, Note on the Point-Convective Model for the. *R. E. Marshak* . . 362

Sun in the Ultraviolet, Spectral Energy-Curve of the. *Edison Pettit* . . 159

PAGE

Sunspot Variations. II. The Mathematical Characteristics of. *John Q. Stewart and Forrest C. Eggleston* 72

Thomas-Fermi Method as Applied to Stars, The Generalized. *R. E. Marshak and H. A. Bethe* 239

Venus, Note on the Surface Temperature of. *Rupert Wildt* 266

White Dwarfs, Subdwarfs, and Binary Stars, New. *G. P. Kuiper* . . . 269

Wolf-Rayet Spectroscopic Binary HD 193576, The. *O. C. Wilson* . . 379

Wolf-Rayet Stars, Physical Characteristics of the. *O. C. Wilson* . . . 394

INDEX OF AUTHORS

PAGE

ABETTI, G. Review of: *Atlas der Restlinien von 30 chemischen Elementen.* A. Gatterer and J. Junkes 479

ADEL, ARTHUR, and C. O. LAMPLAND. Atmospheric Absorption of Infrared Solar Radiation at the Lowell Observatory. II. The Spectral Interval: 5.5–8 μ 1

ADEL, ARTHUR, and C. O. LAMPLAND. Atmospheric Absorption of Infrared Solar Radiation at the Lowell Observatory. III and IV. The Spectral Intervals: 8.0–11.0 μ and 11.0–14.0 μ 481

BATES, D. R., and H. S. W. MASSEY. The Continuous Absorption of Light by Negative Hydrogen Ions 202

BETHE, H. A., and R. E. MARSHAK. The Generalized Thomas-Fermi Method as Applied to Stars 239

BLITZER, LEON. The Excitation Temperature of the Solar Reversing Layer from *CN* (λ 3883) 421

BREIT, G., and E. TELLER. Metastability of Hydrogen and Helium Levels 215

CARLSON, DOROTHY. Some Corrections to Dreyer's Catalogues of Nebulae and Clusters 350

CHAPMAN, S. Erratum 368

CHRISTIE, WILLIAM H. Integrated Photographic Magnitudes of Sixty-eight Globular Clusters 8

COOK, EDWARD M., DONALD H. MENZEL, and LEO GOLDBERG. An Investigation of the Rowland Intensity Scale 320

DODSON, HELEN W. The Spectrum of 25 Orionis, 1933–1939 126

DUFAY, J. *CH* Bands in Comet Spectra 91

EBBIGHAUSEN, E. G. Proper Motions in the Galactic Cluster M 67 . . 244

EGGLESTON, FORREST C., and JOHN Q. STEWART. The Mathematical Characteristics of Sunspot Variations. II. 72

GIOVANELLI, R. G. The Motion of Eruptive Prominences 83

GIOVANELLI, R. G. Solar Eruptions 334

GOLDBERG, LEO, EDWARD M. COOK, and DONALD H. MENZEL. An Investigation of the Rowland Intensity Scale 320

GREENSTEIN, JESSE L. The Spectrum of υ Sagittarii 438

PAGE

HENYEY, L. G., and PHILIP C. KEENAN. Interstellar Radiation from Free Electrons and Hydrogen Atoms 625

HUFFER, C. M., A. E. WHITFORD, and JOEL STEBBINS. The Colors of 1332 B Stars 20

JEHLE, HERBERT. On the Evolution of Comets 473

KEENAN, PHILIP C. Spectral Types of Stars of the North Polar Sequence 113

KEENAN, PHILIP C. Spectroscopic Luminosities of Stars of Types G and K in Two Selected Fields 506

KEENAN, PHILIP C., and L. G. HENYEY. Interstellar Radiation from Free Electrons and Hydrogen Atoms 625

KING, ROBERT B., and DONALD C. STOCKBARGER. Absolute *f*-Values by the Method of Total Absorption 488

KRIEGER, C. J. The Contours of $H\gamma$ in A-Type Stars 476

KUIPER, G. P. New White Dwarfs, Subdwarfs, and Binary Stars . . 269

KUIPER, G. P. Note on Ross 22 366

LAMPLAND, C. O., and ARTHUR ADEL. Atmospheric Absorption of Infrared Solar Radiation at the Lowell Observatory. II. The Spectral Interval: 5.5–8 μ 1

LAMPLAND, C. O., and ARTHUR ADEL. Atmospheric Absorption of Infrared Solar Radiation at the Lowell Observatory. III and IV. The Spectral Intervals: 8.0–11.0 μ and 11.0–14.0 μ 481

MACCRACKEN, C. D., and JOHN Q. STEWART. The General Illumination during a Total Solar Eclipse 51

MCLAUGHLIN, DEAN B. The Relation between Absorption Velocity and Rate of Decline for Galactic Novae 369

MARSHAK, R. E. Note on the Point-Convective Model for the Sun . . 362

MARSHAK, R. E., and H. A. BETHE. The Generalized Thomas-Fermi Method as Applied to Stars 239

MASSEY, H. S. W., and D. R. BATES. The Continuous Absorption of Light by Negative Hydrogen Ions 202

MENZEL, DONALD H., LEO GOLDBERG, and EDWARD M. COOK. An Investigation of the Rowland Intensity Scale 320

MENZEL, DONALD H., and GEORGE H. SHORTLEY. Physical Processes in Gaseous Nebulae. IX. On the Excitation of Fractional Multiplets by Electron Capture 307

MILNE, E. A. Cosmological Theories 129

PAGE

OORT, J. H. Some Problems concerning the Structure and Dynamics of the Galactic System and the Elliptical Nebulae NGC 3115 and 4494 . 273

PETTIT, EDISON. Radiation Measurements on the Eclipsed Moon . . 408

PETTIT, EDISON. Spectral Energy-Curve of the Sun in the Ultraviolet . 159

REBER, GROTE. Cosmic Static 621

ROJANSKY, V. The Hypothesis of the Existence of Contraterrene Matter 257

SEYFERT, CARL K. The Distribution of Color in Spirals 528

SEYFERT, CARL K. Emission Nebulae in Messier 101 261

SEYFERT, CARL K. Magnitudes and Colors of Stars of Large Proper Motion 117

SHERMAN, FRANCES, and OTTO STRUVE. The Effect of Continuous Balmer Absorption upon the Equivalent Widths of Stellar Absorption Lines . 428

SHORTLEY, GEORGE H., and DONALD H. MENZEL. Physical Processes in Gaseous Nebulae. IX. On the Excitation of Fractional Multiplets by Electron Capture 307

STEBBINS, JOEL, C. M. HUFFER, and A. E. WHITFORD. The Colors of 1332 B Stars 20

STEWART, JOHN Q., and FORREST C. EGGLESTON. The Mathematical Characteristics of Sunspot Variations. II. 72

STEWART, JOHN Q., and C. D. MACCRACKEN. The General Illumination during a Total Solar Eclipse 51

STOCKBARGER, DONALD C., and ROBERT B. KING. Absolute *f*-Values by the Method of Total Absorption 488

STRUVE, O. Review of: *Tabelle der Hauptlinien der Linienspektren aller Elemente*, H. Kayser and R. Ritschl 367

STRUVE, OTTO, and FRANCES SHERMAN. The Effect of Continuous Balmer Absorption upon the Equivalent Widths of Stellar Absorption Lines 428

STRUVE, O., and P. SWINGS. Spectrographic Observations of Peculiar Stars 546

STRUVE, O., and A. UNSÖLD. On the Number of Balmer Lines in Early-Type Stars 365

SWINGS, P., and O. STRUVE. Spectrographic Observations of Peculiar Stars 546

TELLER, E., and G. BREIT. Metastability of Hydrogen and Helium Levels 215

TRUMPLER, ROBERT J. Galactic Star Clusters 186

PAGE

UNSÖLD, A., and O. STRUVE. On the Number of Balmer Lines in Early-Type Stars 365

VAN MAANEN, ADRIAAN. The Photographic Determination of Stellar Parallaxes with the 60- and 100-Inch Reflectors. Seventeenth Series 503

VYSSOTSKY, A. N. A Meteor Spectrum of High Excitation 264

WHITFORD, A. E., C. M. HUFFER, and JOEL STEBBINS. The Colors of 1332 B Stars 20

WILDT, RUPERT. Note on the Surface Temperature of Venus . . . 266

WILSON, O. C. Physical Characteristics of the Wolf-Rayet Stars . . . 394

WILSON, O. C. Relative Populations of 2^1S and 2^3S States of Helium in the Orion Nebula 360

WILSON, O. C. The Wolf-Rayet Spectroscopic Binary HD 193576 . . 379

WURM, KARL. On the Physical Significance of the M−S Differentiation . 103

VOLUME 91 NUMBER 5

Yerkes Obs. JUL 5 1940

THE ASTROPHYSICAL JOURNAL

JUL 3 1940

AN INTERNATIONAL REVIEW OF SPECTROSCOPY AND ASTRONOMICAL PHYSICS

Founded in 1895 by GEORGE E. HALE *and* JAMES E. KEELER

Edited by

HENRY G. GALE
Ryerson Physical Laboratory of the University of Chicago

FREDERICK H. SEARES
Mount Wilson Observatory of the Carnegie Institution of Washington

OTTO STRUVE
Yerkes Observatory of the University of Chicago

JUNE 1940

ATMOSPHERIC ABSORPTION OF INFRARED SOLAR RADIATION AT THE LOWELL OBSERVATORY. III AND IV. THE SPECTRAL INTERVALS: 8.0–11.0 μ AND 11.0–14.0 μ - - - - - - - - - - - - - - - - *Arthur Adel and C. O. Lampland* 481

ABSOLUTE *f*-VALUES BY THE METHOD OF TOTAL ABSORPTION *Robert B. King and Donald C. Stockbarger* 488

THE PHOTOGRAPHIC DETERMINATION OF STELLAR PARALLAXES WITH THE 60- AND 100-INCH REFLECTORS. SEVENTEENTH SERIES - - *Adriaan van Maanen* 503

SPECTROSCOPIC LUMINOSITIES OF STARS OF TYPES G AND K IN TWO SELECTED FIELDS - - - - - - - - - - - - - - - - - - *Philip C. Keenan* 506

THE DISTRIBUTION OF COLOR IN SPIRALS - - - - - - - - *Carl K. Seyfert* 528

SPECTROGRAPHIC OBSERVATIONS OF PECULIAR STARS - *P. Swings and O. Struve* 546

NOTES

COSMIC STATIC - *Grote Reber* 621

INTERSTELLAR RADIATION FROM FREE ELECTRONS AND HYDROGEN ATOMS *L. G. Henyey and Philip C. Keenan* 625

INDEX - 631

THE UNIVERSITY OF CHICAGO PRESS
CHICAGO, ILLINOIS, U.S.A.

June 1940 Vol. 91, No. 5

THE ASTROPHYSICAL JOURNAL

AN INTERNATIONAL REVIEW OF SPECTROSCOPY AND ASTRONOMICAL PHYSICS

Edited by

HENRY G. GALE
Ryerson Physical Laboratory of the University of Chicago

FREDERICK H. SEARES
Mount Wilson Observatory of the Carnegie Institution of Washington

OTTO STRUVE
Yerkes Observatory of the University of Chicago

WITH THE COLLABORATION OF

WALTER S. ADAMS, Mount Wilson Observatory
JOSEPH S. AMES, Johns Hopkins University
HENRY CREW, Northwestern University
CHARLES FABRY, Université de Paris
ALFRED FOWLER, Imperial College, London
EDWIN HUBBLE, Mount Wilson Observatory
HEINRICH KAYSER, Universität Bonn
ROBERT A. MILLIKAN, Institute of Technology, Pasadena
HUGH F. NEWALL, Cambridge University
FRIEDRICH PASCHEN, Reichsanstalt, Charlottenburg
HENRY N. RUSSELL, Princeton University
FRANK SCHLESINGER, Yale Observatory
HARLOW SHAPLEY, Harvard College Observatory
F. J. M. STRATTON, Cambridge University

Former Editors:

GEORGE E. HALE JAMES E. KEELER EDWIN B. FROST

The Astrophysical Journal is published by the University of Chicago at the University of Chicago Press, 5750 Ellis Avenue, Chicago, Illinois, during each month except February and August. ¶The subscription price is $10.00 a year; the price of single copies is $1.50. Orders for service of less than a full year will be charged at the single-copy rate. ¶Postage is prepaid by the publishers on all orders from the United States, Mexico, Cuba, Puerto Rico, Panama Canal Zone, Republic of Panama, Dominican Republic, Canary Islands, El Salvador, Argentina, Bolivia, Brazil, Colombia, Chile, Costa Rica, Ecuador, Guatemala, Honduras, Nicaragua, Peru, Hayti, Uruguay, Paraguay, Hawaiian Islands, Philippine Islands, Guam, Samoan Islands, Balearic Islands, Spain, and Venezuela. ¶Postage is charged extra as follows: for Canada and Newfoundland, 30 cents on annual subscriptions (total $10.30); on single copies, 3 cents (total $1.53); for all other countries in the Postal Union, 80 cents on annual subscriptions (total $10.80), on single copies, 8 cents (total $1.58). ¶Patrons are requested to make all remittances payable to The University of Chicago Press, in postal or express money orders or bank drafts.

The following are authorized agents:

For the British Empire, except North America, India, and Australasia: The Cambridge University Press, Bentley House, 200 Euston Road, London, N.W. 1, England. Prices of yearly subscriptions and of single copies may be had on application.

For Japan: The Maruzen Company, Ltd., Tokyo.

For China: The Commercial Press, Ltd., 211 Honan Road, Shanghai. Yearly subscriptions, $10.00; single copies, $1.50, or their equivalents in Chinese money. Postage extra, on yearly subscriptions 80 cents, on single copies 8 cents.

Claims for missing numbers should be made within the month following the regular month of publication. The publishers expect to supply missing numbers free only when losses have been sustained in transit, and when the reserve stock will permit.

Business correspondence should be addressed to The University of Chicago Press, Chicago, Illinois.

Communications for the editors and manuscripts should be addressed to: Otto Struve, Editor of THE ASTROPHYSICAL JOURNAL, Yerkes Observatory, Williams Bay, Wisconsin.

One copy of the corrected galley proof should be returned as soon as possible to the editor, Yerkes Observatory, Williams Bay, Wisconsin. Authors should take notice that the manuscript will not be sent to them with the proof.

The cable address is "Observatory, Williamsbay, Wisconsin."

The articles in this journal are indexed in the *International Index to Periodicals*, New York, N.Y.

Applications for permission to quote from this journal should be addressed to The University of Chicago Press, and will be freely granted.

Entered as second-class matter, January 17, 1895, at the Post-Office, Chicago, Ill., under the act of March 3, 1879.
Acceptance for mailing at special rate of postage provided for in Section 1103, Act of October 3, 1917, authorised on July 15, 1918.

PRINTED IN THE U.S.A.

Publishers: G. E. STECHERT & Co., New York . DAVID NUTT, London . NICOLA ZANICHELLI, Bologna FELIX ALCAN, Paris . AKADEMISCHE VERLAGSGESELLSCHAFT m. b. H., Leipsig . RUIZ HERMANOS, Madrid . F. KILIAN'S NACHFOLGER, Budapest . F. ROUGE e CIE, Lausanne . THE MARUZEN COMPANY, Tokyo.

1940 34th Year

"SCIENTIA"

INTERNATIONAL REVIEW OF SCIENTIFIC SYNTHESIS

Published every month (each number containing 100 to 120 pages)

Editors: G. B. BONINO - F. BOTTAZZI - G. BRUNI - A. PALATINI - F. SEVERI - General Secretary: PAOLO BONETTI

IS THE ONLY REVIEW the contributors to which are really international.

IS THE ONLY REVIEW that has a really world-wide circulation.

IS THE ONLY REVIEW of synthesis and unification of science, that deals in its articles with the newest and most fundamental problems of all branches of knowledge: scientific philosophy, history of science, scientific teaching and advancement, mathematics, astronomy, geology, physics, chemistry, biological sciences, physiology, psychology, history of religions, anthropology, linguistics; articles sometimes constituting real and proper enquiries, such as those on the contribution given by the different nations to the advancement of science; on determinism; on the most fundamental physical and chemical questions, and particularly on relativity, on the physics of the atom and of radiations; on vitalism. "Scientia" thus studies all the main problems interesting the intellectual circles of the whole world.

IS THE ONLY REVIEW that among its contributors can boast of the most illustrious men of science in the whole world.

The articles are published in the language of their authors, and every number has **a supplement containing the French translation of all the articles that are not French. The review is thus completely accessible to those who know only French.** (*Write for a free copy to the* General Secretary of "Scientia," Milan, *sending a sixpence in one stamp of your country, merely to cover packing and postage.*)

SUBSCRIPTION: $11.50

Substantial reductions are granted to those who take up more than one year's subscription.

For information apply to **"SCIENTIA" Via A. De Togni, 23, Milano (Italy)**

Astronomical

LANTERN SLIDES

Since 1903, the Yerkes Observatory of the University of Chicago has been reproducing in lantern slides, transparencies, and prints the original astronomical photographs made at Williams Bay.

The lantern slides are uniformly 4×3¼ inches in size. The frequent call for small sets of slides for school and lecture purposes has led to the preparation of a list of 100 representative slides (price $62.50), a catalogue of which may be obtained upon request to the University of Chicago Press, 5750 Ellis Avenue, Chicago.

Prints as well as slides can be furnished, and for many subjects window transparencies are also supplied.

For catalogue and further information write

The University of Chicago Press

5750 Ellis Avenue, Chicago, Ill.

POPULAR ASTRONOMY

A magazine now in its forty-sixth year, devoted to the elementary aspects of Astronomy and allied sciences.

Published monthly, except July and September.

Yearly subscription rates: Domestic $4.00; Canadian $4.25; Foreign $4.50.

Address

POPULAR ASTRONOMY

CARLETON COLLEGE

NORTHFIELD, MINNESOTA, U.S.A.

ASTROPHYSICAL MONOGRAPHS

Sponsored by the Editors of the Astrophysical Journal

A series designed to provide a growing library of precise, up-to-date, authoritative material of modern astronomy and astrophysics for astronomers, physicists, mathematicians, and chemists. By combining the advantages of an advanced textbook with the interest of a research narrative, the monographs will serve as reference volumes for astronomers and as manuals for teachers.

Just published

THE MASSES OF THE STARS, WITH A GENERAL CATALOGUE OF DYNAMICAL PARALLAXES

By HENRY NORRIS RUSSELL and CHARLOTTE E. MOORE

This list is unique as it contains all the available information of binary components in double stars secured from observations extending over several hundred years. Stellar masses range in size from about one-tenth to several hundred times the mass of the sun, and an exact knowledge of the amount of matter contained in a star is required before the riddle of the generation of stellar energies can be solved. Discussions of the methods used for the determination of the masses of the stars and the results obtained by the authors are included. *236 pages, 53 tables, paper, $3.50*

Ready early summer

SPECTRA OF LONG-PERIOD VARIABLE STARS

By PAUL W. MERRILL

This monograph is devoted largely to the observational side of the subject, but some discussion of the physical significance of various spectral features is included. A brief introduction and a historical chapter are inserted for the benefit of the reader who is not a specialist in stellar spectra. The spectra at maximum light and their chief periodic variations are then described. Following chapters are concerned with certain technical problems and with individual variables of special interest. The monograph concludes with a brief discussion of a few general problems of long-period variables. (?) *$2.50*

Published

AN INTRODUCTION TO THE STUDY OF STELLAR STRUCTURE

By S. CHANDRASEKHAR

Treats in a deductive manner the subject of stellar interiors. The necessary physical theories and mathematical methods are fully explained. Includes accounts of the foundations of thermodynamics, the theory of radiation, the quantum theory of a perfect gas, and a discussion of the elements of nuclear physics. "The material is throughout presented with enviable crispness and clarity of expression. The work will undoubtedly become an indispensable handbook for future researchers in this field."—*Nature* (England). *502 pages, 22 pages of engravings, $10.00*

THE DISTRIBUTION OF THE STARS IN SPACE

By BART J. BOK

". . . . an extremely important contribution to the field of galactic structure, invaluable alike to both students and research workers in the field."—*Science*. The large number and variety of researches carried out in this field during the past fifteen years are discussed critically in this study with clarity and dispatch. *124 pages, paper, $2.50*

THE UNIVERSITY OF CHICAGO PRESS